TECHNISCHE UNIVERSITÄT MÜNCHEN

Fakultät für Medizin

In vivo CRISPR screens to dissect regulatory genes controlling T cell transmigration and macrophage polarization in animal models of Multiple Sclerosis

Arek Kendirli

Vollständiger Abdruck der von der Fakultät für Medizin der Technischen Universität München zur Erlangung des akademischen Grades eines

Doctor of Philosophy (Ph.D.)

genehmigten Dissertation.

Vorsitzender: Prof. Dr. Maximilian Reichert

Betreuer: Prof. Dr. Martin Kerschensteiner

Prüfer der Dissertation:

1. Prof. Dr. Marc Schmidt-Supprian

2. Prof. Dr. Thomas Korn

Die Dissertation wurde am 28.01.2022 bei der Fakultät für Medizin der Technischen Universität München eingereicht und durch die Fakultät für Medizin am 18.03.2022 angenommen.

Nerede olursan ol

İçerde dışarda derste sırada

Yürü üstüne üstüne

Tükür yüzüne celladın

Fırsatçının fesatçının hayının

Dayan kitap ile

Dayan iş ile

Tırnak ile diş ile

Umut ile sevda ile düş ile

Ahmed Arif

Abstract

Multiple Sclerosis (MS) is an inflammatory demyelinating autoimmune disease of the brain and spinal cord. In healthy conditions, the infiltration of immune cells into the central nervous system (CNS) is tightly controlled by the blood-brain barrier (BBB). In MS, however, activated myelin-specific T cells can cross the BBB and accumulate in the CNS. After re-activation, they then recruit and instruct other immune cells including monocyte-derived macrophages that contribute to tissue damage. In my thesis, I used CRISPR gene editing in MS models to perform a comprehensive characterization of two critical steps in the disease pathogenesis, the CNS infiltration of T cells and the local instruction of phagocyte phenotypes.

In the first part of my thesis work, we used an adoptive T-cell transfer EAE model in Lewis rats to perform an *in vivo* genome-wide loss-of-function CRISPR screen in Myelin Basic Protein (MBP)-specific T cells (T_{MBP}). Our CRISPR screen identified the essential genes required for T_{MBP} cell transmigration into the CNS, which included previously reported regulators such as Itga4, Fermt3, Cxcr3, as well as novel regulators such as Grk2. *In vivo* two-photon imaging experiments performed by our collaborators revealed that Grk2-deficient T_{MBP} cells can attach to the intraluminal surface of the blood vessels and crawl similarly to control T_{MBP} cells, but they fail to extravasate to the abluminal side, which also prevents EAE. This impaired transmigration phenotype was rescued upon the knockout (KO) of Sphingosine-1-phosphate receptor (S1pr1), suggesting that Grk2 executes its function on transmigration through the S1pr1 regulation. We also found that Ets1 acts as an inhibitor of T cell migration, since Ets1-deficient T_{MBP} cells were enriched in CNS compartments. Overall, our genome-wide *in vivo* CRISPR screen identified regulators of MBP-specific T cell migration, paving the way for the discovery of new therapeutic targets in MS.

In the second part of my thesis, I focused on the molecular regulation of phagocyte phenotypes in the inflamed CNS. This is of interest as monocyte-derived macrophages, a highly abundant cell type in MS and EAE inflammatory lesions, can perform dual functions and contribute to both the formation and resolution of CNS lesions. When exposed to lesion microenvironments, these phagocytes develop into pro-(M_{iNOS}) and anti-(M_{Arg1}) inflammatory phenotypes, which are

associated with microbicidal activity and tissue repair, respectively. Here, we developed a novel method for studying the polarization dynamics of macrophages *in vivo* in the inflamed CNS by the adoptive transfer of Hoxb8 cells, immortalized bone marrow progenitor cells, into EAE-induced mice. Given the unlimited proliferative capacity of Hoxb8 cells *in vitro*, CRISPR manipulations could be introduced before transferring them to EAE-induced animals. We showed that *in vitro* myeloid-primed Hoxb8 cells complete their differentiation into monocytes *in vivo*, which are then recruited to the inflamed spinal cord in a Ccr2-dependent manner during EAE. In the CNS, they become macrophages and exhibit polarization characteristics comparable to endogenous macrophages. We performed an *in vivo* CRISPR screen using this Hoxb8 transfer model, targeting cytokine receptors and their key signaling intermediates, and discovered that TGF-β and GMCSF are both required to drive cells to the M_{Arg1} phenotype, while IFN-γ and TNF-α are required to drive cells to the M_{iNOS} phenotype. Surprisingly, none of the classical M_{Arg1} driving cytokines such as IL4, IL13, or IL10 play a role in our active EAE model. Moreover, we demonstrated the synergistic effects of TGF-β and GMCSF on M_{Arg1} polarization and IFN-γ and TNF-α on M_{iNOS} polarization in classical bone marrow-derived macrophages (BMDMs) *in vitro*. Overall, our *in vivo* CRISPR screen in Hoxb8-derived macrophages identified cytokines that regulate macrophage activation and polarization towards M_{Arg1} and M_{iNOS} phenotypes, shedding light on the complex cytokine milieu of the inflamed spinal cord during EAE. Furthermore, our Hoxb8 transfer model offers a highly useful tool for studying the role of monocytes/macrophages in health and disease *in vivo*.

Overall, I believe that using *in vivo* CRISPR screens in animal models of MS to identify essential regulators of T cell transmigration and macrophage polarization will improve our understanding of disease initiation, progression, and resolution, and thus contribute to the development of targeted therapeutic strategies for MS.

Table of Contents

List of Abbreviations

AJs	Adherens Junctions
APC	Antigen-Presenting Cells
Arg1	Arginase 1
BBB	Blood-Brain Barrier
BCSFB	Blood-Cerebrospinal Fluid Barrier
BFP	Blue Fluorescent Protein
BMDM	Bone Marrow-Derived Macrophages
CFA	Complete Freund's Adjuvant
CIS	Clinically Isolated Syndrome
CNS	Central Nervous System
CRISPR	Clustered Regularly Interspaced Short Palindromic Repeats
CSF	Cerebrospinal Fluid
DMT	Disease-Modifying Therapies
DSB	Double-Strand Break
EAE	Experimental Autoimmune Encephalomyelitis
EBV	Epstein-Barr Virus
FACS	Fluorescence-Activated Cell Sorting
FBS	Fetal Bovine Serum
gDNA	genomic DNA
GFP	Green Fluorescent Protein
GM-CSF	Granulocyte-Macrophage Colony-Stimulating Factor
GPCRs	G-Protein-Coupled Receptors
guide RNA	gRNA
GWAS	Genome-Wide Association Studies
HDR	Homology-Directed Repair
InDels	Insertions and Deletions
i.p.	intraperitoneal
i.v.	intravenous
iNOS	inducible Nitric Oxide Synthase
iPSCs	induced Pluripotent Stem Cells
JCV	John Cunningham Virus
KO	Knock-Out
LAFUGA	Laboratory for Functional Genome Analysis
LPS	Lipopolysaccharides
M1-like	pro-inflammatory type of Macrophages
M2-like	anti-inflammatory type of Macrophages
MACS	Magnetic-Activated Cell Sorting
MBP	Myelin Basic Protein
MHCII	Major Histocompatibility Complex II
MMPS	Matrix Metalloproteinases

MMPs	Multipotent Progenitors
MOG	Myelin Oligodendrocyte Glycoprotein
MOI	Multiplicity Of Infection
MRI	Magnetic Resonance Imaging
mRNA	messenger RNA
MS	Multiple Sclerosis
NHEJ	Non-Homologous End Joining
NK cell	Natural Killer cell
NO	Nitric Oxide
NT	Non-Targeting
o/n	overnight
OVA	Ovalbumin
PAM	Protospacer-Adjacent Motif
PBS	Phosphate Buffered Saline
PLP	Proteolipid Protein
PML	Progressive Multifocal Leukoencephalopathy
PPMS	Primary Progressive MS
PRMS	Progressive Relapsing MS
PTX	Pertussis Toxin
RIS	Radiologically Isolated Syndrome
RNAi	RNA Interference
RNP	Ribonucleoprotein
ROS	Reactive Oxygen Species
RRMS	Relapsing-Remitting MS
RT	Room Temperature
S1P	Sphingosine-1-Phosphate
shRNAs	short-hairpin RNAs
siRNAs	short-interfering RNAs
SPMS	Secondary Progressive MS
TALENs	Transcription Activator-Like Effector Nucleases
TEER	Transendothelial Electrical Resistance
Th1	T helper 1
Th17	T helper 17
TJs	Tight Junctions
T_{regs}	Regulatory T cells
UVB	Ultraviolet B-light
vs	versus
ZFNs	Zinc-Finger Nucleases

1. INTRODUCTION

1.1 Multiple Sclerosis

1.1.1 Epidemiology and Risk Factors

Multiple Sclerosis (MS) is an autoimmune disease of the central nervous system (CNS), where the dysregulated immune system targets myelin proteins, leading to impaired function of the nervous system. Based on a 2020 global study, approximately 2.8 million people worldwide have MS (The Multiple Sclerosis International Federation, September 2020). This disease affects mostly young adults with an onset age range of 20 to 45 years. The prevalence and incidence of MS are higher in Western developed countries and the female to male ratio of MS is 3:1 (**Figure 1**), both of which suggest that several genetic and environmental factors might play a role (Alonso & Hernán, 2008) (Palacios, Alonso, Brønnum-Hansen, & Ascherio, 2011) (Napier et al., 2016). Although the direct cause of MS remains unknown, it has been shown that a combination of genetic and environmental factors can contribute to the disease development. Epstein-Barr virus (EBV) infection, low vitamin D levels, exposure to ultraviolet B-light (UVB), obesity and smoking are well known environmental risk factors for MS development (Ascherio, 2013) (Ramagopalan, Dobson, Meier, & Giovannoni, 2010) (Olsson, Barcellos, & Alfredsson, 2017). In a more recent study involving a cohort of 10 million people over the course of 20 years, it was discovered that after infection with EBV, the risk of developing MS increased 32-fold, with no link to other viruses (Bjornevik et al., 2022). As for the genetic factors, genome-wide association studies (GWAS) have identified over 230 genetic risk variants for MS mainly including polymorphisms in HLA class I and II genes and in other genes associated with immune function such as TNFR1, IL7R, IL2RA (Cotsapas & Mitrovic, 2018) (Beecham et al., 2013). A more recent GWAS has identified MS risk genes not only in peripheral innate and adaptive immune cells but also in CNS resident microglia cells, however it failed to associate any to astrocytes or neurons (International Multiple Sclerosis Genetics Consortium, 2019).
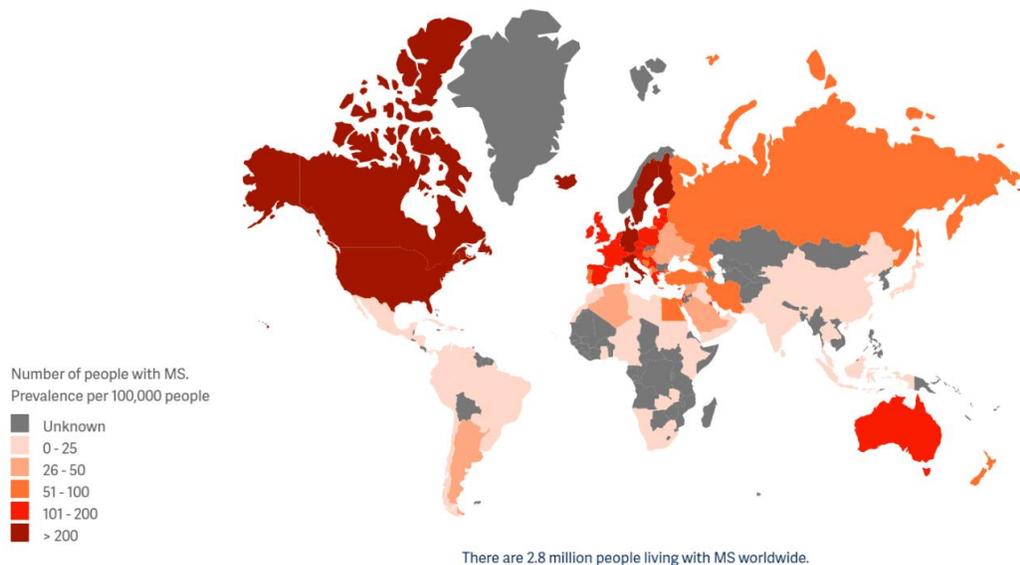
Figure 1 | Worldwide prevalence of MS. Around 2.8 million people worldwide have MS with a high prevalence in Western countries. Image taken from The MS International Federation's Atlas of MS, 2020.

1.1.2 Clinical Features of MS

As MS lesions can occur throughout the CNS a broad range of neurological symptoms can be observed that often affect vision and locomotion (McAlpine, Lumsden, & Acheson, 1972). There are four types of MS that have been defined based on the clinical course of the disease by the International Advisory Committee on Clinical Trials of MS (Lublin et al., 2014) (**Figure 2**). Typically, when a person develops an initial clinical attack resembling MS, it is classified as a clinically isolated syndrome (CIS). The majority (about 85%) of MS patients develop relapsing-remitting MS (RRMS), which is characterized by clinical attacks at irregular intervals with full or partial recovery. Secondary progressive MS (SPMS), characterized by progressive worsening of the disease, is developed by most patients with RRMS 10-15 years after onset. Primary progressive MS (PPMS) affects approximately 10% of MS patients, showing a gradual and continued disease progression without early relapses or remissions. Lastly, a rare form of MS, progressive relapsing MS (PRMS), is seen in less than 5% of the patients and shows progressive disease course from the onset with no remission intervals. Each MS type can have active or inactive lesions in the brain and spinal

cord, detected by magnetic resonance imaging (MRI). MRI scans are not only the key to diagnosing MS, but also very useful to follow disease progression and to evaluate response to treatments. In addition to MRI scans, clinical signs and cerebrospinal fluid (CSF) examinations are considered for the diagnosis of MS along with other guidelines included in the McDonald criteria (A. J. Thompson et al., 2018). MS-like abnormalities detected with MRI in the absence of clinical symptoms are classified as asymptomatic MS or radiologically isolated syndrome (RIS) (De Stefano et al., 2018). Approximately 34% of people with RIS develop MS in the next 5 years (Okuda et al., 2014), indicating a potential window for pre-symptomatic diagnosis.
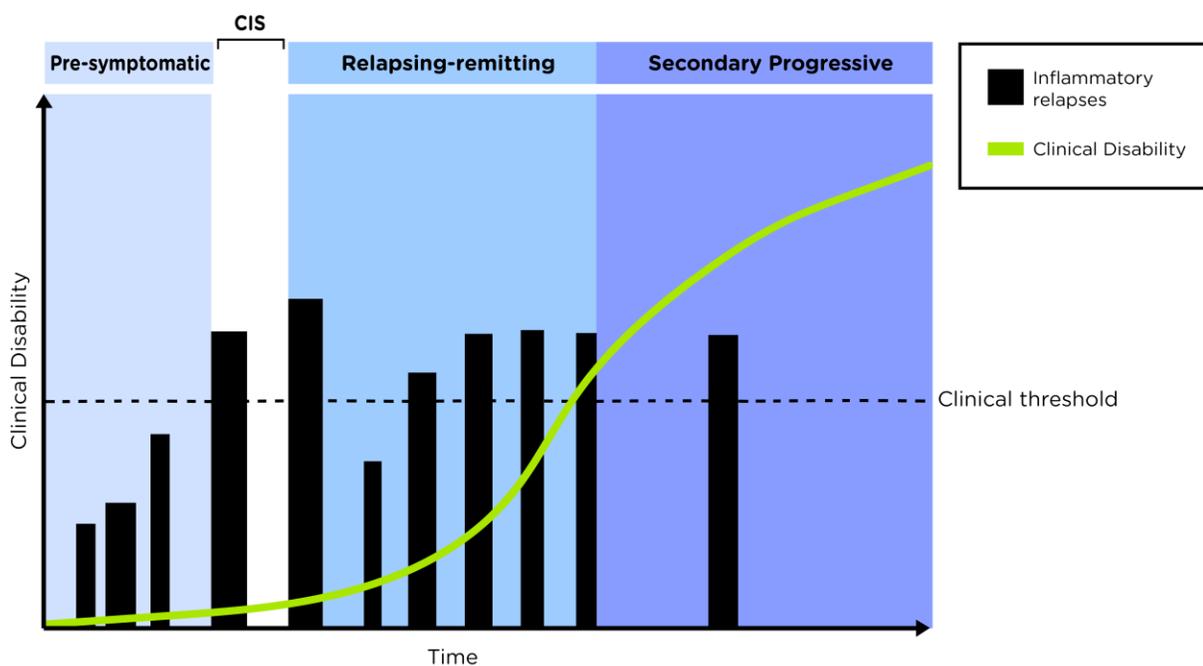
Figure 2 | Clinical course of MS. The first episode of clinical symptoms before developing MS is referred to clinically isolated syndrome (CIS). Relapsing-remitting MS (RRMS) is characterized by inflammatory relapses at irregular intervals. Secondary Progressive MS (SPMS) is characterized by progressive and irreversible clinical disability. Based on Figure 1 from (Massimo Filippi et al., 2018)

1.1.3 Treatment options for MS

Until now, there is no FDA-approved curative treatment for MS. Currently, available treatments include disease-modifying therapies (DMT) directed to reduce disease activity and progression, and treatments aimed at reducing the main symptoms in order to improve quality of life. Acute MS relapses can be treated with short-term high-dose corticosteroids to reduce the duration of the relapse and to minimize the neurological damage (La Mantia et al., 1994). Although there are

several available DMTs with different mechanisms of action, they are mostly used to treat RRMS patients as they show no or only limited benefits for PPMS patients (Filippini et al., 2013), indicating the need for better understanding of MS pathology in order to provide better treatments for the different types of disease. Current DMTs are either immunomodulatory such as interferon-beta (IFNβ), glatiramer acetate, and teriflunomide, or immunosuppressants such as fingolimod, natalizumab, and ocrelizumab. Immunomodulatory DMTs are often used as first-line treatment for RRMS patients as they show moderate but safe effects. On the other hand, immunosuppressant DMTs, are more commonly used as a second-line treatment, as they are more effective but with a higher risk profile (M. Filippi et al., 2018). More recently, the success of depleting B cells in MS with anti-CD20 therapies revealed the importance of B cells in MS pathology (Greenfield & Hauser, 2018). The anti-CD20 monoclonal antibody, Ocrelizumab, is the first FDA-approved drug used for the treatment of patients with PPMS (Montalban et al., 2017). In addition to the DMTs, treatments with neuroprotective and remyelinating functions are in clinical trials and may show beneficial effects with fewer side effects compared to existing DMTs (T. Kapoor & Mehan, 2021) (Hooijmans et al., 2019). In a more recent study, an mRNA vaccine, coding for disease-related autoantigens, has been shown to provide antigen-specific immune tolerance with no other effect on immune function, resulting in the suppression of disease in animal models of EAE (Krienke et al., 2021). Developing mRNA vaccines to induce immunosuppression towards autoantigens stands as a very promising therapy for MS and points out the importance of personalized medicine.

1.1.4 Immunopathology of MS

Inflammatory demyelinating lesions in the white and gray matter of the brain and spinal cord are the pathological hallmarks of MS. MS is traditionally thought to be a two-stage disease, with the early inflammatory phase causing relapsing–remitting disease and the neurodegenerative phase causing non-relapsing disease (Steinman, 2001) (Leray et al., 2010). These two phases implicate multiple cell types in MS pathology, as they link peripheral innate and adaptive immune systems with CNS resident cells. Macrophages and CD8+ T cells are the predominant cell types in the early stages of active demyelinating lesions, when inflammation is more pronounced, whereas CD4+ T cells, CD20+ B cells, and plasma cells are found in smaller numbers at first, increasing as the

disease progresses (Chard et al., 2002). Although recent studies have shown that interactions between the peripheral immune system and CNS can exist through skull channels and meningeal lymphatic vessels (Cugurra et al., 2021) (Brioschi et al., 2021), the CNS is thought to be an immune-privileged tissue, with tightly controlled trafficking of immune cells by the blood-brain barrier (BBB), which protects the neurons in the CNS (Forrester, McMenamin, & Dando, 2018). During MS, BBB breakdowns due to the effect of pro-inflammatory cytokines and chemokines such TNF, IFN-γ, IL-6, IL1-β produced by CNS resident cells, endothelial cells, or infiltrating immune cells, allows more trans-endothelial migration of activated T cells, B cells, and macrophages which further contributes to inflammation and neurodegeneration (Ortiz et al., 2014) (Frohman, Racke, & Raine, 2006). The pro-inflammatory environment is also sensed by CNS resident cells, such as microglia and astrocytes, which makes them involved in neuro-axonal damage through the production of neurotoxic mediators and reactive oxygen species (ROS) (J. M. Frischer et al., 2009).

Cortical gray matter lesions, which are more prominent in PPMS and SPMS patients, have characteristics of lower degree BBB breakdown, less inflammation, and more efficient remyelination compared to white matter lesions, underlying different pathophysiological mechanisms of lesion formation and resolution between gray and white matter (Vercellino et al., 2009) (Strijbis, Kooi, van der Valk, & Geurts, 2017). Synaptic loss has been also observed in MS patients with normal-appearing cortex even outside of demyelinated cortical lesions (Jürgens et al., 2016). A recent study in an animal model of MS has shown that activated microglia and invading macrophages can cause synaptic removal by phagocytosis (Jafari et al., 2021).

Remyelination can occur in demyelinated lesions (Strijbis et al., 2017). Although the degree of remyelination differs based on several factors such as the location of a lesion, the duration of inflammation, the presence of myelin-producing oligodendrocyte and its progenitors, it is more pronounced at early phases of MS and in younger individuals, whereas it decreases in PPMS and SPMS patients (Goldschmidt, Antel, König, Brück, & Kuhlmann, 2009). Since demyelination is a key factor in MS pathology, it has been considered that CNS autoantigens, which can be composed of myelin-derived peptides, are the main drivers of autoreactive T cells. Indeed, it has been shown that antigens such as myelin basic protein (MBP), proteolipid protein (PLP), and

myelin oligodendrocyte glycoprotein (MOG) can be recognized by circulating CD4+ T helper cells (Bielekova et al., 2004). The antigens can be presented to T cells by antigen-presenting cells (APCs) such as dendritic cells, macrophages, and B cells both in the periphery and CNS (Bar-Or, 2008). There are two main types of CD4+ T helper cells that contribute to the disease progression by secreting their signature cytokines; IFN-γ secreting T helper 1 (Th1) cells and IL-17 secreting T helper (Th17) cells (Cao et al., 2015). CD4+ T cells are also known to produce Granulocyte-macrophage colony-stimulating factor (GM-CSF) which contributes to inflammation by activating myeloid cells (Rasouli et al., 2015). Another aspect of aberrant autoreactive T cells activation is inadequate suppressor function of regulatory T cells (T$_{regs}$) which can express anti-inflammatory cytokines such as IL-10 (Kaskow & Baecher-Allan, 2018).

The role of B cells in MS has been recently more appreciated due to the success of selective anti-CD20 treatment, including in progressive MS (Montalban et al., 2017). B cells expressing pro-inflammatory cytokines such as IL-6, GM-CSF, and TNF and reduced expression of the regulatory cytokine IL-10 have been found in MS patients (Bar-Or et al., 2010).

As one of the abundant cell types in lesions, macrophages play a dual role in MS pathology by contributing both to the initiation and resolution of inflammation (Brück et al., 1996). Pro-inflammatory macrophages can cause demyelination and axonal damage, whereas anti-inflammatory macrophages contribute to tissue repair and resolution of inflammation (see section 1.4 for more detailed discussion). Their functional plasticity is dictated by cytokines secreted from other immune cells and CNS resident cells. While most available treatments are focused to reduce the trafficking or depleting leukocytes, targeting macrophage plasticity to drive them into a further tissue repair phenotype holds a potential therapeutic approach (Nally, De Santi, & McCoy, 2019).

1.2 Animal models of MS

Experimental autoimmune encephalomyelitis (EAE) is a broadly used animal model to study MS pathology. EAE was initially induced by delivering CNS tissue homogenate as a source of CNS autoantigens which required multiple injections to achieve robust disease incidence (Rivers, Sprunt, & Berry, 1933). Later, by the discovery of complete Freund's adjuvant (CFA), a mix of

Freund's Adjuvant, which enhances the immunogenicity of antigens, and heat-inactivated mycobacteria tuberculosis as a strong immune stimulant (Kabat, Wolf, Bezer, & Murray, 1951), and by the identification of disease-causing CNS autoantigens such as MBP, MOG, PLP, highly reproducible EAE models were obtained (Mendel, Kerlero de Rosbo, & Ben-Nun, 1995). Since then, several EAE models have been established to cover multiple different aspects of MS pathology such as inflammation, demyelination, and glial scar formation (Lassmann & Bradl, 2017).

1.2.1 Passive T-cell transfer model

The concept that MS might initially be driven by auto-aggressive T cells found in the periphery originated after studies in animal models showed that adoptive transfer of antigen-specific T cells that are propagated *in vitro* is sufficient to trigger an encephalomyelitis in healthy recipients (Ben-Nun, Wekerle, & Cohen, 1981). In the Lewis rat model described by Ben-Nun et al (1981), the transfer of MBP-specific encephalitogenic T cells, but not of ovalbumin (OVA)-specific T cells, induced strong inflammation in the CNS, leading to clinical signs three days after the transfer, followed by clinical recovery in the next few days with the resolution of inflammation. These T cells are activated CD4 T_H1 lymphocytes that are activated by recognizing MBP peptides via MHC class II. Rapid inflammatory CNS pathology following adoptive transfer of T cells is not restricted to myelin antigens only; T cells that are specific to autoantigens derived from neurons and astrocytes can also induce EAE (Wekerle, Kojima, Lannes-Vieira, Lassmann, & Linington, 1994), although pathology induced by specific autoantigens shows differences in location and cellular content of inflammation (Berger et al., 1997). MBP-specific T cells induce massive inflammation in the spinal cord, while the forebrain is mostly unaffected. Upon intravenous transfer of MBP-specific T cells, a small number of cells can be found in the CNS before the onset, but the majority of cells travel first to lymph nodes, the lung, and the spleen, where they gain a functional migratory phenotype by changing their gene expression profile to overcome the BBB and reach the CNS (Flügel et al., 2001) (Bartholomäus et al., 2009) (Odoardi et al., 2012). Cells that encounter antigens in the CNS become reactivated, leading to massive inflammation and further breakdown of the BBB (Kawakami et al., 2005). Although the disease course is monophasic and there is little demyelination, the passive T cell transfer model is particularly suitable to study two key aspects

of T cell-mediated CNS pathology that can shed light on our understanding of MS: how T cells overcome the BBB and enter the CNS and how they remain in there and how their reactivation contributes to the inflammation.

Passive EAE can also be induced in mice by adoptive transfer of *in vitro* polarized CD4+ Th subtypes (Th1, Th17, Th9), obtained from MOG-specific TCR transgenic mice (2D2), to naïve syngeneic recipients (Jäger, Dardalhon, Sobel, Bettelli, & Kuchroo, 2009). The lesion pathology induced in the CNS by each subset of Th cells differs anatomically (Peters et al., 2011) and mechanistically (Rothhammer et al., 2011), indicating the various contributions of different Th subtypes to the disease.

1.2.2 Active EAE model

Active immunization of myelin antigens emulsified with CFA also requires the injection of pertussis toxin (PTX), a protein-based exotoxin produced by the bacterium *Bordetella pertussis*, to generate more robust disease incidence in mice (Bernard & Carnegie, 1975). The exact mechanism of PTX remains unknown, however, studies have shown that PTX can increase the permeability of BBB (Lu et al., 2008), and can enhance auto aggressive T cells activation by inhibiting peripheral anergy (Kamradt, Soloway, Perkins, & Gefter, 1991) or suppressing regulatory T cells (Chen et al., 2006). The most widely used antigens for sensitization in C57BL/6 mice are recombinant MOG35-55 or MOG1-125, which induce acute EAE with clinical signs within 10-12 days followed by remission and recovery of symptoms (Bettadapura, Menon, Moritz, Liu, & Bernard, 1998). Different types of EAE can also be induced by using different genetic backgrounds, different antigens, or different peptide epitopes. For example, PLP139-151 peptide-induced EAE in SJL mice and MOG-induced EAE in Biozzi ABH mice show a relapsing disease course (Whitham et al., 1991) (Amor et al., 1994), whereas MOG-induced EAE in NOD mice follows a progressive course (Basso et al., 2008). Identification of new peptides and epitopes that drive autoreactive T cells will help researchers to establish different EAE models (Siewert et al., 2012). Active EAE generates strong MHCII-restricted autoreactive CD4+ T cells (Th1 and Th17) responses which cause acute inflammation and axonal damage exclusively in the spinal cord, while the forebrain is mostly not affected as in the passive T cell transfer Lewis rat model (Nikić et al., 2011). The relative contribution of Th1 and Th17 cells to the pathology has not been very clear yet as

the expression of both signature cytokines IFN-γ and IL17A is enhanced in lesions, and they might even be simultaneously expressed (Kebir et al., 2009).

Although EAE is a heterogeneous disease depending on the genetic background of the mice and antigen used, mouse EAE models present a powerful tool to improve our understanding regarding different aspects of the disease.

1.3 T cell trafficking into the CNS

CNS homeostasis is protected from rapid changes in the bloodstream by the endothelial BBB in parenchymal and meningeal microvessels and the epithelial blood-cerebrospinal fluid barrier (BCSFB) in the choroid plexus. In addition to BBB, the glia limitans, composed of astrocytic endfeet and basal membrane of the parenchyma, provides a second barrier to protect the CNS parenchyma (Coisne & Engelhardt, 2011) (Owens, Bechmann, & Engelhardt, 2008). The BBB tightly controls the movement of molecules as well as migration of peripheral immune cells due to their highly complex network of adherens junctions (AJs) and tight junctions (TJs), expressed by endothelial cells of the CNS, compared to peripheral vascular endothelial cells (Daneman, 2012). For example, VE-cadherin, Claudin-5, Occludin, and junctional adhesion molecules (JAMs), expressed by CNS endothelial cells, are important for BBB function (Abbott, Patabendige, Dolman, Yusof, & Begley, 2010). It has been also shown that CNS endothelial cells can present myelin antigens to T cells via MHCII to facilitate the migration of T cells (Lopes Pinheiro et al., 2016).

As a part of normal CNS immunosurveillance, immune cells can enter the CSF-draining perivascular and leptomeningeal spaces to search for CNS antigens by interacting with APCs remaining outside of the CNS parenchyma. However, during EAE, clinical signs occur when immune cells also penetrate through the glial limitans in order to reach the CNS parenchyma where they cause tissue damage. Adoptive transfer of non-CNS antigen-specific T cells (T$_{OVA}$) leads to their accumulation within the leptomeninges but not in the CNS parenchyma, compared to T$_{MBP}$ cells, therefore causing no clinical signs (Bartholomäus et al., 2009). CNS antigen autoreactive T cells become licensed in the lung and gain migratory capacity in the periphery by downregulating some activation markers and upregulating chemokine and adhesion molecules on their surface to be able to cross the BBB to the CNS where they get reactivated and contribute

to inflammation (Flügel et al., 2001) (Odoardi et al., 2012). Those chemokine and adhesion molecules are then required to interact with endothelial cells on the BBB to complete the multi-step process of T cell transmigration, starting with rolling and capture of T cells at the endothelium, continuing by chemokine-induced integrin activation, followed by arrest and crawling, and finally diapedesis (extravasation) of cells (Engelhardt & Ransohoff, 2005) (**Figure 3**).

Upon antigen recognition during CNS immunosurveillance, the initial steps of neuroinflammation start by triggering the endothelial cells to upregulate signals to enhance T cell tethering and rolling. Live imaging analysis during EAE has shown that the interaction between inflamed brain and spinal cord microvessels and T cells is mediated by PSGL-1 with its endothelial ligand P-selectin (Kerfoot & Kubes, 2002). High levels of PSGL-1 expression have been also found on CD4+ T cells of MS patients (Bahbouhi et al., 2009). However, the lack of either PSGL-1 or P/E-selectin did not prevent T cell invasion to CNS parenchyma and therefore EAE development in mice, although T cell rolling was abrogated (Sathiyanadan, Coisne, Enzmann, Deutsch, & Engelhardt, 2014). After tethering and rolling, the firm adhesion of T cells to the vascular endothelium requires activation through signaling mediated by G-protein-coupled receptors (GPCRs) on the surface of T cells (Piccio et al., 2002). This signaling leads to clustering and a conformational change in the integrin molecules, increasing the ligand-receptor binding affinity. Several chemokines such as CCL19 and CCL21 are expressed on the luminal side of the BBB have been found to trigger CCR7+ T cell arrest during EAE (Holman, Klein, & Ransohoff, 2011). It has also been shown that MBP-specific T cells upregulate chemokine receptors such as CXCR3, CXCR4, and CCR5 before entering the leptomeninges and CNS parenchyma, and blockage of CXCR3 or CCR5 prevents T cell entrance to the CNS (Schläger et al., 2016).

In EAE, inflammation upregulates the expression of adhesion molecules ICAM-1 and VCAM-1 in endothelial cells at the BBB, and in epithelial cells at the BCSFB, facilitating the arrest of encephalitogenic T cells by binding to their respective ligands LFA-1 (αLβ2) and VLA-4 (α4β1) (Steffen, Butcher, & Engelhardt, 1994). The interaction of LFA-1 with ICAM-1 and VLA-4 with VCAM-1 has been shown to cause a firm adhesion of T cells on the cerebral vessels *in vitro* (Greenwood, Wang, & Calder, 1995) as well as in MS lesions (Sobel, Mitchell, & Fondren, 1990). Although T cell arrest is mediated by both interactions, LFA-1 interaction with ICAM-1 and ICAM-

2 is necessary for the polarization and crawling of cells to find a spot for diapedesis on the endothelium. However, in the absence of ICAM-1 and ICAM-2, T cells can still get arrested by VLA-4 and VCAM-1 interaction (Steiner, Coisne, Cecchelli, et al., 2010). Different subtypes of T cells can preferentially use one or the other of the interactions to enter the CNS. For example, antibody-mediated inhibition of the VLA-4 and VCAM-1 interaction prevents Th1 cells to enter the spinal cord, whereas Th17 entry into the CNS parenchyma is dependent on LFA-1 and ICAM-1 interaction (Rothhammer et al., 2011). Furthermore, EAE driven by Th1 mediated adoptive transfer of T_{MBP} cells in Lewis rats is strongly reduced with anti-VLA-4 antibody but unaffected by anti-LFA-1 treatment, although treatment of both antibodies instantly detaches T cells from the luminal walls (Bartholomäus et al., 2009). Natalizumab, a monoclonal anti-VLA-4 antibody, has been approved for RRMS and has been shown to be beneficial in slowing the disease progression (Hutchinson, 2007). On the other hand, Natalizumab is not beneficial for the progressive forms of MS (R. Kapoor et al., 2018), indicating differences in the immunopathological mechanisms of MS types.

Arrested T cells crawl along the CNS microvessels to find a permissive site for diapedesis. Transendothelial migration of T cells can happen through intercellular junctions and through cell bodies, referred to as paracellular and transcellular migration, respectively (Mickael et al., 2021). Tight junctions on the endothelial barrier undergo rapid remodeling to facilitate paracellular migration (Winger, Koblinski, Kanda, Ransohoff, & Muller, 2014). During the transmigration, ICAM-1 and VCAM-1 cluster, forming cup-like transmigratory structures (Carman & Springer, 2004), which trigger phosphorylation cascades, production of nitric oxide (NO), and ROS by endothelial cells (Martinelli et al., 2009). Although the mechanisms of choice for transmigration routes remain to be investigated, there are several factors that can play a role, such as shear force, type of T cells, inflammatory induced changes in the expression of junctional and adhesion proteins. For example, studies have shown that inflammation-induced high cell surface levels of ICAM-1 favor transcellular migration of T cells (Abadier et al., 2015) by recruiting ICAM-1 to caveola- and F-actin-rich areas (Millán et al., 2006).

After transmigration of T cells to the other side of the endothelial barrier, as the last step of immune trafficking into the CNS, the cells need to cross the glia limitans. The interaction of

laminin α4 at the endothelial basement membrane with α6β1 integrin on T cells facilitates migration across glia limitans. Indeed α4-laminin deficient mice are less susceptible to EAE, although this is partially due to migration inhibitory effect of laminin α5 (Wu et al., 2009). During EAE, CXCR7 upregulation leads to internalization of endothelial CXCL12 which removes the migration inhibitory effect of CXCL12, allowing T cell migration (Cruz-Orengo et al., 2011). In comparison to the endothelial basement membrane, glial limitans are enriched for laminin α1 and α2, which T cells have no ligands for (Sixt et al., 2001). Therefore, T cells are dependent on matrix metalloproteinases (MMPs) such as MMP-2 and MMP-9 to cleave β-dystroglycan anchoring astrocyte endfeet to the parenchymal basement membrane (Agrawal et al., 2006) and enhance T cell transmigration during EAE (Song et al., 2015).

Transmigration of lymphocytes is a multi-step process and involves multiple different cell types, which contributes to the complex regulation of the process. Therefore, further understanding of the process will be helpful to target each step more specifically.
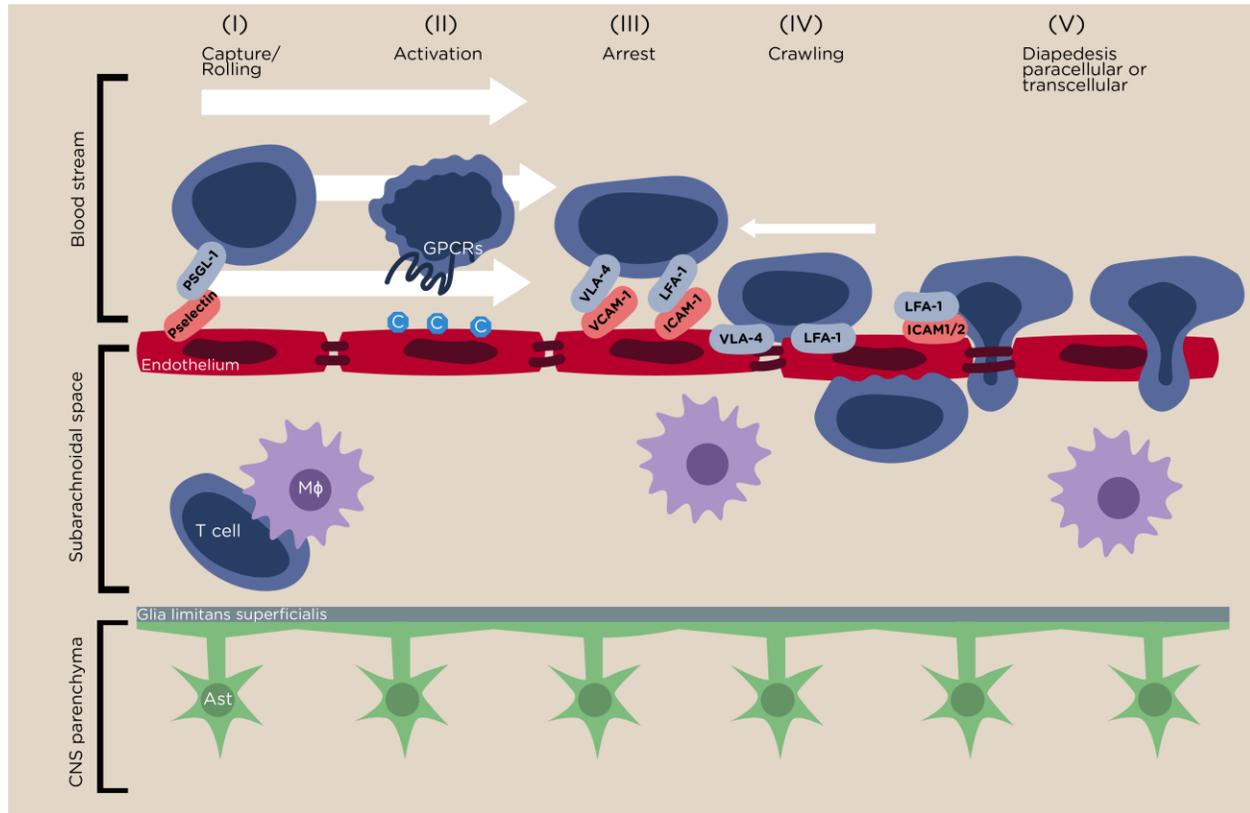
Figure 3 | Multi-step T cell transmigration across the BBB. During neuroinflammation T cells and endothelial cells express adhesion molecules to enhance the initial steps of T cell transmigration, capture and rolling (I). T cells then undergo chemokine(C)-induced integrin activation (II) mediated by GPCR signaling. The interactions between VLA-4 (α4β1) with VCAM-1 and LFA-1 (αLβ2) with ICAM-1 are required for T cell arrest on the endothelium (III). T cells can crawl on the luminal surface of endothelium against the direction of blood to search for a spot for diapedesis (V). After diapedesis, T cells interact with macrophages (Mφ) in the subarachnoidal space to enhance the inflammation. To enter CNS parenchyma, T cells finally need to across the glia limitans barrier, composed of astrocytic (Ast) end-feet and basal membrane of the parenchyma. Based on Figure 3 from (Engelhardt & Ransohoff, 2012).

1.4 Macrophage polarization in lesions

CNS homeostasis is maintained by the CNS parenchyma resident macrophages (microglia), derived from embryonic yolk sac progenitors during embryonic development. Microglia, therefore, enter the CNS before BBB formation. Microglia play an important role in the homeostatic function of the nervous system and provide immunosurveillance in the CNS

(Nimmerjahn, Kirchhoff, & Helmchen, 2005). Although CNS resident non-parenchymal macrophages such as perivascular, meningeal, and choroid plexus macrophages are also derived from the same embryonic progenitor populations, choroid plexus macrophages can be replaced by blood-borne monocytes (Goldmann et al., 2016). On the other hand, macrophages that are massively recruited during EAE or MS are mostly derived from peripheral monocytes which are not present in the CNS in healthy conditions (Henderson, Barnett, Parratt, & Prineas, 2009) (Ajami, Bennett, Krieger, McNagny, & Rossi, 2011). A recent study has also shown that the bone marrow of the skull and vertebrae can supply monocytes/macrophages to the meninges during CNS neuroinflammation through specialized channels between the skull and dura. These bone marrow-recruited monocyte/macrophages display different transcriptional profiles compared to their blood-derived counterparts (Cugurra et al., 2021)

As one of the major cell types of inflammatory lesions in MS and in EAE, macrophages gained attention after it was shown that disease severity during EAE correlates with the number of infiltrating monocyte/macrophages, regardless of the specificity and number of T cells (Berger et al., 1997) (McQualter et al., 2001) (Brück et al., 1996). Activated macrophages can secrete several soluble factors associated with tissue damage such as NO, ROS, MMPs, proteases, and excitotoxins (Redford et al., 1997). On the other hand, macrophages can also contribute to the lesion resolution by their tissue repair functions and secretion of neuroprotective factors (Hohlfeld, Kerschensteiner, Stadelmann, Lassmann, & Wekerle, 2000). The high degree of the functional plasticity of macrophages, mostly regulated by secreted chemokines and cytokines by other cell types in the lesion area, allows them to have a dynamic spectrum of activation and to play a dual role in MS. Macrophages responsible for tissue damage or tissue repair are defined as two ends of the spectrum, pro-inflammatory (M1-like) and anti-inflammatory macrophages (M2-like), respectively (Murray et al., 2014).

One of the well-known chemoattractants of monocytes for their traffic to the site of inflammation is CCL2, which mediates its function by binding to the CCR2 receptor on monocytes. CCR2 is highly expressed on Ly6C+ blood monocytes that are ready to migrate and CCR2 deficient mice have higher numbers of monocytes in bone marrow due to a lack of egress (C.-L. Tsou et al., 2007). The absence of CCR2 or blockage of the ligand CCL2 also prevents EAE and CNS histopathology by

preventing infiltration of monocytes to CNS (Fife, Huffnagle, Kuziel, & Karpus, 2000) (Huang, Wang, Kivisakk, Rollins, & Ransohoff, 2001). GM-CSF, a pro-inflammatory cytokine expressed by Th subsets, has been shown to regulate the pathological signature of CCR2+ monocytes during EAE (Croxford et al., 2015). A recent study with single-cell RNA sequencing of blood monocytes during EAE identified Cxcl10+ and Saa3+ monocytes, which are derived from early myeloid progenitors but not from Ly6C+ monocytes, as a pathogenic subtype of blood monocytes (Giladi et al., 2020).

Upon entry of monocytes to the CNS, they become activated and differentiate into myeloid-derived dendritic cells or macrophages with heterogeneous functions dictated by the chemokines and cytokines in the tissue microenvironment (Mantovani et al., 2004). T cells can produce pro-inflammatory cytokines such as IFN-γ, TNF-α, GM-CSF, IL-6 in EAE lesions, which can direct the spectrum of macrophage polarization towards a pro-inflammatory (M1-like) phenotype characterized by the expression of iNOS, MHCII, IL-12p40, IL6, IL1-α/β, IL23, CXCL9/10 (King, Dickendesher, & Segal, 2009). The inflammatory cytokines secreted by M1-like macrophages as well as NO and ROS fuel the inflammation and eventually cause tissue damage and axonal loss (Nikić et al., 2011). Axonal loss is also likely related to the activity of pro-inflammatory in MS lesions (Josa M. Frischer et al., 2009) with high expression of iNOS (Bö et al., 1994) co-localizing with CD64+ macrophages and with markers of myelin damage such as nitrotyrosine and MBP fragments (Hill, Zollinger, Watt, Carlson, & Rose, 2004). While pro-inflammatory macrophages are associated with tissue damage, macrophages can also play a role in tissue repair as well, putting them on the other side of the spectrum of polarization with an anti-inflammatory (M2-like) phenotype. M2-like macrophages are associated with the resolution of inflammation, tissue remodeling, promotion of angiogenesis, and pathogen clearing (Martinez & Gordon, 2014). A gradual shift from the M1-like phenotype, which predominates during the early stages of disease, to the M2-like phenotype, which predominates throughout the remission phase, has been observed in EAE by tracing iNOS and Arg1, canonical markers of M1 and M2 like phenotypes, in macrophages (Locatelli et al., 2018). Similarly, M2-like CD206+ macrophages have been found in inactive lesions, whereas high iNOS expression has been found in active lesions of EAE (Giles et al., 2018). A dual phenotype of macrophages has been also observed in MS lesions (Vogel et al., 2013). Based on *in vitro* studies, classical M2-like phenotype inducing cytokines are IL-4, IL-13, IL-

10, and TGF-β. Unlike M1-like phenotype-inducing cytokines, the source of M2-like phenotype inducing cytokines is less clear during neuroinflammation. Different combinations of cytokines can induce differential transcriptional profiles, resulting in various subtypes of M2-like phenotypes. IL-10 has been shown to be upregulated in the remission phase of EAE, which is associated with the inhibition of the pro-inflammatory microenvironment (Kennedy, Torrance, Picha, & Mohler, 1992). IL-4 mediated Arg1 induction is also known to suppress iNOS activity as the two enzymes compete for the same substrate L-arginine. Adoptive transfer of *in vitro* M2-like polarized macrophages has been found to be beneficial for EAE, although it has been suggested that this beneficial effect might be mediated peripherally rather than centrally (Mikita et al., 2011). M2-like macrophages can also promote remyelination by enhancing oligodendrocyte differentiation through TGF-β family molecule Activin-A (Miron et al., 2013). Increased TGF-β levels have been observed in the CSF of patients in remission compared to patients in relapse (Carrieri et al., 1997). Although a main therapeutic target of existing DMTs for MS is the lymphocyte population of T and B cells, several studies have shown that DMTs can also enhance an M2-like phenotype on monocyte/macrophages (B. S. Liu, Janssen, & Boonstra, 2012) (H. J. Kim et al., 2004). Modulating macrophage polarization toward the M2-like tissue repair phenotype may hold therapeutic promise. However, a better understanding of the cytokines involved in the lesion microenvironment at various stages of disease is required (**Figure 4**).
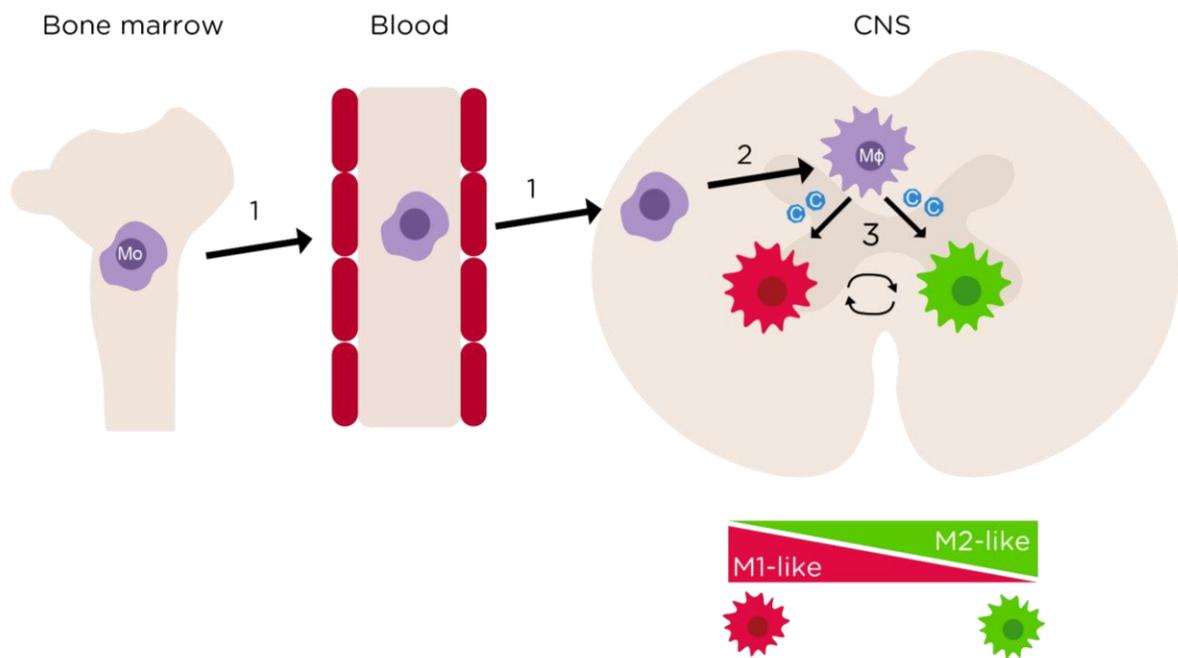
Figure 4 | Involvement of monocytes/macrophages in EAE. During neuroinflammation, monocytes (Mo) from the bone marrow and blood start to infiltrate inflammation sites in the CNS in response to the Ccr2 ligand (1). Monocytes become activated and develop into macrophages (Mφ) upon entering the CNS (2). Macrophages adopt pro- (M1-like) and anti- (M2-like) inflammatory functional phenotypes in response to cytokines (C) in the tissue microenvironment. A phenotypic transition can occur depending on external and internal factors (3).

1.5 CRISPR and *in vivo* screens

The study of gene function often relies on activation or inactivation of genes through the engineering of biological systems and correlating the observed phenotypes to these induced alterations. In this effort, several reverse-genetics tools have been developed in the last decades. For example, the discovery of RNA interference (RNAi) and its applications in different organisms made it possible to study functionality by silencing the expression of the genes (Fire et al., 1998) (Elbashir et al., 2001). Although the method's ease of use makes it a highly valuable and practical tool, it does have some drawbacks, including the inability to induce a complete loss of function phenotype (Housden et al., 2017). To overcome the partial suppression of gene function in the RNAi approach, genome-modification tools have been established and they mostly utilized the DNA nucleases to bring the targeted alterations. Zinc-finger nucleases (ZFNs), transcription

activator-like effector nucleases (TALENs), CRISPR-associated protein 9 (Cas9) nuclease constituted the most common DNA endonucleases employed in genome engineering (Gaj, Gersbach, & Barbas, 2013). These programmable, site-specific nucleases can generate a complete loss of function as they direct the disruption of genes by introducing double-stranded DNA breaks on the targeted regions (Zhang, Zhang, & Yin, 2019). The double-stranded DNA breaks primarily induce the error-prone DNA repair-machinery; non-homologous end joining (NHEJ), which leads to small insertions or deletions (InDels) at the nuclease cleavage site and perturb the locus. Although ZFNs and TALENs require de novo engineering of the nuclease proteins for each target gene, Cas9 does not require this as it can act in a sequence-independent manner and just requires a directory signal from a target-specific guide-RNA (gRNA) sequence which is designed for the gene of interest (Boettcher & McManus, 2015). The CRISPR (clustered regularly interspaced short palindromic repeat)/Cas9 system, discovered as a bacterial immune defense system, has been adapted and used as a versatile and powerful genome-editing tool in a variety of organisms. In this technology, target specific gRNA sequences together with the protospacer adjacent motif (PAM) on the DNA, an NGG/NAG motif adjacent to the recognition sequence enable the pairing of the RNA-DNA on the target site for further Cas9 nuclease functioning and gene disruption (Anders, Niewoehner, Duerst, & Jinek, 2014). Easy design and modular use of the gRNAs allowed CRISPR/Cas9 technology to be the most widely used and powerful genome-editing tool in mammalian cells as well (Adli, 2018). Importantly, further modifications to the Cas9 enzyme also allowed the engineering tools to expand. For example, the generation of an enzymatically inactive Cas9 in combination with transcription repressors or activators made it possible to inhibit (CRISPRi) or activate (CRISPRa) genes without disturbing the locus (Horlbeck et al., 2016) (Bester et al., 2018) (Kampmann, 2018). Similarly, by inactivating the single nuclease domain of Cas9 with a point mutation (Cas9 D10A on the RuvC domain or Cas9 H840A on the HNH domain), a Cas9 nickase, which is capable of cleaving only one strand of DNA, was generated. The use of a Cas9 dual nickase enabled researchers to target a single gene with two independent sgRNAs located on the opposite strands of DNA, which was reported to lower the probability of off-target editing (Cong et al., 2013). Fusing Cas9 nickase with cytidine or adenosine deaminase has allowed base editing on DNA by creating C to T (or G to A) and A to G (or T to C) change, respectively (Komor, Kim, Packer, Zuris, & Liu, 2016) (Gaudelli et al., 2017), whereas fusing Cas9

nickase with reverse transcriptase made it possible to make precise gene editing on the target genes without induction of double strand breaks (Anzalone et al., 2019). Base and prime editing technologies offer a potential therapeutic window especially for diseases caused by single nucleotide polymorphism. Very recently, three ancestor proteins of Cas nucleases, namely IscB, IsrB, and TnpB, have been discovered and engineered to create new genome editing tools (Altae-Tran et al., 2021). Other Cas protein endonucleases have also been identified, broadening the genome editing applications. For instance, Cas12 (Cpf1) recognizes T-rich PAM sequences, offering access to previously unreachable PAM regions with NGG (of Cas9) (Zetsche et al., 2015). Cas12 has been further modified to diversify PAM recognition (Kleinstiver et al., 2019). The Cas13 enzyme, on the other hand, targets RNA instead of DNA as an RNA editing tool (Abudayyeh et al., 2016). CRISPR also allows genomic knock-ins via the HDR pathway when an exogenous DNA template is supplied with homology arms. CRISPR knock-ins have revolutionized the field of transgenic mice as it has become easier to generate mice carrying reporter and conditional alleles (Yang et al., 2013). Viral delivery systems like Lenti-, Retro-, and Adeno-associated-viruses (AAV) and non-viral delivery systems like nucleofection (electroporation)made it possible to deliver Cas9 protein and gRNAs to a variety of cells *in vitro* and *in vivo*, allowing genetic manipulations (L. Li, Hu, & Chen, 2018).

To systematically target multiple genes, genome-wide gRNA libraries have been developed (**Figure 5**). gRNA libraries allowed researchers to identify essential regulators of various cellular processes (T. Wang et al., 2017) (Parnas et al., 2015). Since genome-wide gRNA libraries require a higher number of cells to keep the gRNA distribution homogeneous, CRISPR screens were mostly performed *in vitro* (Shalem, Sanjana, & Zhang, 2015). However, *in vitro* screens fail to fully recapitulate *in vivo* physiological environments, whereas *in vivo* screens can offer an understanding of the biological processes of cells in their natural niche by considering the impact of complex cell interactions, the immune response, tissue architecture, and the endocrine system (Kuhn, Santinha, & Platt, 2021). For example, an *in vivo* screen performed to identify cancer-driving genes in glioblastoma identified hits that were not picked by *in vitro* screens performed in parallel (Miller et al., 2017). *In vivo* CRISPR screens are still challenging due to the need for large numbers of cells and efficient delivery methods. Current techniques, such as generating transgenic lines for each perturbation, are slow, costly, and laborious, thus optimizing *in vivo*

CRISPR screens to overcome those limitations is critical to speeding up functional genetic studies. So far, CRISPR *in vivo* screens were successfully applied in several studies to identify essential genes involved in various biological process (Manguso et al., 2017) (LaFleur et al., 2019) (Weber, Braun, Saur, & Rad, 2020) (Bradley, 2019). Therefore, establishing methods to move from *in vitro* to *in vivo* screens will be a key factor in deciphering the functions of genes in health and disease, potentially aiding the design of better therapeutic approaches (Kuhn et al., 2021).
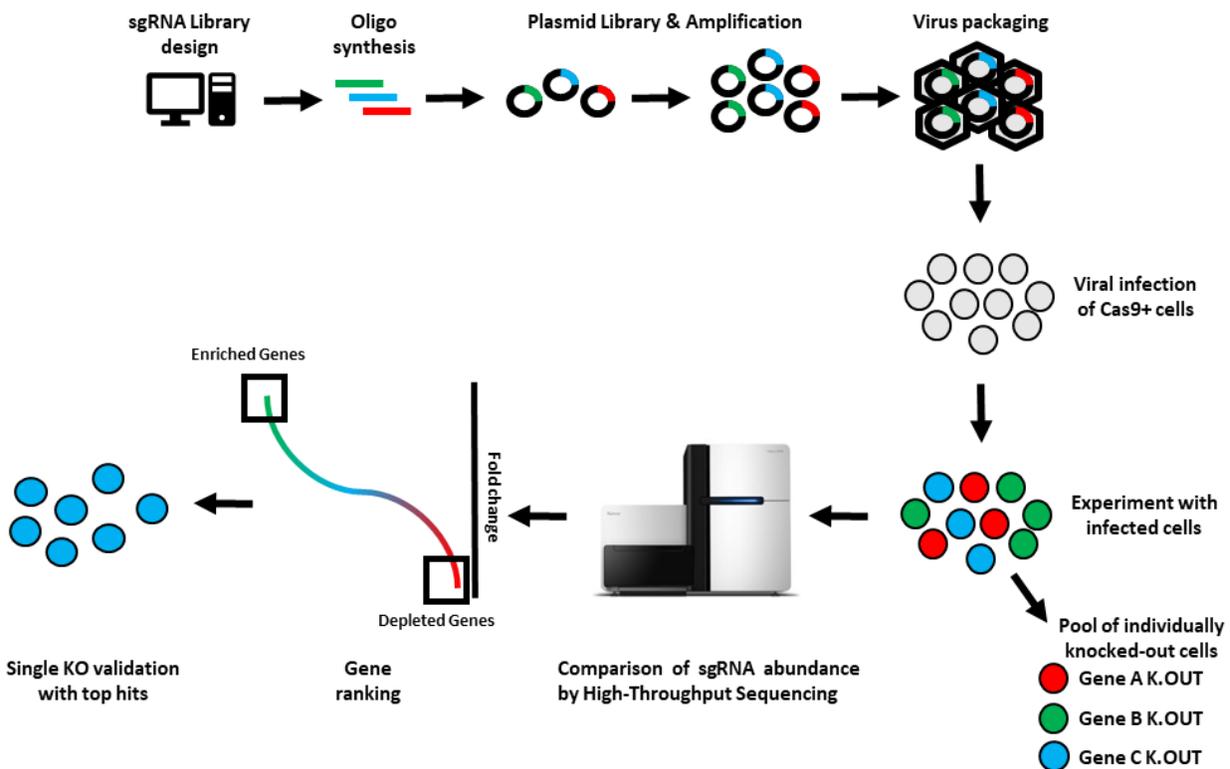
Figure 5 | Framework of a CRISPR/Cas9 based knock-out screen. Commercially synthesized oligos are amplified by PCR and cloned into viral plasmids. A pool of sgRNA constructs is packaged into viral particles to transduce target cells to produce a pool of individually knocked-out cells. sgRNA counts in a population are identified by using high-throughput next-generation sequencing (NGS) and ranked for enrichment or depletion phenotype. Top hits are picked for further confirmation of the phenotype.

1.6 Aim of the study

The BBB tightly regulates the trafficking of immune cells in order to protect neurons in the CNS from potential immune-mediated damage. However, during neuroinflammatory conditions such as MS, antigen-specific T cells transmigrate from the periphery to the CNS, where they get re-activated and secrete signals to recruit and activate monocytes/macrophages to initiate the lesion formation.

CRISPR is a powerful gene-editing tool, and CRISPR screens enable researchers to identify the key regulators of a specific phenotype on a large scale. So far, the majority of CRISPR screen studies have been conducted *in vitro*. Moving from *in vitro* to *in vivo* CRISPR screens, on the other hand, has become essential as *in vitro* conditions fail to mimic complex *in vivo* environments (Kuhn et al., 2021). In this project, I aimed to establish CRISPR *in vivo* screens to understand T cell transmigration and macrophage polarization in disease pathogenesis.

A) T cell transmigration is a multi-step process involving interactions with multiple cell types on the barrier. A better understanding of the molecular mechanisms of T cell transmigration can offer new therapeutic targets in MS. Most commonly, in T cell trafficking studies, *in vitro* BBB models are used, however these models cannot fully mimic the physiological conditions of the BBB during the disease. Therefore, in my thesis I aimed the followings:

- Establishing CRISPR-Cas9 mediated gene editing in rat T_{MBP} cells *in vitro*
- Conducting an *in vivo* genome-wide CRISPR KO screen in T_{MBP} cells to identify essential regulators of T cell transmigration in Lewis rats with an adoptive-transfer EAE model
- Validating the candidates identified by the CRISPR screen by *in vivo* single KO experiments
- Characterizing the mechanisms of the selected candidates by RNA sequencing and two-photon imaging

B) During EAE, the number of infiltrating monocytes/macrophages correlates with the disease severity. Macrophages exhibit high functional plasticity, contributing to both lesion formation and resolution. Chemokines, cytokines, and tissue-specific signals secreted by other cell types in the lesion area govern the macrophage phenotypes. Studying the molecular mechanism of macrophage phenotype switch can enable us to manipulate them towards a lesion recovery

phenotype. The most difficult aspect of studying macrophage phenotypes is to introduce the genetic perturbations, as creating compound mutant transgenic mouse models for each perturbation is a time-consuming, expensive, and labor-intensive process. Therefore, in my thesis I aimed the followings:

- Establishing a novel *in vivo* model system that allows studying monocytes/macrophages in an active EAE mouse model by using conditionally immortalized Hoxb8 cells
- Conducting an *in vivo* CRISPR screen in monocytes/macrophages to identify essential regulators of macrophage phenotypes in the inflamed spinal cord of EAE induced mice
- Validating the candidates identified by the CRISPR screen by in vivo single KO experiments
- Characterizing the mechanisms of the selected candidates in BMDMs *in vitro*

Overall, the discovery of essential regulators *in vivo* that may play a role in disease initiation and progression has the potential to open up new therapeutic avenues for MS.

2. MATERIALS & METHODS

2.1 Materials

2.1.1 Equipment

Product	Description	Distributor
Agilent 2100 Bioanalyser	Bioanalyser	Agilent
CFX Connect Real-Time PCR	Quantitave PCR	BioRad
FACS Aria III	Cell Sorter	Becton Dickinson
FACS Fusion	Cell Sorter	Becton Dickinson
Nanodrop 2000C/2000	Spectrophotometer	Thermo Fisher
Amaxa 4D-Nucleofector System	Electroporator	Lonza
FlowJo Dongle	Flow Cytometry	Becton Dickinson
Odyssey® Fc	Imaging system	LI-COR Biosciences
Qubit 4	Fluorometer	Thermo Fisher

2.1.2 Consumables

Material	Provider	Cat. Number
1 mL Tissue Grinder, Dounce	Wheaton	357538
100mm Tissue Culture-Treated Culture Dish	Sigma	CLS430167
2-Mercaptoethanol (50 mM)	Thermo Fisher Scientific	31350010
Accutase® solution	Sigma	A6964-500ML
ACK Lysing Buffer	Thermo Fisher Scientific	A10492-01
Agarose	Sigma	A9539
Agilent DNA 1000 Kit	Agilent Technologies	5067-1504
Alt-R® Cas9 Electroporation Enhancer	IDT	1075916
Alt-R® CRISPR-Cas9 crRNA	IDT	custom
Alt-R® CRISPR-Cas9 tracrRNA	IDT	1072534
Alt-R® S.p. HiFi Cas9 Nuclease V3	IDT	1081060
BD Cytofix/Cytoperm	BD Biosciences	554714
beta-Estradiol	Sigma	E2758-250MG
Carbenicillin Disodium Salt BioChemica	Panreac AppliChem	A1491,0001
Cd11b (Microglia) MicroBeads	Miltenyi Biotec	130-093-636
Cell strainer 100 um	BD Falcon	352360
Collagenase D	Roche	11088866001
Collibri™ 3´ mRNA Library Prep Kit for Illumina	Thermo Fisher Scientific	A38110024

Deoxynucleotide Solution Mix	NEB	N0447S
DMEM, low glucose, GlutaMAX	Thermo Fisher Scientific	21885108
DMSO	Sigma	D8418-100ML
DNase I grade II, from bovine pancreas	Roche	10104159001
DNeasy Blood and Tissue Kit	Qiagen	69504
Dulbecco's Phosphate Buffered Saline	Sigma	D8537-24X500ML
Endofree Plasmid Maxi Kit	Qiagen	12362
FastAP Alkaline Phosphatase (1 U/µL)	Fermentas	EF0654
FastDigest Bpil	Thermo Fisher Scientific	FD014
FastDigest EcoRI	Thermo Fisher Scientific	FD0274
FastDigest XhoI	Thermo Fisher Scientific	FD0694
FBS SUPERIOR stabil®	Bio&SELL	FBS. S 0615
Freund's Adjuvant, Incomplete	Sigma	F5506-10X10ML
G418 (Geneticin)	Invitrogen	ant-gn-1
Gibson Assembly® Master Mix	NEB	E2611S
IDTE (1X TE Solution)	IDT	11-01-02-02
Invitrogen qubit Assay Tubes	Thermo Fisher Scientific	Q32856
LS Columns	Miltenyi Biotec	130-042-401
M. Tuberculosis H37 Ra	BD Difco	231141
Millex-HV Filter, 0,45 µm	Merck	SLHV033RS
MOG1-155	in house	
Molecular BioProducts™ RNase™ AWAY	Thermo Fisher Scientific	10666421
Molecular Probes Quant iT RNA HS Assay Kit	Thermo Fisher Scientific	Q32852
NEB Stable Competent cells	NEB	C3040I
Nuclease-Free Water	Qiagen	129114
Nucleotide Removal Kit	Qiagen	28304
oPools™ Oligo Pools	IDT	
P4 Primary Cell 4D-Nucleofector® X Kit S	Lonza	V4XP-4032
Penicillin Streptomycin (10,000 U/mL)	Thermo Fisher Scientific	15140122
Percoll	Sigma	P1644-500ML
Pertussis toxin from Bordetella pertussis	Sigma	P7208
Primocin, 500 mg (10 x 1 ml tubes)	Invivogen	ant-pm-1
Puromycin Dihydrochloride	Thermo Fisher Scientific	A1113803
Q5 High-Fidelity DNA Polymerase	NEB	M0491L
QIAamp DNA Micro Kit	Qiagen	56304
QIAprep Spin Miniprep Kit	Qiagen	27106
QIAquick Gel Extraction Kit	Qiagen	28706
QIAquick PCR Purification Kit	Qiagen	28104
Quick Ligation Kit	NEB	M2200L
QuickExtract™ DNA Extraction Solution 1.0	biozym	101098 (QE0905T
Recombinant Murine GM-CSF	PeproTech	315-03

Recombinant Murine M-CSF	PeproTech	315-02-50ug
Recombinant Murine TNF-α	PeproTech	315-01A
Recombinant mouse TGF-β1	BioLegend	763102
Restriction Enzymes	NEB	
Retronectin	Takara	T100A
RevertAid H Minus First Strand cDNA synthesis kit	Thermo Fisher Scientific	K1632
Rnasin Plus RNase Inhibitor	Promega	N2615
RNeasy Plus Micro Kit	Qiagen	74034
RNeasy Plus Mini Kit	Qiagen	74134
RPMI-1640	Sigma	R0883
SPRIselect Reagent	Beckman Coulter	B23317-5mL
SsoAdvanced™ Universal SYBR® Green Supermix	BioRad	1725272
Stellar™ Competent Cells	Clontech	636763
T4 DNA Ligase	NEB	M0202T
T4 DNA Ligase Reaction Buffer	NEB	B0202S
T4 Polynucleotide Kinase	NEB	M0201S
TransIT-LT1 Transfection Reagent	MoBiTec	MIR2305
Trypsin-EDTA (0.25%), phenol red	Thermo Fisher Scientific	25200056
Ultracomp eBeads™ Compensation Beads	Thermo Fisher Scientific	01-2222-42
PhosSTOP™	Sigma-Aldrich	000000004906845001
cOmplete™ ULTRA Tablets	Sigma-Aldrich	000000005892791001
Tris Glycine Transfer Buffer (25X)	Thermo Fisher Scientific	LC3675
Tris-Glycine SDS Running Buffer (10X)	Thermo Fisher Scientific	LC2675
WedgeWell™ 4 to 12%, Tris-Glycine, Protein Gel	Thermo Fisher Scientific	XP04120BOX
Pierce™ RIPA Buffer	Thermo Fisher Scientific	89900
NuPAGE Sample Reducing Agent (10X)	Thermo Fisher Scientific	NP0009
Tris-Glycine SDS Sample Buffer (2X)	Thermo Fisher Scientific	LC2676
Bovine Serum Albumin	Sigma-Aldrich	A9647-50G

2.1.3 Antibodies

Antigen	Fluorophore	Provider	Clone	Cat. Number	Dilution
Arg1	PE	Invitrogen	A1exF5	12-3697-80	1:100
Arg1	APC	Invitrogen	A1exF5	17-3697-82	1:100
CD11b	PerCP	BioLegend	M1/70	101230	1:100
CD11b	APC	BioLegend	M1/70		1:100
CD11c	e450	Invitrogen	N418	48-0114-80	1:100
CD11c	PE-Cy7	BioLegend	N418		1:100
CD45	BV785	BioLegend	38-F11	103149	1:100
F4/80	PE	BioLegend	BM8	123109	1:100

iNOS	e450	eBioscience	CXNFT	48-5920-80	1:100
iNOS	APC	eBioscience	CXNFT	17-5920-80	1:100
iNOS	PerCP-eFluor 710	eBioscience	CXNFT	46-5920-80	1:100
iNOS	PE-Cy7	eBioscience	CXNFT	46-5920-80	1:100
Iso control	APC	eBioscience	eBR2a	17-4321-81	1:100
Ly6C	e450	Invitrogen	HK1.4	48-5932-80	1:100
Ly6G	BV785	BioLegend	1A8	127645	1:100
Ly6G	APC	BioLegend	1A8	127613	1:100
Ly6G	PE-Cy7	BioLegend	1A8		1:100
MHC II	e450	Invitrogen	M5/114.15.2	48-5321-80	1:100
MHC II	APC	Biolegend	M5/114.15.2		1:100
NK1.1	APC	BioLegend	PK136		1:100
Siglec F CD170	PE	Invitrogen	1RNM44N	12-1702-80	1:100
TruStain Fc Block CD16/32		BioLegend	93	101320	1:50
LIVE/DEAD™ Fixable Near-IR	Near-IR	Invitrogen		L10119	1:1000
ETS-1 Rabbit mAb		CST	D8O8A	14069S	1:1000
β-Actin Antibody (C4) HRP		Santa Cruz		sc-47778 HRP	1:250000
mouse anti-rabbit IgG-HRP		Santa Cruz		sc-2357	1:10000

2.1.4 Cells & Plasmids

Material	Provider	Cat. Number
HEK293T cells	ATCC	crl-3216
Flt3L-producing B16 melanoma cell line	provided by Seren Baygün	
LentiCas9-EGFP vector	Addgene	63592
MSCV-pU6-(BbsI)-CcdB-(BbsI)-Pgk-Puro-T2A-BFP	Addgene	86457
pKLV2-U6gRNA5(BbsI)-PGKpuro2ABFP-W	Addgene	67974
MSCV-Cas9-EGFP-Neo	in house cloning	
MSCV-pklv2-U6-(BbsI)-Pgk-Puro-T2A-GFP	in house cloning	
pMSCV-pklv2-U6-(sgNon-Targeting)-Pgk-Puro-T2A-tdtomato	in house cloning	
pMSCV-pklv2-U6-(BbsI)-Pgk-Puro-T2A-BFP	in house cloning	
psPAX2	Addgene	12260
pMD2.G	Addgene	12259
pCL-Eco	Provided by PD. Dr. Naoto Kawakami	
pMSCV-neo	Provided by PD. Dr. Naoto Kawakami	

2.1.5 Oligos

Library preparation primers	
Oligo_Amp_F	GCAGATGGCTCTTTGTCCTA
Oligo_Amp_R	GGCGACGAGAAGACTAAAAC
Fwd-Lib	AATGATACGGCGACCACCGAGATCTACACTCTTTCCCTACACGACGCTCTTCCGATCT
Rev-Lib	CAAGCAGAAGACGGCATACGAGAT**NNNNNNNN**GTGACTGGAGTTCAGACGTGTGCTCTTCCGATCT
	NNNNNNNN: Barcode
Fwd-Lib-1	AATGATACGGCGACCACCGAGATCTACACTCTTTCCCTACACGACGCTCTTCCGATCTTTGTGGAAAGGACGAAACACCG
Fwd-Lib-2	AATGATACGGCGACCACCGAGATCTACACTCTTTCCCTACACGACGCTCTTCCGATCT**C**TTGTGGAAAGGACGAAACACCG
Fwd-Lib-3	AATGATACGGCGACCACCGAGATCTACACTCTTTCCCTACACGACGCTCTTCCGATCT**GC**TTGTGGAAAGGACGAAACACCG
Fwd-Lib-4	AATGATACGGCGACCACCGAGATCTACACTCTTTCCCTACACGACGCTCTTCCGATCT**AGC**TTGTGGAAAGGACGAAACACCG
Fwd-Lib-5	AATGATACGGCGACCACCGAGATCTACACTCTTTCCCTACACGACGCTCTTCCGATCT**CAAC**TTGTGGAAAGGACGAAACACCG
Fwd-Lib-6	AATGATACGGCGACCACCGAGATCTACACTCTTTCCCTACACGACGCTCTTCCGATCT**TGCACC**TTGTGGAAAGGACGAAACACCG
Fwd-Lib-7	AATGATACGGCGACCACCGAGATCTACACTCTTTCCCTACACGACGCTCTTCCGATCT**ACGCAAC**TTGTGGAAAGGACGAAACACCG
Fwd-Lib-8	AATGATACGGCGACCACCGAGATCTACACTCTTTCCCTACACGACGCTCTTCCGATCT**GAAGACCC**TTGTGGAAAGGACGAAACACCG
Rev-Lib-1	CAAGCAGAAGACGGCATACGAGAT**TCGCCTTG**GTGACTGGAGTTCAGACGTGTGCTCTTCCGATCTCGACTCGGTGCCACTTTTTCAA
Rev-Lib-2	CAAGCAGAAGACGGCATACGAGAT**ATAGCGTC**GTGACTGGAGTTCAGACGTGTGCTCTTCCGATCTCGACTCGGTGCCACTTTTTCAA
Rev-Lib-3	CAAGCAGAAGACGGCATACGAGAT**GAAGAAGT**GTGACTGGAGTTCAGACGTGTGCTCTTCCGATCTCGACTCGGTGCCACTTTTTCAA
Rev-Lib-4	CAAGCAGAAGACGGCATACGAGAT**ATTCTAGG**GTGACTGGAGTTCAGACGTGTGCTCTTCCGATCTCGACTCGGTGCCACTTTTTCAA
Rev-Lib-5	CAAGCAGAAGACGGCATACGAGAT**CGTTACCA**GTGACTGGAGTTCAGACGTGTGCTCTTCCGATCTCGACTCGGTGCCACTTTTTCAA
Rev-Lib-6	CAAGCAGAAGACGGCATACGAGAT**GTCTGATG**GTGACTGGAGTTCAGACGTGTGCTCTTCCGATCTCGACTCGGTGCCACTTTTTCAA
Rev-Lib-7	CAAGCAGAAGACGGCATACGAGAT**TTACGCAC**GTGACTGGAGTTCAGACGTGTGCTCTTCCGATCTCGACTCGGTGCCACTTTTTCAA
Rev-Lib-8	CAAGCAGAAGACGGCATACGAGAT**TTGAATAG**GTGACTGGAGTTCAGACGTGTGCTCTTCCGATCTCGACTCGGTGCCACTTTTTCAA
Rev-Lib-9	CAAGCAGAAGACGGCATACGAGAT**CGGTTCAA**GTGACTGGAGTTCAGACGTGTGCTCTTCCGATCTCGACTCGGTGCCACTTTTTCAA
Rev-Lib-10	CAAGCAGAAGACGGCATACGAGAT**GCTGGATT**GTGACTGGAGTTCAGACGTGTGCTCTTCCGATCTCGACTCGGTGCCACTTTTTCAA

qPCR	Forward primer sequence (5'-3')	Reverse primer sequence (5'-3')
Cas9	AAACAGCAGATTCGCCTGGA	CATCCGCTCGATGAAGCTCT
Gapdh	CAAGGTCATCCATGACAACTTTG	GTCCACCACCCTGTTGCTGTAG
Actb	ATTGCCGACAGGATGCAGAA	GCTGATCCACATCTGCTGGAA
Ets1	CAGATGTCCCACTGTTAACTCC	CAGTCGCTGCTGCTCTTT
Itga4	TCAAGCAGTGGAGAGAAATGTAG	ATGATGCCCAAGGTGGTATG

Cxcr3	CTTTCGAGCTATGAGGCTAGTG	ACTCCCACGTCCATAAGGATA
Prf1	CATCACATCTACGGATGCTTATCT	CTCCACGAGGGATGGTTATTG
Ccr6	GCCAATCGCCTACTCCTTAAT	ATGGACCTGGCTTTCTTGTAG
Il17a	AAACGCCGAGGCCAATAA	GAAGTGGAACGGTTGAGGTAG
Tnfrsf9	TCCAGAGAGAGAATCAGGAGAG	GCACAGAGAACCAGAGAATGA
Nkg7	CTGAGCACTGACTTCTGGATAG	GACCTGTGTCACGTGGATATAA

Target	gRNA
Non-Targeting	GCTGCATGGGGCGCGAATCA
Cd4	CATCACGGCCTATAAGAGTG
Itga4	GATGCTGTTGCTGTACTTCG
Hsp90b1	GTCTCACGGGAAACATTGAG
Ccr2	ATCATCGTAGTCATACGGTG
Cxcr3	TCTGCGTGTACTGCAGCTAG
Gnai2	TGGGTGGTCAGCGATCTGAG
S1pr1	GCGGCTTCGAGTCCTCACCA
Arih1	GGAGGAAGATTACCGCTACG
Ube2l3	GCTTGAAGGGATACTCTGCT
Grk2	GATTTGTCAGAACCTCCGAG
Ets1	TGCTGCTCGGAGTTAACAGT
Tgfbr	AGAGCGTTCATGGTTCCGAG
Csf2ra	TTGGTCGTGACCGGTCGGAG
Il6ra	CTGTGCGTTGCAAACAGTGT
Ifngr1	TTCAGGGTGAAATACGAGGA
Tnfrsf1a	AGACCTAGCAAGATAACCAG
Il4ra	TGAGGCCCCAGTACAGAATG
Stat6	ATAAAGCGCTGTGAGCGGAA
Arg1	GTATGACGTGAGAGACCACG

2.2 Methods

2.2.1 Cell lines and primary cells

All cells except T_{MBP} cells were incubated in a humidified incubator at 37°C and 5% CO_2. All cell mediums were supplemented with 10% FBS and 1% Pen/Strep. HEK293T cells were kept in DMEM GlutaMAX, Bone marrow cells and Hoxb8 cells were kept in RPMI GlutaMAX. Hoxb8 cells were additionally supplemented with 0.1% 2-Mercaptoethanol, 1 µM β-estradiol, and supernatant from an Flt3L-producing B16 melanoma cell line with a final concentration of 35 ng/ml. Macrophage medium was additionally supplemented with M-CSF (10-20ng/ml).

T_{MBP} cells were incubated at 37°C with 10% CO_2. T_{MBP} cells were cultured in DMEM medium supplemented with 10% heat-inactivated horse serum and 2% supernatant from an IL-2 producing PMA stimulated EL4 cell line. Re-stimulation medium of T_{MBP} cells was supplemented with 1% rat serum, MBP peptide (10µg/ml) and thymocytes (50 Gy irradiated) isolated from the thymus. For freezing cells, 10% DMSO and 90% FBS mixture were used and cryovials were kept in a freezing box for several days at -80°C before transferring to liquid nitrogen. Cell lines were tested for the absence of mycoplasma. HEK239T cells were detached by using 0.05% Trypsin-EDTA. Macrophages were detached with Accutase solution.

2.2.2 Animals

R26-Cas9-eGFP animals were ordered from Jackson Lab (024858) and backcrossed to C57BL/6 background several times. All experimental procedures involving animals and their care were carried out in accordance with regulations of the relevant animal welfare acts and protocols approved by the respective regulatory office (Regierung von Oberbayern).

2.2.3 Generation of Cas9 expressing T_{MBP} cells

MBP-specific T cells were kindly generated by PD. Dr. Naoto Kawakami by immunizing Lewis rats with MBP as described previously (Ben-Nun et al., 1981). A Cas9-p2a-Egfp construct was PCR amplified from LentiCas9-EGFP vector (Addgene, 63592) by using primers Forward: 5'-cttctctaggcgccgggcgctgccaccatggacaaga-3',   Reverse: 5'-

tacccggtagaattagatctcattcttacttgtacagctcgtccat-3'. The PCR product was then Gibson assembled into EcorI + XhoI digested pMSCV-neo backbone plasmid. The retrovirus packaging cell line GP+E cells were transfected with pMSCV-Cas9-EGFP-neo by Trans-IT and co-cultured with T_{MBP} cells. Transduced cells were enriched in a medium with Neomycin (G418) (0.4mg/ml). After several rounds of expansion GFP+ cells were sorted with BD FACSAria IIIu.

2.2.4 Genome-wide rat gRNA library construction

A list of sgRNA designs for the Rat genome was kindly provided by the Functional Genomics Consortium of Broad Institute. For the genome-wide library 4 sgRNA/gene were picked. An oligo pool containing 87,690 oligos was purchased from Twist Bioscience. Each oligo is 79-mer in length and has a sequence of 5'-GCAGATGGCTCTTTGTCCTAGACATCGAAGACAACACCGN_{20}GTTTTAGTCTTCTCGTCGCC-3', where N_{20} indicates sgRNA sequences. Oligo pools were dissolved in Qiagen TE buffer at 10ng/ul stock concentration. The single-stranded oligos (1ng) were PCR amplified 10 cycles with Q5 High-Fidelity DNA Polymerase by using Oligo_Amp_F and Oligo_Amp_R primers. A total of 24 reactions were pooled. The PCR products were purified with the Nucleotide Removal Kit. Amplified double-stranded DNAs were digested with FastDigest BpiI for 2h at 37°C in a total of 20 reactions and then purified with the Nucleotide Removal Kit. Ligation was performed with a T4 DNA Ligase by using 3ng insert and 40ng BpiI-digested MSCV-pU6-(BbsI)-CcdB-(BbsI)-Pgk-Puro-T2A-BFP for 16h at 16°C per reaction in a total of 30 reactions. The ligated product was cleaned with a PCR Purification Kit and the concentration was measured with Qubit 4. 10ng of the ligated product was transformed into 50ul of NEB Stable Competent cells in a total of 45 reactions and incubated at 30°C overnight. >100x Library representation was confirmed by plating transformed competent cells in serial dilutions. The plasmid DNA was prepared with an Endofree Plasmid Maxi Kit.

For the validation library, 2 additional sgRNA were added per gene (6 sgRNA/gene) to increase the confidence of the hits. An oligo pool containing 12,000 oligos was purchased from Twist Bioscience and plasmid DNA was prepared as the genome-wide library.

2.2.5 Virus production and transduction of T$_{MBP}$ cells

$6x10^6$ HEK293T cells were seeded per 10cm dish 18-24h before transfection. The transfection mixture was prepared by adding 10ug of cargo plasmid and 10ug of packaging and envelope plasmid (pCL-Eco) in 2ml RPMI medium without serum or antibiotic. 60µl of the transfection reagent TransIT-LT1 were added into the mixture, vortexed, and left for 30 min incubation at room temperature (RT) before adding dropwise onto HEK cells. The supernatant of cells containing the virus was harvested 48-72h after transfection and used freshly for transduction. The day before transduction non-TC treated 12 well plates were coated with a final concentration of 10µg/ml Retronectin in PBS at 4°C. Before transduction, the retronectin was removed and the plates were blocked for 30min at RT with 2%BSA in PBS. Two days after re-stimulation of T$_{MBP}$ cells in culture, Nycoprep gradient was performed to remove thymocytes and dead cells. Live T$_{MBP}$ cells were then seeded into the retronectin-coated plates and spin-infected for 1h at 1200g at RT. The next day, Puromycin was added at a final concentration of 0.5µg/ml to select retrovirus infected cells. For the genome-wide retroviral library, 300M T$_{MBP}$ cells were transduced at a multiplicity of infection (MOI) of 0.4 or below (<30% Transduction efficiency) to prevent multiple integrations into one cell and to keep 1000x representation of each of the 87,690 gRNAs.

2.2.6 Adoptive transfer and isolation of T$_{MBP}$ cells

Ten million BFP+ T$_{MBP}$ cells per rat were transferred intravenously (i.v.). On day 3, animals with a mild clinical score or body weight loss were sacrificed to collect organs. EAE score was evaluated as followed: 0, no clinical signs; 0.5, partial tail weakness; 1, tail paralysis; 1.5, gait instability or impaired righting ability; 2, hind limb paresis; 2.5, hind limb paresis with dragging of one foot; 3, total hind limb paralysis. Organs from multiple animals were combined before the isolation of cells. Cells were isolated from the blood and the spleen as peripheral organs and from the meninges and the parenchyma as CNS organs. Single-cell suspensions for each organ were prepared by PD. Dr. Naoto Kawakami and Katrin Lämmle, GFP+BFP+ T$_{MBP}$ cells from the spleen for the genome-wide library were sorted to purity with BD FACSAria IIIu. For each replicate, a minimum of 9M cells was sorted to keep the coverage >100x. For the validation library, cells from all organs were sorted to purity.

2.2.7 Amplification and NGS sequencing of sgRNAs from genomic DNA

Genomic DNA (gDNA) from GFP+BFP+ T_{MBP} cells was isolated with the DNeasy Blood and Tissue Kit. An amplification PCR was performed with Q5 High Fidelity DNA Polymerase by using 2.5ug of gDNA per reaction with Fwd-Lib (mix of 8 staggered primers), Rev-Lib (consists of 8bp of unique barcode) primers for a total of 24 cycles. Illumina adapters were introduced together with the amplification primers. The PCR products were purified with SPRIselect with a ratio of 1:0.8 (DNA to beads) and eluted in nuclease-free water. 250bp Amplicons were confirmed with Agilent Bioanalyzer on DNA 1000 Chips and sent to The Laboratory for Functional Genome Analysis (LAFUGA) in the Gene Center Munich for sequencing single-end 50bp on a HiSeq 1500.

2.2.8 QPCR and 3` bulk mRNA sequencing

Total RNA from cells was isolated with either a RNeasy Plus Mini or a Micro (for less than 100k cells) kit. Total RNA from fixed cells was isolated with a modified protocol, cells were incubated with 100µl PBS, 100ul AL Lysis buffer and 15µl Proteinase K at 56°C for 1h for the de-crosslinking of fixed RNA. AL Lysis buffer and Proteinase K were used from DNeasy Blood and Tissue Kit. After the incubation, 300µl RLT Plus buffer and 270µl 96-100% Ethanol were added. Total RNA, then, was isolated according to the Rneasy Plus Mini or Micro kit. RNA concentrations were measured with Nanodrop or Qubit 4. RNA samples were stored at -80°C not longer than a week before preparation for mRNA sequencing. For QPCR, cDNA was synthesized using RevertAid H Minus First Strand cDNA synthesis kit with 100-500ng total RNA and Oligo (dt) primers. Quantitative PCR (qPCR) was carried out on Bio-Rad CFX Connect Real-Time PCR system using SsoAdvanced™ Universal SYBR® Green Supermix. All qPCR reactions were run in duplicate and the housekeeping genes GAPDH or β-Actin was used as an internal control to normalize the variability in expression level. Results were quantified using the $\Delta\Delta C_t$ method. For 3` bulk mRNA sequencing, total RNA samples were processed till submission for NGS by using the Collibri 3' mRNA Library Prep Kits for Illumina Systems. Amplification of transcripts was confirmed with Agilent Bioanalyzer on DNA 1000 Chips and sent to LAFUGA for sequencing single-end 50bp on a HiSeq 1500.

2.2.9 Western blotting

Cells were rinsed with cold PBS and lysed with 200µl RIPA buffer including protease and phosphatase inhibitor cocktail tablets. Protein concentration was determined using BCA protein assay kit. Lysates were mixed with Laemmeli buffer and reducing agent (1x) and boiled at 95°C for 5 min. 4-12% Tris-Glycine gels were used for protein separation. Primary antibodies were incubated o/n at 4°C in 5% BSA-TBST buffer. Secondary antibodies were incubated at RT for 2h. Blots were analyzed using enhanced chemiluminescence with HRP-conjugated anti-mouse and anti-rabbit secondary antibodies.

2.2.10 Molecular cloning

For single sgRNA CRISPR targeting, 20nt length sgRNAs were picked from GPP sgRNA designer tool from Broad Institute. sgRNA sequence and reverse complemented sequence were ordered as two separate oligos from Metabion with overhangs on the 5` side of CAAC for forward and AAAC for reverse. The nucleotide 'G' was added as a first nucleotide to increase the efficiency of the gRNA expression by hU6 promoter (Ran et al., 2013). Complementary oligos with overhangs were phosphorylated and annealed in the presence of 10X T4 Ligation Buffer and T4 PNK by increasing the temperature to 95°C and ramping down to 25°C at 5°C/min. Annealed oligos were ligated into Bpil- digested gRNA cargo plasmid by Quick Ligase for 6 min at RT. Ligated plasmids were then transformed into Stellar competent cells with heat shock at 42°C for 55sec. Bacteria plates were grown overnight (o/n), single clones were picked and prepped with the Qiagen plasmid miniprep kit. The correct ligation product was confirmed with Sanger sequencing using hU6 primer.

To generate MSCV-pU6-(BbsI)-Pgk-Puro-T2A-GFP, the pU6-Pgk-Puro-T2A construct was PCR amplified from pKLV2-U6gRNA5(BbsI)-PGKpuro2ABFP-W (Addgene), the EGFP construct was PCR amplified from pMSCV-Cas9-EGFP-neo (in house). The PCR products were then Gibson assembled into SalI + XhoI digested pMSCV-neo backbone plasmid. To generate MSCV-pU6-(sgNon-Targeting)-Pgk-Puro-T2A-tdtomato, the same pU6-Pgk-Puro-T2A construct and tdtomato construct, PCR amplified from AAV-CAG-CRE-p2a-tdtomato (in house), were Gibson assembled into SalI + XhoI digested pMSCV-neo. To generate MSCV-pU6-(BbsI)-Pgk-Puro-T2A-BFP, the pU6-

Pgk-Puro-T2A-BFP construct was PCR amplified with overhangs for SalI + XhoI from pKLV2-U6gRNA5(BbsI)-PGKpuro2ABFP-W (Addgene) digested and ligated into SalI + XhoI digested pMSCV-neo with Quick Ligase.

2.2.11 RNP delivery with nucleofection

Target specific sequences for Alt-R CRISPR-Cas9 crRNA were picked from GPP sgRNA designer tool and ordered from Integrated DNA Technologies (IDT) without overhangs and without additional G at the first base. For duplex formation, Alt-R CRISPR-Cas9 crRNA and tracRNA were suspended in IDTE buffer to a final concentration of 200µM and mixed in equimolar concentration. The mix was then heated to 95°C for 5min and allowed to cool at RT. For RNP complex formation, 1µl of duplex and 1µl of Alt-R HiFi Cas9 V3 (61µM stock) enzyme were mixed and incubated for 20min at RT. 2 or 3 days after re-stimulation, 5M T_{MBP} cells were washed twice with PBS and resuspended in nucleofection solution provided from the P4 Primary Cell 4D-Nucleofector X Kit. 2µl of RNP complex together with 1µl of 100uM Alt-R Cas9 Electroporation Enhancer were added to the mix and 25µl of cell:RNP complex mixture was transferred to the 16-well Nucleocuvette module. T_{MBP} cells were then electroporated with the program CM137 by using an Amaxa 4D-Nucleofector. Electroporated cells were immediately transferred to an incubator with the prewarmed medium. The nucleofection program for T_{MBP} cells was picked from literature (Seki & Rutz, 2018), and the high efficiency of RNP complex delivery with minimal cell death was confirmed by assessing KO efficiency of target genes with protein (flow cytometry) and DNA levels (TIDE assay). For Cas9 expressing T_{MBP} cells, the crRNA:tracRNA duplex was delivered alone without RNP formation with Cas9.

2.2.12 Tide assay

For gene editing assessment at a DNA level for single gRNAs, gDNA was isolated by using DNeasy Blood & Tissue Kit or QuickExtract™ DNA Extraction Solution. PCR amplification was performed with specific primers for each target by using Q5 High-Fidelity DNA Polymerase. PCR mixtures were run on a 0.8-1% Agarose gel and amplicons at the expected size were purified with QIAquick Gel Extraction Kit. Samples were submitted for Sanger sequencing. INDELs and KO efficiency were assessed by using two different web-based tools, TIDE software tool (Tracking of Indels by

DEcomposition) (Brinkman, Chen, Amendola, & van Steensel, 2014) and ICE v2 (Inference of CRISPR Edits) (Hsiau et al., 2019).

2.2.13 Hoxb8-FL generation

Cas9 expressing Hoxb8 lines kindly generated and provided by Seren Baygün from Prof. Dr. Marc Schmidt-Supprian`s lab. Shortly, bone marrow cells were harvested from femur and tibia of 6-10 weeks old animals and cultured in RPMI supplemented with recombinant mouse IL-3 (5 ng/ml), IL-6 (20 ng/ml), and 1% cell culture supernatant from SCF-producing B16 melanoma cells. After 2 days, the cells were spin infected with MSCV-ERHBD-Hoxb8 carrying retrovirus. A day after spin infection the cells were cultured in Hoxb8 medium till infected cells enrich in culture in the presence of β-estradiol (Redecke et al., 2013).

2.2.14 Custom Oligo Pools for *in vivo* screen in Hoxb8 cells

sgRNAs for mouse Cytokine Receptor library were also picked from GPP sgRNA designer tool and ordered from IDT as custom oPools with 50 pmol/oligo. In the Cytokine Receptor library, each gene was targeted with 3 different sgRNAs (Stat6 with 4 sgRNAs) and 15 Non-Targeted control gRNAs were included (337 oligos in total). The Oligo pool was dissolved in Qiagen TE buffer to get 100µM stock concentration. The single-stranded oligos (10ng) were PCR amplified 2 cycles in one reaction in order to generate a double-stranded pool with the Q5 High-Fidelity DNA Polymerase by using Oligo_Amp_F and Oligo_Amp_R primers. The final library plasmid was prepared the same as the genome-wide and validation libraries for T_{MBP} cells. The MSCV-pU6-(BbsI)-Pgk-Puro-T2A-GFP (in house) backbone was used for the Cytokine Receptor library.

2.2.15 Virus production and transduction of Hoxb8 cells

Retroviral particles from Cytokine Receptor library or single sgRNA constructs were produced similarly as for T_{MBP} cells by using HEK293T cells. Hoxb8 cells were spin infected for 1h 1200g at RT with the freshly harvested virus. Puromycin was added at a final concentration of 5µg/ml to select retrovirus infected cells. MOI of 0.4 or below (<30% Transduction efficiency) was used to prevent multiple integrations into one cell. Two days after puromycin selection, cells expressing fluorescent markers (e.g. GFP) were sorted to purity to ensure the expression of gRNA and high

expression of the fluorescent marker by using BD FACSAria IIIu. After sorting, Hoxb8 cells were expanded in the Hoxb8 medium. Primocin (100µg/ml final) was added to the medium for 2 days to prevent contamination that might come from sorting.

2.2.16 EAE induction and transfer of Hoxb8 cells

EAE was induced in 6-12 weeks old C57BL/6 animals by immunizing them with in-house purified recombinant MOG1-125 (400µg) and CFA containing 650µg Mycobacterium tuberculosis emulsion subcutaneously. PTX dissolved in PBS (200ng) was administered intraperitoneally (i.p.) on day 0 and day 2 of immunization. Animals were scored daily for weight loss and clinical score. EAE score was evaluated as followed: 0, no clinical signs; 0.5, partial tail weakness; 1, tail paralysis; 1.5, gait instability or impaired righting ability; 2, hind limb paresis; 2.5, hind limb paresis with dragging of one foot; 3, total hind limb paralysis; 3.5, hind limb paralysis and forelimb paresis; 4, hind limb and forelimb paralysis; 5, death. The first day of the clinical sign was considered as onset, onset +2,3 days were considered as the peak of disease.

In vitro expanded Hoxb8 cells were washed twice with PBS and cultured in a Macrophage medium for 2 days. On Day 9 of EAE induction, cells were washed twice with PBS. 10-15M cells in 200µl of PBS were transferred by i.v. through the tail vein of animals. M-CSF treated Hoxb8 cells were allowed to complete their differentiation to myeloid cells *in vivo* for at least 6 days.

2.2.17 Flow cytometry

Animals with EAE clinical signs were sacrificed. Blood samples were collected immediately after euthanasia from the heart and the animal got perfused with PBS-heparin before collecting the spleen, bone marrow (femur and vertebra), and spinal cord. Blood was washed with PBS and incubated with ACK Lysis buffer for 20min on ice. When insufficient removal of red blood cells, ACK incubation was repeated. Bone marrow cells were flushed out or crushed out with PBS. Spleen and spinal cord tissues were homogenized with a glass dounce homogenizer and transferred into a PBS solution containing Collagenase D (0.8mg/ml final) and DNase I (10ng/ml final) and incubated for 20 min at 37°C with shaking (1000rpm) for dissociation of cells. Spleen and Bone marrow cells were treated with ACK for 5 min. Spinal cord cells were run on Percoll

gradient to remove myelin. Cells were resuspended with 1ml of 100% FBS mixed with 9ml of 33% Percoll (in PBS) and 1ml of 10% FBS (in PBS) was added on the top slowly to form a layer. Samples were centrifuged without brakes for 15min at 4°C with a speed of 800g. The myelin layer was carefully sucked with vacuum and pelleted cells were washed with PBS to get rid of the Percoll solution. All the cells were then transferred to 96-well U bottom plates for flow cytometry staining.

For the Cytokine Library experiment, 5 to 10 animals (depending on the disease score) were combined for one replicate. Before starting flow cytometry staining, monocytes/macrophages from the spleen and bone marrow were enriched with MACS using Cd11b microbeads to reduce sorting time. All cells were blocked with TruStain fcX™ (anti-mouse CD16/32) and stained with Live/Dead stain to exclude dead cells during blocking for 30min at 4°C. After washing with PBS, cells were stained for extracellular markers for 30min at 4°C with anti-Cd11b antibody to include monocytes/macrophages and anti-Ly6G antibody to exclude granulocytes. Cells from the spinal cord were then fixed (15min at 4°C) and permeabilized with Cytofix/Cytoperm solution for intracellular staining. Cells then were stained with anti-Arg1 and anti-iNOS antibodies for 30min at 4°C in permeabilization solution. Populations of interest were sorted for purity with BD FACSAria IIIu. Genomic DNA from sorted cells was isolated by using QIAamp DNA Micro Kit. Cells were lysed in the presence of Proteinase K at 56°C overnight instead of 10min for more efficient de-crosslinking of fixed DNA before DNA isolation. Samples for the CRISPR library were prepared for NGS as T_{MBP} cells. Antibodies used in characterization experiments are listed in the Materials section. For RNA isolation experiments, cells were kept in solutions with 1:100 Rnasin Plus RNase Inhibitor after the fixation step to prevent RNA degradation.

For in vitro macrophage polarization experiments, Hoxb8 cells or bone marrow-derived cells were cultured in the Macrophage medium (10-20ng/ml MCSF) for 5-7 days to allow differentiation. Differentiated cells were then re-seeded and respective recombinant mouse cytokines (IL4, IL6, TGF-β, GMCSF, IFN-γ, TNF-α) were incubated at a concentration of 20ng/ml for 24 or 48h before FACS.

2.2.18 Analyses of CRISPR screens and bulk RNA sequencing

Data processing was conducted by using the Galaxy platform (Afgan et al., 2018). Raw fastq.gz files obtained from sequencing were de-multiplexed with Je-Demultiplex-Illu. Cutadapt and Trimmomatic were used to obtain a 20bp length gRNA sequence. Raw sgRNA counts were obtained by using MAGeCK (W. Li et al., 2014). Raw counts were normalized across samples using R (R Development Core Team, 2021) by the geometric mean, setting a 50 raw counts quality threshold for exclusion before normalization. sgRNAs were discarded when they had counts below the quality threshold in more than two replicates for the same tissue. MAGeCK test was then run with default parameters except for no normalization and no removal of zero counts. After MAGeCK, all other data manipulations were conducted in R.

To design the Validation library, we included all genes in the Meninges vs Blood comparison and in the Parenchyma vs Blood comparison with a log2(fold change) above 0.5 or below -0.5. We then filtered genes based on detected expression in T_{MBP} cells by using the data from (Schläger et al., 2016). Next, we selected top candidate genes from other comparisons (Meninges or Parenchyma vs Spleen and Spleen vs Blood) with more astringent thresholds: |log2(fold change)| > 1 & good sgRNAs >= 2 or |log2(fold change)| > 0.6 & good sgRNAs > 2.

For Bulk RNA analysis, data processing was conducted by using the Galaxy platform and R. Fastq files were aligned to the reference genomes by using RNA STAR (version 2.7.2b) with default parameters without trimming. Then, transcript counts were determined with HTSeq-count (version 1.0.0). Differential expression analysis was conducted with DESeq2 (version 2.11.40.7+galaxy1), with default parameters except for Method for estimateSizeFactors being poscounts. The batch correction was applied when applicable. Further analysis was conducted in R.

2.2.19 Statistics and Software

Flow cytometry files were analyzed by using FlowJo version 10 (BD Biosciences). GraphPad Prism version 9 (GraphPad Software) was used to perform statistical analyses and to generate plots. Total cell numbers and other calculations were performed using Excel (Microsoft Office). Adobe Illustrator (Adobe Systems) and PowerPoint (Microsoft Office) were used for figure preparations.

3. RESULTS

3.1 Trafficking of T$_{MBP}$ cells in EAE

3.1.1 Generation of Cas9 expressing T$_{MBP}$ cells and establishment of gene editing in T$_{MBP}$ cells

In order to perform gene editing with CRISPR in rat T$_{MBP}$ cells, we first introduced the Cas9 protein with a retroviral vector together with a p2a-linked to the fluorescent marker eGFP to be able to assess Cas9 expression (**Figure 6A**). We confirmed Cas9 expression by both GFP expression on FACS and by qPCR with Cas9 specific primers, and we sorted the high GFP population to ensure enough and homogenous expression of Cas9 (**Figure 6B-C**). We then wanted to assess genome editing efficiency by delivering sgRNAs targeting Itga4 and Cd4 with separate retroviral vectors carrying the fluorescent marker BFP and the selection marker puromycin (**Figure 6D**). We could successfully KO Itga4 and Cd4 in T$_{MBP}$ Cas9 expressing cells, as confirmed with FACS staining (**Figure 6E**). Since delivering retroviral vectors to T$_{MBP}$ cells twice and stable expression of Cas9 might cause physiological disturbance in T cells, we also established a method where we deliver with nucleofection either the gRNA duplex alone to Cas9 expressing T$_{MBP}$ cells or together with Cas9 (RNP) to non-transduced T$_{MBP}$ cells, in which Cas9 expression is transient. Nucleofection of T$_{MBP}$ cells with Itga4 gRNA duplex also resulted in high efficiency of genome editing confirmed by FACS (**Figure 6F**). We also delivered the Cas9 protein alone to gRNA expressing T$_{MBP}$ cells, however, KO efficiency was lower when compared to other delivery methods, which could be due to less efficient Cas9 gRNA complex formation inside of the cells. Overall, we confirmed that delivering gRNA and Cas9 either with double virus or nucleofection method results in efficient gene editing in rat T$_{MBP}$ cells.
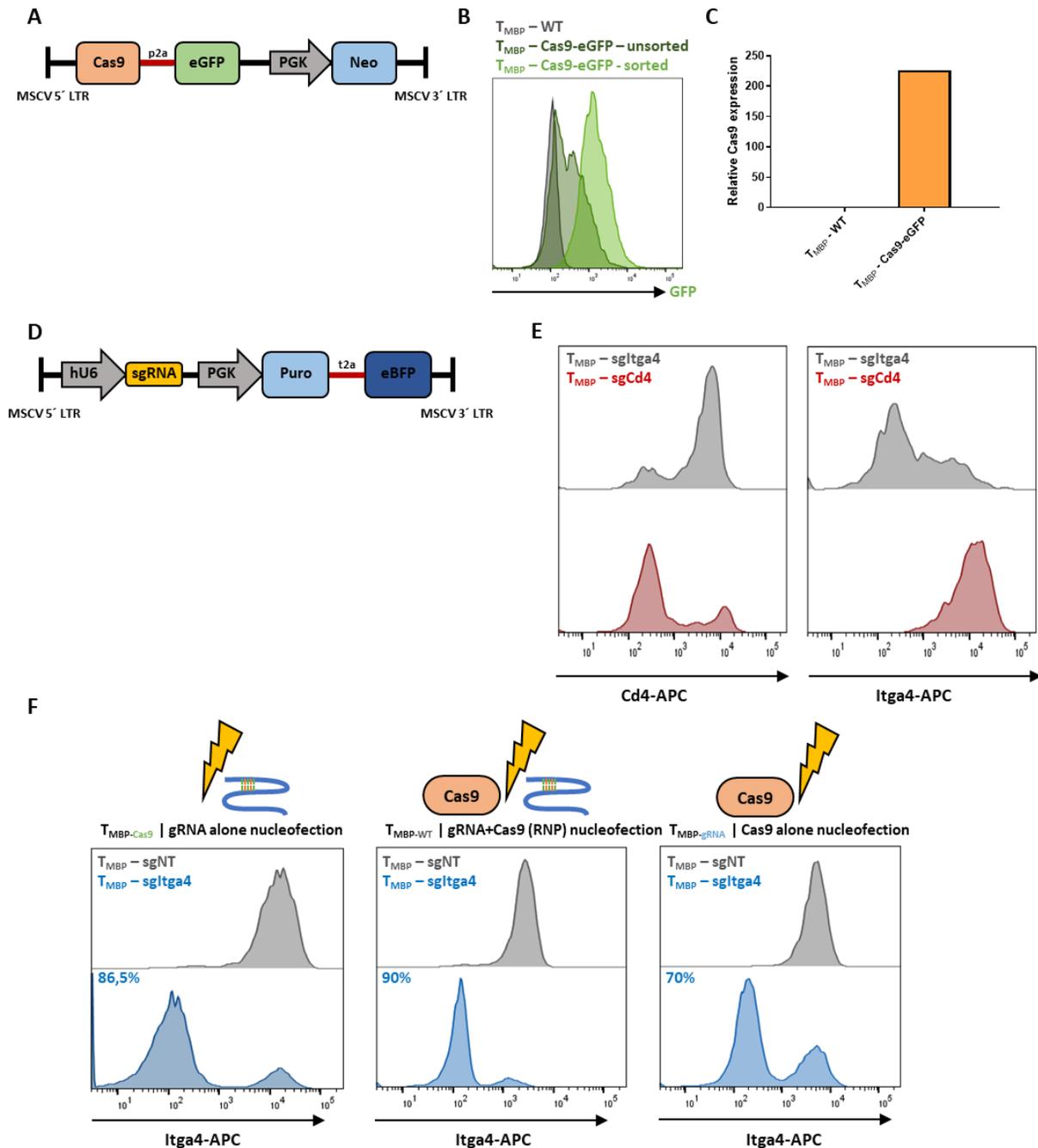
Figure 6 | Gene editing in T_MBP cells. A. Retroviral Cas9 expression cassette. **B.** Representative FACS plots of T_MBP cells transduced with the retroviral Cas9-p2a-eGFP vector. **C.** Confirmation of Cas9 transcription in T_MBP cells by QPCR using Cas9 specific primers. **D.** Retroviral sgRNA expression cassette. **E.** Representative FACS plots of Cas9-T_MBP cells transduced with retroviral sgRNA vector, targeting Itga4 or Cd4, illustrating the KO efficiency. **F.** Representative FACS plots of Cas9-T_MBP cells nucleofected with Itga4 or NT gRNA duplex, WT-Cas9-T_MBP cells nucleofected with Itga4 or NT gRNA duplex + Cas9 (RNP), gRNA-T_MBP cells nucleofected with Cas9 protein alone. Numbers indicate the percentages of the Itga4⁻ population. FACS data are representative of at least 2 experiments. qPCR was performed once for the confirmation of Cas9 expression.

3.1.2 Genome-wide *in-vivo* CRISPR KO migration screen in Cas9 expressing T$_{MBP}$ cells

Once we were able to confirm successful gene editing in T$_{MBP}$ cells, we designed a sgRNA library consisting of 87,690 sgRNAs (4gRNA/gene) targeting all protein-coding genes and miRNAs in the genome and included 800 NT gRNAs as control. We adoptively transferred T$_{MBP}$ cells expressing the gRNA library to Lewis rats and sacrificed them on day 3 when they show first symptoms of disease, namely body weight loss or a clinical score of ≥0.5. We isolated cells from the blood and spleen as a representative of peripheral organs, and from the meninges and parenchyma as a representative of CNS organs (**Figure 7A**). We confirmed the BFP expression in T cells from each organ by FACS (**Figure 7B**) and performed the experiments for a total of 3 replicates. We pooled 8-10 animals per replicate to get enough number of cells for library representation. After the isolation of cells from tissues, we performed gDNA extraction to the whole tissue lysate. Due to the low percentage of BFP+ T$_{MBP}$ cells in the spleen, we sorted them to purity before the isolation of gDNA. We first looked for the correlation of gRNA counts among the replicates as quality control for each organ (**Figure 7C**). The correlation gets better when a higher number of counts is detected, indicating that a higher representation of gRNAs is necessary for better quality. Therefore, we decided to filter out counts below 50 before we analyzed the data using MAGeCK, a computational tool developed to identify hits from CRISPR-Cas9 KO screens (W. Li et al., 2014). As a positive control we used Itga4 a well-established regulator of T cell migration across the BBB. Indeed, Itga4 was one of the top depleted hits in comparisons of CNS vs peripheral organs (**Figure 7D**), confirming that our genome-scale CRISPR screen can identify migration relevant genes in T$_{MBP}$ cells.
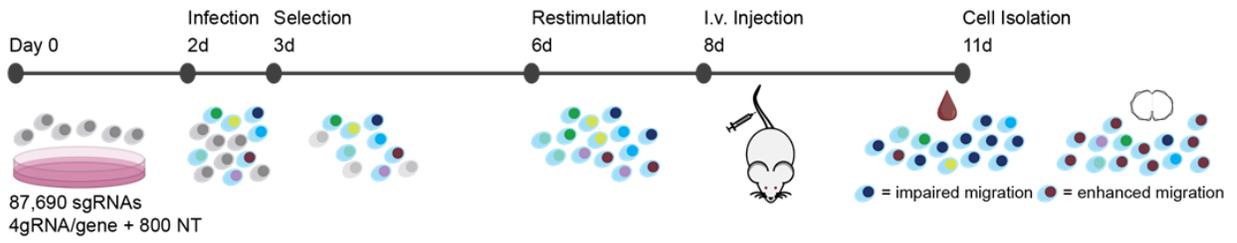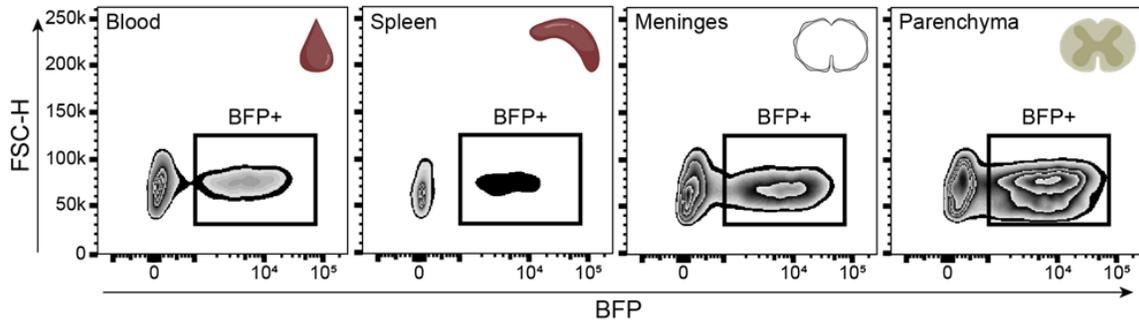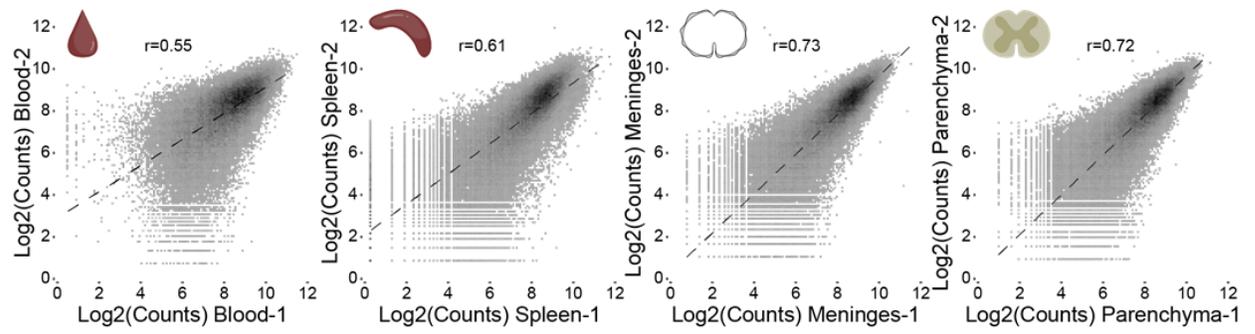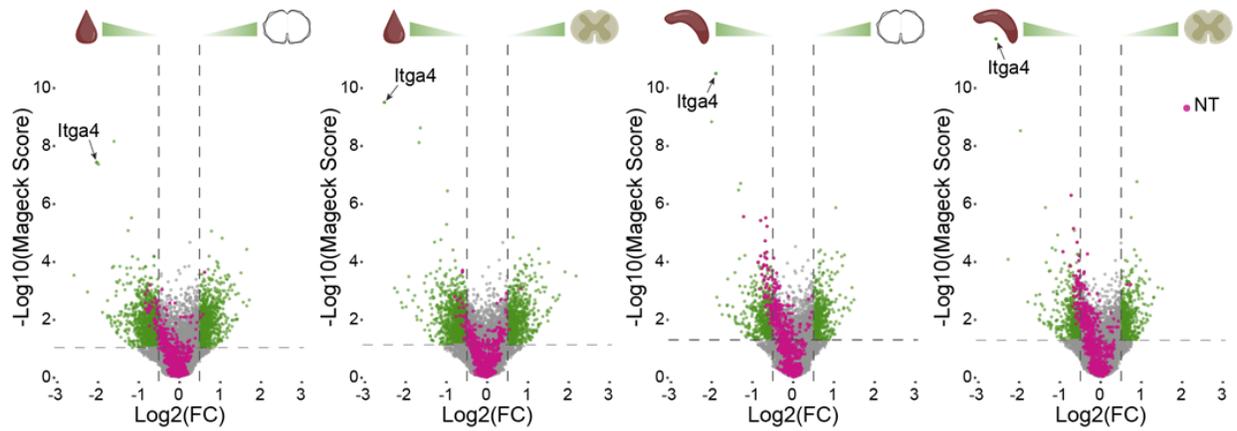
Figure 7 | Genome-wide CRISPR screen of T cell migration to the CNS. A. Scheme of the experimental approach. **B.** Representative FACS plots of the BFP+ cells for (left to right) blood, spleen, meninges, and parenchyma. **C.** Correlation of individual replicates of the genome wide screen sgRNA log2 counts for (left to right) blood, spleen, meninges, and parenchyma. **D.** Volcano plots of 4 comparisons (from left to right, meninges vs blood, parenchyma vs blood, meninges vs spleen and parenchyma vs spleen). Green indicates significant candidates at adjusted p-value < 0.05 and |log2(Fold-Change)| > 2 standard deviations of the log2(FC) distribution. Pink indicates Non-Targeted (NT) sgRNA controls. NT spread in comparisons (left to right) for meninges vs blood -0.124 ± 0.218, meninges vs spleen 0.183 ± 0.228, parenchyma vs blood -0.078 ± 0.236, parenchyma vs spleen -0.172 ± 0.220.

3.1.3 A deeper secondary pooled library to validate hits with higher confidence

As genome-wide screens can be noisy due to the large size of the sgRNA library, we decided to design a targeted validation library, composed of 12,000 sgRNAs, based on the results from the genome-wide screen to reduce false positive and negative hits. We included 6 gRNAs per gene to increase the sensitivity and specificity of each phenotype (**Figure 8A**). To design the targeted validation library, we kept fold change selection criteria low (0.5), to avoid missing real hits, and we added a couple of genes from pathways enriched in the top hits. We performed 3 replicates of the targeted validation library. Moreover, for the validation library, we sorted BFP+ cells from all organs to purity. It allowed us to make more precise calculations on the amount of gDNA to use for each amplification PCR. Indeed, the correlation of replicates improved in the validation library (**Supplementary Figure 1A**). In the analyses of the validation library, we first focused on candidates which have an impact on T cell migration from the periphery into the CNS. CNS organs had similar fold changes for most of the top candidates in comparison to the peripheral organs, indicating that common molecular mechanisms regulate the migration to the meninges and CNS parenchyma in our experimental setup (**Supplementary Figure 1B**). We ranked top depleted and enriched candidates across comparisons with MAGeCK (**Figure 8B-E**). A strength of the CRISPR KO screen is that it allows for the identification of essential regulators of a phenotype. Therefore, we decided to look at molecular classes which are expected to play a role in T cell migration to identify gene members that are essential for this process, such as 'Adhesion Molecules', 'Cytokine Receptors', 'Chemokine Receptors', 'Transcription Factors', 'GPCR Receptor Signaling'.

Among the cluster of 'Adhesion Molecules', Itga4 and Fermt3 had the highest fold change difference, indicating their indispensable role in T cell migration to CNS (**Figure 8F**). The effect of Itga4 KO on migration is in line with Natalizumab studies and its efficacy to prevent T cells migration by blocking VLA-4 and VCAM-1 interaction (Hutchinson, 2007). Surprisingly, deficiency of another subunit of VLA-4, Itgb1, had a milder fold change, suggesting that the involvement of Itgb1 in the adhesion step might be redundant compared to Itga4. Fermt3 and Tln1 are both cytoplasmic proteins that bind to α4β1 integrins to modulate their activation for ligand binding (E. J. Park, Yuki, Kiyono, & Shimaoka, 2015). Similarly, Tln1 had a milder fold change compared to Fermt3, suggesting they might have differential importance in the migration of T$_{MBP}$ cells.

Among the 'Cytokine Receptors', we found no genes that are significantly regulated across all four comparisons (**Figure 8G**), suggesting that cytokine receptors do not play an essential role in T$_{MBP}$ migration.

Among the 'Chemokine Receptors', knocking out Cxcr3, which is a receptor for inflammatory chemokines CXCL9, CXCL10 and CXCL11, showed significantly impaired migration phenotype (**Figure 8H**) confirming previously observed function of Cxcr3 in the same adoptive transfer EAE model (Schläger et al., 2016). Overall, our validation CRISPR screen confirmed the role of several known regulators of T cell adhesion such as Itga4, Fermt3, Tln1, Itgb1 and chemokine receptor involvement such as Cxcr3, indicating the strength of our unbiased approach to identify essential regulators of T$_{MBP}$ transmigration in an EAE model.

Among the cluster of 'Transcription Factors', Cbfb (Core-binding factor subunit beta), and Foxo1 (Forkhead box protein O1) had the highest fold change differences (**Figure 8I**). Cbfb is known to be involved in different stages of T cell development (Zhao et al., 2007) and Foxo1 is important for Cd4 T cells homeostasis (Newton et al., 2018), however, it was not previously known that they also impact the migration of already differentiated MBP specific Cd4+ T cells.

In addition to the known regulators, our CRISPR screen also identified several previously unknown candidates for T cell migration from the periphery into the CNS. Among the cluster of 'GPCR Receptor Signaling', Grk2 (Beta-adrenergic receptor kinase 1), and Gnai2 (Guanine nucleotide-binding protein G(i) subunit alpha-2), had the highest fold change differences (**Figure 8J**). Grk2, as a GPCR kinase, has a major role in the desensitization and internalization of GPCRs by

phosphorylating them (Penela, Ribas, Sánchez-Madrid, & Mayor, 2019). Gnai2 is necessary to activate downstream signaling of GPCRs, and its deficiency has been shown to affect chemoattractant induced T cell motility (I. Y. Hwang, Park, & Kehrl, 2007).

Our CRISPR screen also identified hits that showed an enhanced migration phenotype. Among those, Ets1 was the most robust candidate with a high fold change across conditions (**Figure 8E**). Ets1 is a transcription factor that was previously identified as a risk loci in GWAS of T cells for Atopic Dermatitis, indicating its potential contribution during autoimmune diseases (Paternoster et al., 2015).

Among miRNAs, only 11 (out of 380) of them from the genome-wide library were validated in the targeted validation library, as the rest did not pass our selection criteria. However, none of the miRNAs in the validation library except Mir202 in the meninges vs spleen comparison showed a significant fold change difference, suggesting that none of the miRNAs in our library play an essential role in T cell migration in our experimental setup (**Supplementary Figure 2B-C**).
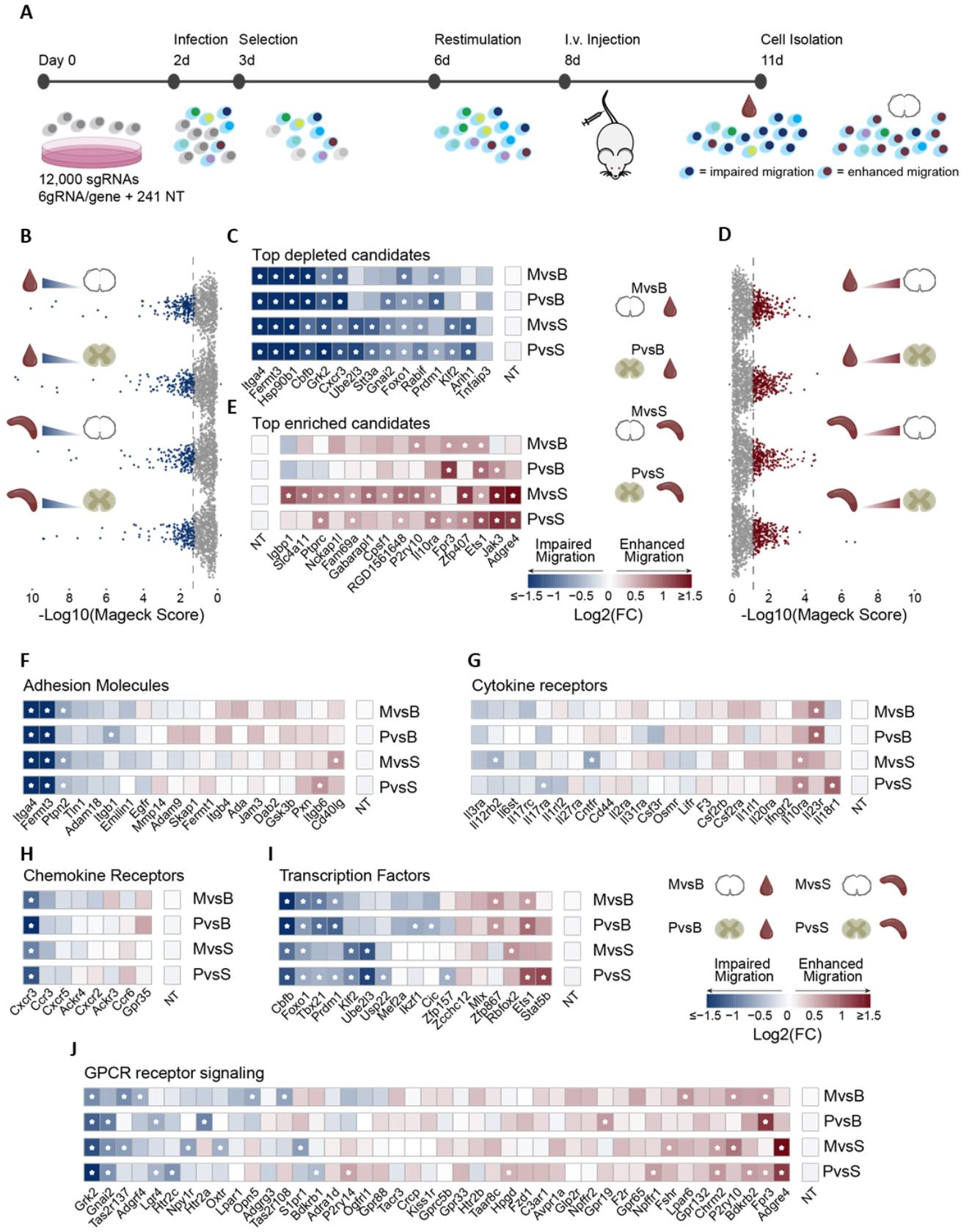
Figure 8 | Validation CRISPR screen of T cell migration to the CNS. **A.** Scheme of the experimental approach. **B.** MAGeCK score plots of all KO depleted in the CNS (from top to bottom meninges vs blood, parenchyma vs blood, meninges vs spleen and parenchyma vs spleen). Blue dots indicate significantly depleted candidates (adjusted p-value < 0.05). **C.** Heatmap of the top depleted candidates across comparisons (from top to bottom meninges vs blood, parenchyma vs blood, meninges vs spleen and parenchyma vs spleen). **D.** MAGeCK score plots of all KO enriched in the CNS. Red indicates significantly enriched (adjusted p-value < 0.05). **E.** Heatmap of the top enriched candidates across comparisons. **F-J.** Heatmaps of the selected moleculer classes across comparisons. Stars indicate significance (good sgRNAs > 3, |log2(Fold-Change)| > 3 standard deviations from the log2(FC) distribution, adjusted p-value < 0.05) (except for GPCR receptor signaling and Transcription Factors, where adjusted p-value < 0.01).

3.1.4 Compartment specific hits

Since we performed the screen with two peripheral and two CNS organs, we also looked at each comparison individually to identify hits that affect the distribution between the two peripheral or central compartments (**Figure 9A-H**). Among the top depleted candidates, Cbfb, the KO of which was significantly depleted in the CNS compared to the periphery, is also significantly depleted in the spleen compared to blood (**Figure 9B**)**,** suggesting that Cbfb KO have a general impaired migration phenotype as cells get stuck in the blood circulation.

Among the top enriched candidates, S1pr1, a known regulator for normal egress of mature T cells from lymph nodes to the bloodstream and a therapeutical target of the FDA-approved MS drug Fingolimod (Cyster & Schwab, 2012), was significantly enriched in the spleen compared to the blood (**Figure 9D**), suggesting that our CRISPR screen can also identify tissue specific migration phenotypes. Other candidates such as Arih1, Ube2l3, Stt3a, Klf2 are significantly depleted in the comparisons of CNS tissues with the spleen but not with the blood (**Figure 8C**). This is partially due to their enrichment in the spleen (**Figure 9D**). Arih1 is an E3 ubiquitin-protein ligase that interacts to E2 ubiquitin-conjugating enzyme Ube2l3 for their function of catalyzing ubiquitination of target proteins (Wenzel, Lissounov, Brzovic, & Klevit, 2011). Deficiency of Arih1 and Ube2l3 led to enrichment in the spleen compared to the blood, therefore, preventing them from reaching the CNS tissues, indicating that their co-function is crucial to exit the spleen. Moreover, Klf2, a transcription factor, is known to regulate S1pr1 expression (Bai, Hu, Yeung, & Chen, 2007), suggesting that its deficiency phenotype might be linked to S1pr1. These data suggest that our

CRISPR screen not only informs us about the molecular mechanism of T cells trafficking into the CNS but also provides candidate regulators that specifically target T cell exit from the spleen or other lymphoid organs.

We also looked at the meninges vs parenchyma comparison to identify hits differentially required for the migration of T_{MBP} cells between two CNS compartments (**Figure 9E-H**). We identified potentially interesting candidates. For instance, the KO of P2ry10, a GPCR, was enriched in the meninges compared to the peripheral organs but absent in the parenchyma. On the other hand, the KO of Itgb3bp, a centromere protein R functions as a transcription co-regulator, was significantly depleted only in the parenchyma. Although most of the top candidates that regulate the migration from the peripheral organs to CNS organs were conserved between the meninges and parenchyma (**Supplementary Figure 1B**), these results suggest that specific regulatory mechanisms may exist to control trafficking of T_{MBP} cells from the meninges to the parenchyma.
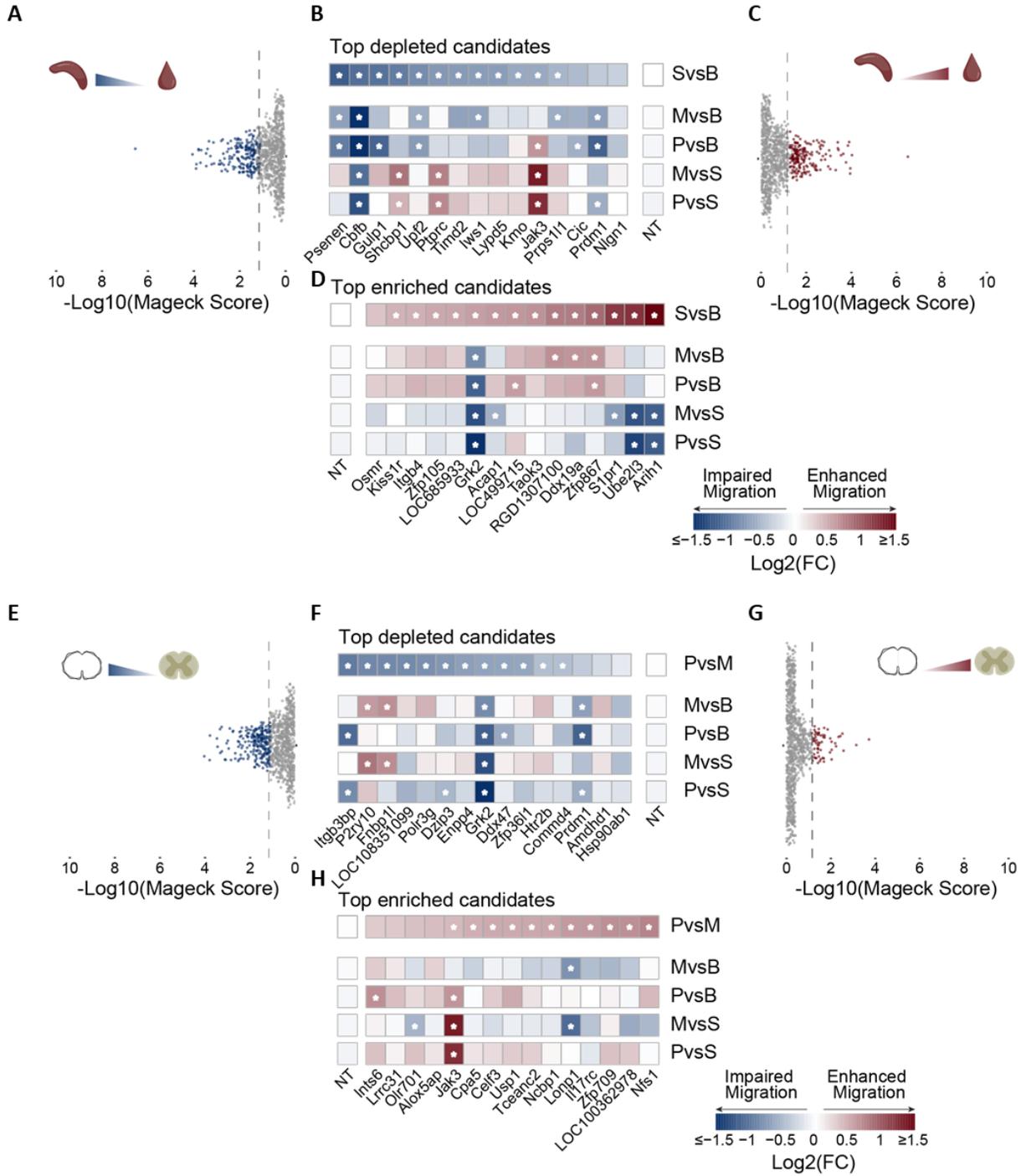
Figure 9 | Regulation of T cell migration in Spleen vs Blood and Parenchyma vs Meninges. A. MAGeCK score plots of all KO depleted in spleen vs blood. Blue dots indicate significantly depleted candidates (adjusted p-value < 0.05). **B.** Heatmap of the top depleted candidates in spleen vs blood across comparisons (from top to bottom spleen vs blood, meninges vs blood, parenchyma vs blood, meninges vs spleen and parenchyma vs spleen). **C** MAGeCK score plots of all KO enriched in spleen vs blood. Red indicates significantly enriched (adjusted p-value < 0.05). **D.** Heatmap of the top enriched candidates in spleen vs blood across comparisons (from top to bottom spleen vs blood, meninges vs blood, parenchyma vs blood, meninges vs spleen and parenchyma vs spleen). **E.** MAGeCK score plots of all KO depleted in the Parenchyma vs Meninges. Blue dots indicate significantly depleted candidates (adjusted p-value < 0.05). **F.** Heatmap of the top depleted candidates in parenchyma vs meninges across comparisons (from top to bottom parenchyma vs meninges, meninges vs blood, parenchyma vs blood, meninges vs spleen and parenchyma vs spleen). **G.** MAGeCK score plots of all KO enriched in the parenchyma vs meninges. Red indicates significantly enriched (adjusted p-value < 0.05). **H.** Heatmap of the top enriched candidates in parenchyma vs meninges across comparisons (from top to bottom parenchyma vs meninges, meninges vs blood, parenchyma vs blood, meninges vs spleen and parenchyma vs spleen). Stars indicate significance (good sgRNAs > 3, |log2(Fold-Change)| > 3 standard deviations from the log2(FC) distribution, adjusted p-value < 0.05).

3.1.5 Validation of identified hits by individual knock-out experiments

Overall, our CRISPR screen in T_{MBP} cells identified several candidates which might regulate the trafficking of autoreactive T cells trafficking into the CNS. However, each candidate requires validation to rule out the possibility of false-positive and negative hits identified by the screen. We performed the CRISPR screen by delivering the sgRNA library with retroviral particles for the second time. To prevent any possible cell disturbance caused by double retroviral integration we decided to perform single KO experiments by editing genes with the nucleofection method by using non-Cas9 expressing T_{MBP} cells in order to have a transient expression of Cas9 and gRNA. To keep the experimental variation to a minimum, we transduced T_{MBP} cells with two different fluorescent proteins, one color for NT control cells and the other one for KO cells. My colleagues, Dr. Naoto Kawakami and Katrin Lämmle, then adoptively co-transferred NT and KO 1:1 mix of cells to rats and compared the ratio of KO cells to NT cells in each compartment (**Figure 10A**). We could successfully confirm the phenotype of Itga4, Hsp90b1, Cxcr3, Gnai2, Grk2, Ets1, S1pr1, Arih1 and Ube2l3 from the CRISPR screen with single knock-out experiments (**Figure 10B**), indicating the robustness of the CRISPR screen. Katrin Lämmle confirmed target DNA perturbations for each gene by TIDE (**Supplementary Table 1**).

Since CRISPR KO can only show the functional phenotypes of the genes, we wanted to understand whether our candidate genes are regulated transcriptionally in T$_{MBP}$ cells. To do that, we adoptively transferred GFP-expressing T$_{MBP}$ cells and sorted cells on onset from the spleen, blood, CSF, meninges, and parenchyma and performed 3`mRNA bulk RNA sequencing. Most of our top candidates identified by the CRISPR KO screen, showed differential expression in different organs (**Supplementary Figure 3A**), suggesting a transcriptional level regulation of migration relevant genes in T$_{MBP}$ cells.
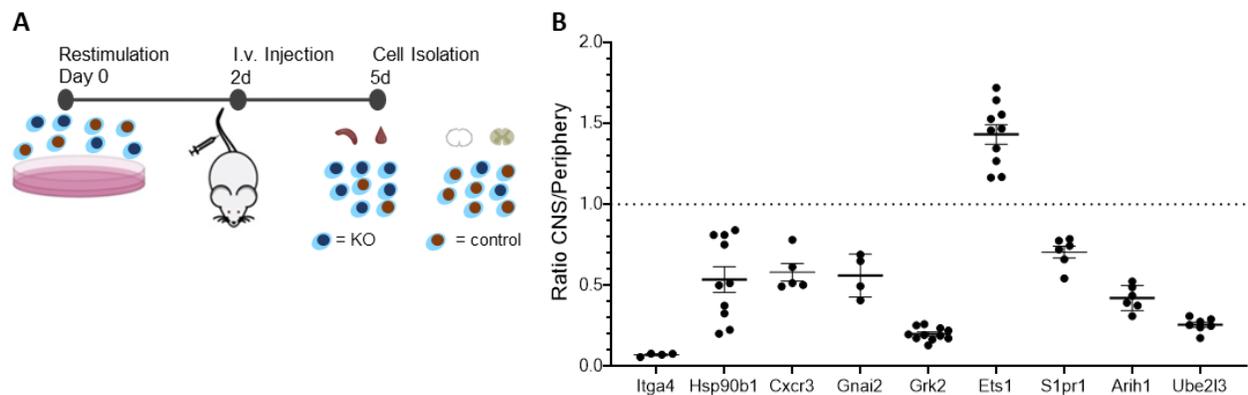
Figure 10 | Validation of identified hits by the CRISPR screen. A. Scheme of the experimental approach for validation of individual KOs. **B.** A ratio of % of KO cells in CNS (meninges + parenchyma) to the periphery (blood and spleen) relative to % of control NT cells (normalized to 1). Each dot represents one rat.

3.1.6 Grk2 regulates S1pr1 for the transmigration of T$_{MBP}$ cells

Among the novel hits identified by our CRISPR screen, we focused on Grk2 to further investigate its impact on T$_{MBP}$ migration into the CNS since our experiments showed that the KO effect of Grk2 on migration is as strong as the KO of Itga4 (**Figure 10B**). Moreover, as protein kinases are major drug targets, targeting Grk2 could be a potential therapeutic approach. Indeed, Paroxetine, an FDA-approved drug for serotonin reuptake inhibition, also inhibits Grk2 kinase activity, and more Paroxetine-based molecules have been being developed to target Grk2 more specifically (S. Keretsu, S. P. Bhujbal, & S. Joo Cho, 2019).

We first wanted to explore which transmigration steps are impaired in Grk2 deficient T$_{MBP}$ cells. To do so, Dr. Naoto Kawakami and Katrin Lämmle adoptively co-transferred NT cells and Grk2 KO cells and performed *in vivo* two-photon imaging (**Figure 11A**). We observed no differences in the speed and path length of Grk2 KO cells compared to NT cells (**Figure 11B-C**), suggesting that Grk2 deficiency does not impair the initial steps (adhesion and crawling) of transmigration. On the other hand, the number of extravasated cells (diapedesis) was significantly lower in Grk2 KO cells compared to NT cells (**Figure 11D**), indicating that Grk2 deficiency impairs the last step of transmigration of T$_{MBP}$ cells. We then wanted to assess the functional relevance of knocking out Grk2 T$_{MBP}$ cells. To do that, Dr. Naoto Kawakami and Katrin Lämmle adoptively transferred Grk2 KO T$_{MBP}$ cells into rats and observed the clinical score development. Rats transferred with Grk2 KO T$_{MBP}$ cells showed a milder disease course compared to rats transferred with NT cells (**Figure 11E**). Milder clinical score correlated with the lower body weight loss (**Figure 11F**). We then performed 3' bulk mRNA sequencing on Grk2 deficient cells from the spleen, however, we did not observe significant changes in the transcriptome of Grk2 KO cells compared to NT cells (**Figure 11G**), suggesting that Grk2 mediated effect is not transcriptionally regulated.

Grk2 mediated S1pr1 desensitization was shown to be necessary for the migration of T and B cells from blood, into the lymph nodes, against the S1P gradient. Impaired migration phenotype of Grk2 deficient cells was restored in S1P deficient mice (Arnon et al., 2011) and by S1pr1 antagonist treatment (I.-Y. Hwang, Park, Harrison, & Kehrl, 2019). Therefore, we hypothesized that Grk2 mediated S1pr1 internalization might also be required for T$_{MBP}$ cells to migrate against the S1P gradient, from blood into the CNS. Dr. Naoto Kawakami and Katrin Lämmle performed transfer experiments with Grk2 KO, S1pr1 KO and Grk2/S1pr1 double KO cells. Indeed, KO of S1pr1 in Grk2 KO cells restored the migration deficient phenotype from blood into the CNS (**Figure 11H**). Overall, these data suggest that Grk2 KO cells lack internalization of S1pr1, preventing them to migrate against the S1P gradient, from blood into the CNS.

A T_MBP – sgNT
   T_MBP – sgGrk2
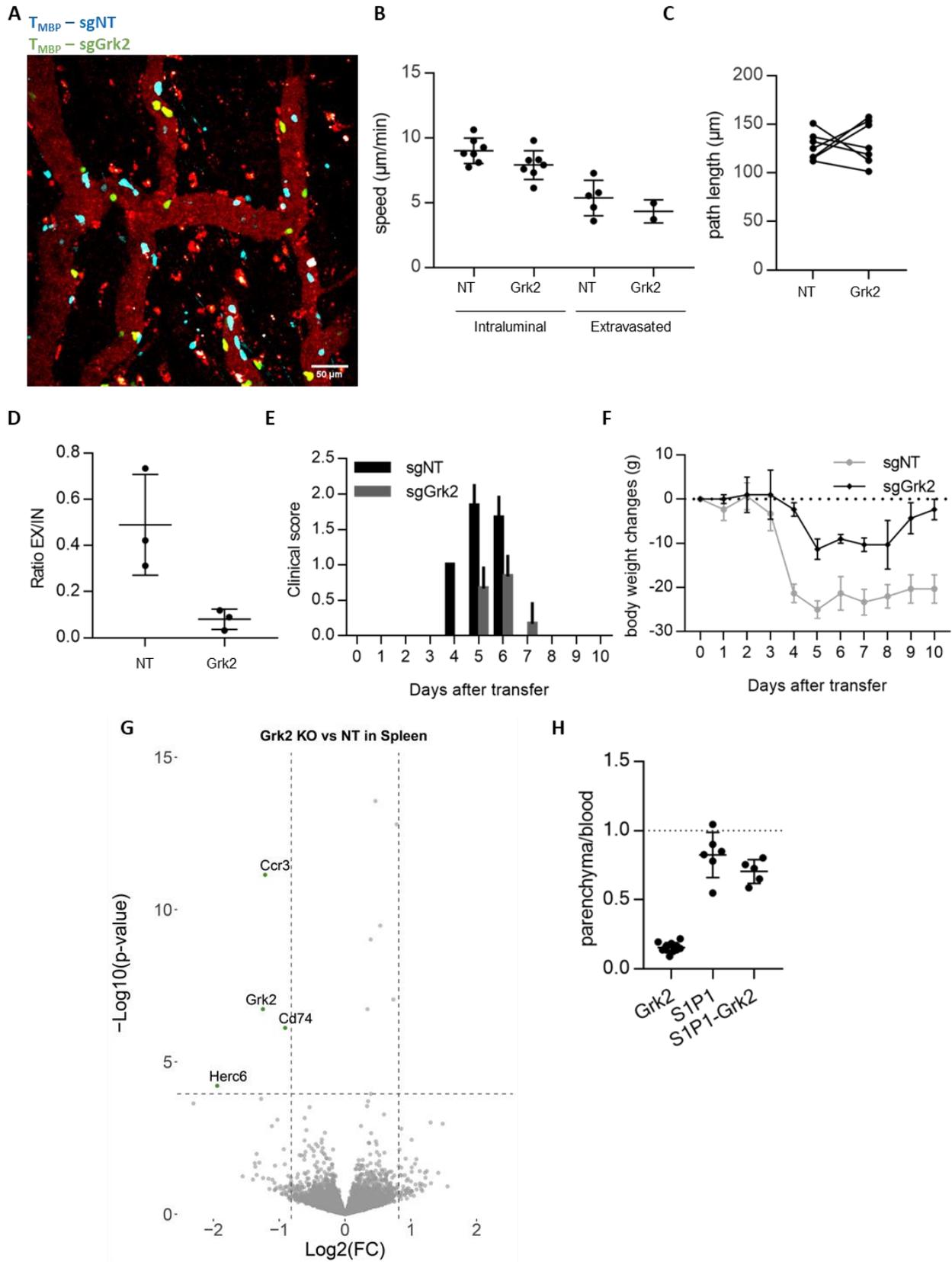
Figure 11 | Grk2 KO T$_{MBP}$ cells fail to extravasate BBB due to lack of S1pr1 sensitization. A. A representative two-photon image of Grk2 KO (GFP) and NT (BFP) injected rats on the onset of the disease. Blood vessel in red. **B.** The speed (velocity) of Grk2 KO and NT cells found on the intraluminal surface and extravasated cells. Each dots represents one video taken from 3 different rats. **C.** The length of the path T cells crawls on the intraluminal surface. **D.** A ratio of the number of extravasated (EX) cells to the number of cells on the intraluminal surface. Each dot represents one rat. **E.** Clinical score and **F.** body weight change in rats adoptively transferred with NT cells or Grk2 cells (n=3 rats). **G.** 3' Bulk mRNA sequencing of Grk2 KO and NT T$_{MBP}$ cells isolated from the spleen. Green dotes indicate significantly regulated transcripts based of FDR adjusted p-value < 0.05 and |log2(Fold-Change)| > 3 standard deviations of the log2(FC) distribution (n=3 rats). **H.** A ratio of % of KO cells parenchyma to the blood relative to % of control NT cells (normalized to 1). Each dot represents one rat.

3.1.7 Ets1 controls T cell activation and cytotoxicity

Ets1 KO T$_{MBP}$ cells are enriched in the CNS, indicating that Ets1 functions as a suppressor of T cell migration. Ets1 has been shown as a negative regulator of Th17 differentiation, and a suppressor of pathogenic T cell response (C.-G. Lee et al., 2019), however, its role in the transmigration of antigen-specific T cells has not been addressed yet. Therefore, we wanted to investigate how the transcriptome of Ets1 deficient cells changes in T$_{MBP}$ cells. To do so, we adoptively co-transferred NT cells and Ets1 KO cells and isolated cells from the parenchyma for 3' bulk mRNA sequencing. We observed that Ets1 KO cells upregulated transcripts associated with cytotoxicity and activation such as Nkg7, Prf1, Tnfrsf9, Il2ra (**Figure 12A**). We also observed an increase in Th17 regulating genes such as IL17a, Ccr6. These results indicate that Ets1 deficiency leads to a more aggressive T cell response in T$_{MBP}$ cells with a higher Th17 phenotype. However further experiments are required to understand how the more aggressive phenotype is mechanistically linked to the enhanced CNS migration in our EAE model. Ets1 transcript depletion was not detected by the 3'mRNA sequencing, this could be because the 3' mRNA sequencing method only captures reads from the 3' end of the mRNA or it could be that frameshift mutations on the target site do not cause mRNA decay. Therefore, we confirmed the deficiency of Ets1 on protein level (**Figure 12B**) with a monoclonal antibody and on RNA level by designing specific primers to the target exon (**Figure 12C**). We also validated top hits from the 3'mRNA sequencing with specific primers by qPCR (**Figure 12C**).
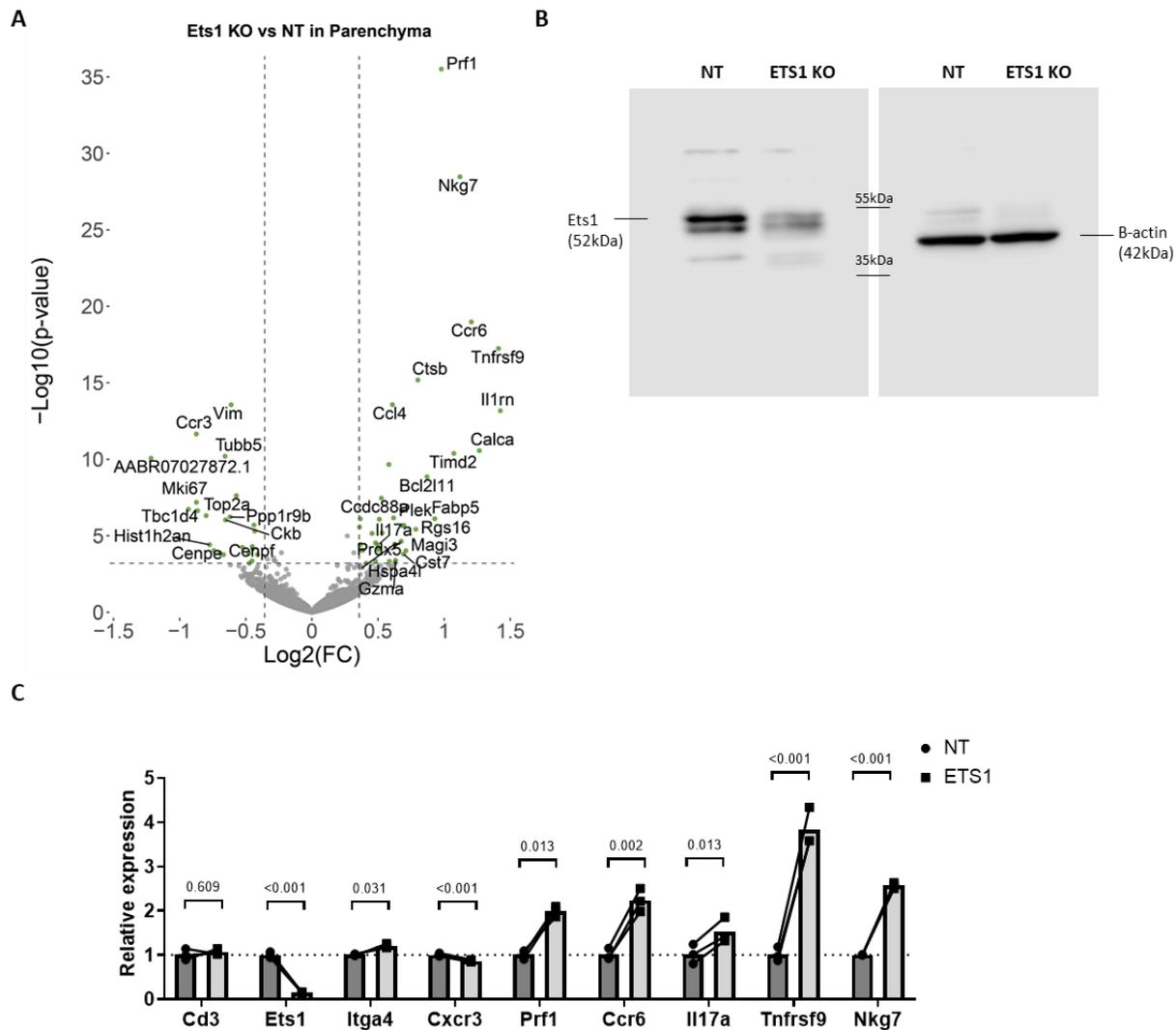
Figure 12 | Ets1 KO T$_{MBP}$ cells are more cytotoxic in the parenchyma. A. 3' Bulk mRNA sequencing of Ets1 KO and NT T$_{MBP}$ cells isolated from the parenchyma. Green dotes indicate significantly regulated transcripts based on FDR adjusted p-value < 0.05 and |log2(Fold-Change)| > 3 standard deviations of the log2(FC) distribution (n=3 rats). **B.** Western Blot analysis for Ets1 (52kDa) from cell culture Ets1 KO and NT T$_{MBP}$ cells. **C.** qPCR analysis of ETS1 KO and NT T$_{MBP}$ cells isolated from the parenchyma (n=3 rats). Multiple paired two-tailed Student's t-test comparing the expression of transcripts in Ets1 KO cells to NT (mean is normalized to 1) .

3.2 Macrophage polarization in EAE

Previous research from our lab demonstrated that during EAE, infiltrating macrophages can adopt a different spectrum of polarization and polarize from M_{iNOS} cells to M_{Arg1} cells. M_{iNOS} cells predominate during the initial inflammatory phase, and gradually shift to a M_{Arg1} phenotype during lesion resolution (Locatelli et al., 2018). I performed the experiments in Locatelli et al., (2018) to identify signals that may regulate this phenotypic shift. To do so, I co-cultured M_{iNOS} polarized (LPS and IFN-γ) bone marrow-derived macrophages (BMDM) with TLR or latex (as a control) beads, as well as a myelin or non-myelin (as a control) fraction of CNS *in vitro*. I also co-cultured BMDMs with primary astrocytes and microglia for 48 hours on a transwell system to allow cells to secrete signals through the transwell membrane. The phenotype of M_{iNOS} and M_{Arg1} was then determined by qPCR measurements of iNOS and Arg1 levels. Relative mRNA abundance revealed that phenotypic shift of macrophages from M_{iNOS} to M_{Arg1} could be due to signals secreted by Astrocytes; however, the presence of latex or TLR beads, myelin or non-myelin fraction of CNS, and Microglia had no effect (**Figure 13A-B**).

We then intended to determine the drivers of M_{iNOS} and M_{Arg1} polarization during EAE as a continuation of the project. *In vitro* polarization BMDMs with recombinant cytokines is, however, a rather limited setup when compared to the inflammatory milieu of EAE lesions, which involves many cell types and tissue specific signals. We first intended to design a setup for performing CRISPR screen in macrophages to uncover regulators of macrophage polarization during EAE because the present tools do not allow us to perform large scale genetic modifications in macrophages *in vivo*.
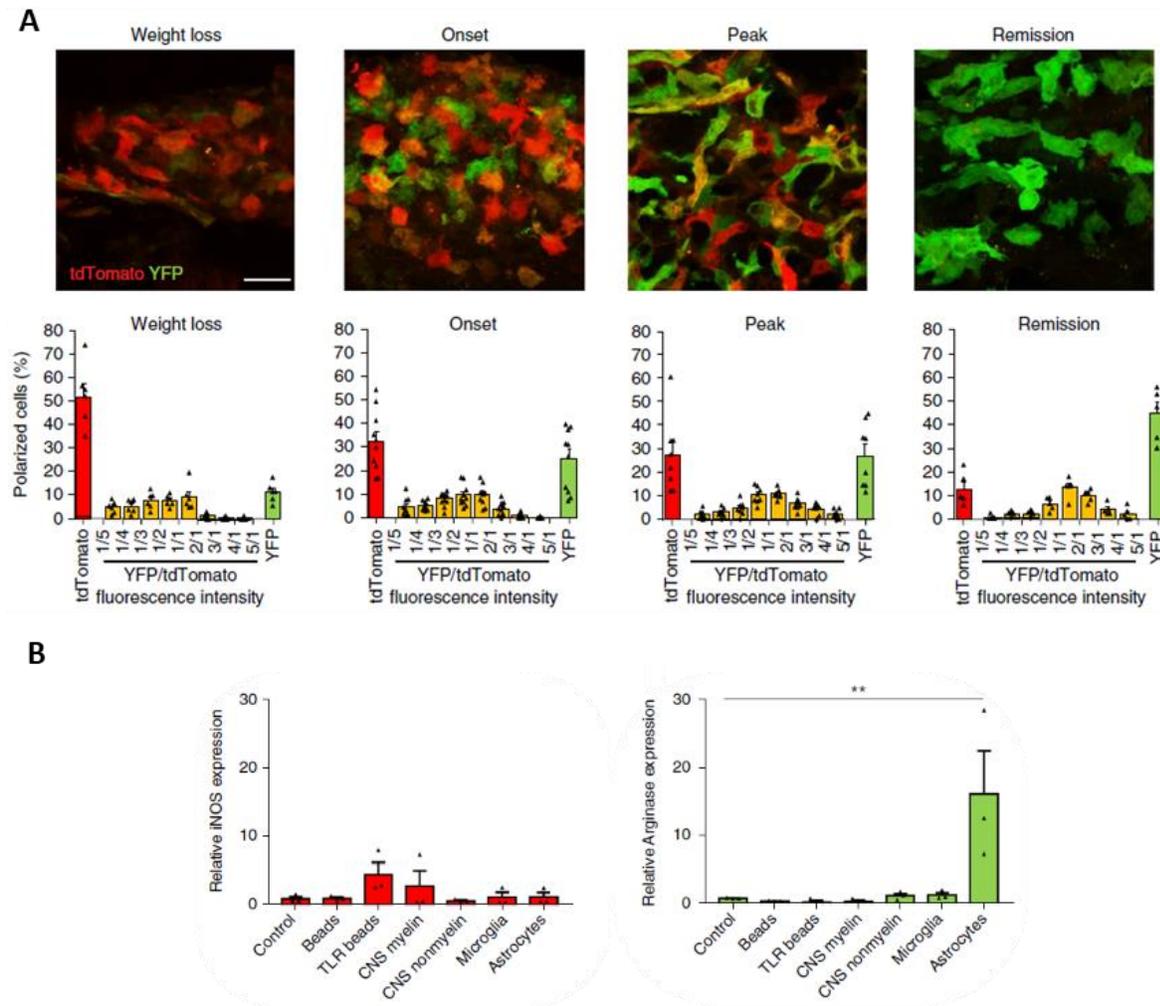
Figure 13 | M$_{iNOS}$ to M$_{Arg1}$ shift of Macrophages in EAE. A. Confocal images of spinal cord lesions and quantitative analysis of MiNOS, MiNOS/Arg1, and MArg1 cells at the indicated EAE timepoints in iNOS-tdTomato-Cre × Arginase-YFP mice (n = 6 mice at weight loss, n = 10 at onset, n = 8 at peak, n = 5 at remission). **B.** Quantitative PCR analysis of iNOS and Arg1 transcription in BMDM polarized *in vitro* for 48 h toward M$_{iNOS}$ with LPS + IFN-γ and analyzed at 24h after culture with medium only (control), latex microspheres (beads), zymosan-coupled bioparticles that stimulate TLR signaling (TLR beads), myelin and nonmyelin fractions of the CNS, or after transwell cultures with isolated microglia or astrocytes (astrocytes). Data from 3 experiments are shown as individual values and as average + s.e.m. (** P < 0.01; one-way ANOVA with Bonferroni post hoc correction, P = 0.0033 (astrocytes vs. control). Figures are taken from Locatelli, G., Theodorou, D., **Kendirli, A**.,. . . Kerschensteiner, M. (2018). Mononuclear phagocytes locally specify and adapt their phenotype in a multiple sclerosis model. Nat Neurosci, 21(9), 1196-1208. doi:10.1038/s41593-018-0212-3

3.2.1 Establishing *in vivo* transfer of Hoxb8 progenitor cells in the EAE model

Hoxb8 cells are immortalized early bone marrow progenitor cells with myeloid and lymphoid potential dependent on the self-renewal and cell differentiation arrest function of the *Hoxb8* gene (G. G. Wang et al., 2006) (Redecke et al., 2013). Hoxb8 expression is estrogen-dependent and upon withdrawal of estrogen and in the presence of M-CSF, cells can differentiate to macrophages and polarize as their counterparts BMDMs (Accarias et al., 2020). The unlimited proliferative capacity of Hoxb8 cells offers the possibility to conduct a wide range of genetic manipulations *in vitro*. Therefore, we assumed the adoptive transfer of Hoxb8 cells before the EAE onset might behave similarly to their endogenous counterparts. We incubated Hoxb8-Bcl2 cells two days in culture in the presence of M-CSF to initiate their differentiation to the myeloid lineage and then transferred them i.v. into EAE induced mice before the onset of the disease. Six days after cell transfer, we isolated cells from different organs for the subsequent analysis (**Figure 14A**).

We first wanted to characterize Hoxb8 derived cells in EAE animals. To do so, we transduced Hoxb8 cells with a retroviral vector expressing GFP to able to distinguish them from the endogenous population. We first looked for their potential to differentiate into myeloid lineage in animals. On Day 0 when they are still in the Hoxb8 medium they did not express Cd11b as expected. After 2 Days in medium with M-CSF, right before the transfer to animals, very few cells started to express Cd11b, whereas almost all Hoxb8 derived cells became Cd45+Cd11b+ myeloid cells in all the compartments we checked in animals on the day of analysis (**Figure 14B**). Notably, they express Cd45 and Cd11b in higher intensity due to the inflamed environment of the spinal cord. Also, there is no progenitor Hoxb8 cells in the bone marrow on the day of analysis, suggesting that there would be no continuous differentiation from the bone marrow niche. Indeed, we observed that Hoxb8-derived cells gradually disappear from the circulation after 8-9 days of transfer (data not shown)

We then studied the percentage of Hoxb8-derived myeloid cells in different organs compared to the endogenous population. Around 20% of myeloid cells in the blood and spinal cord were Hoxb8-derived (**Supplementary Figure 4A,B**), offering enough cells for CRISPR manipulations. The amount of Hoxb8 cells in the body did not significantly interfere with the EAE incidence or clinical score (**Supplementary Figure 4C**).

A

Immunization (MOG + PTX)
Day 0   2d

I.v. injection
9d

Onset
~12d (onset)

Analysis
15d (onset + 2/3)

7d

M-CSF

GFP+ Hoxb8 cells

B

C

Live GFP+

Figure 14 | Transferred Hoxb8 cells become myeloid cells in EAE mice A. Scheme of the experimental approach. Adoptive transfer of Hoxb8 cells transduced with retroviral sgRNA vector, expressing NT sgRNA and GFP fluorophore, into the EAE induced mice. **B.** Representative FACS plots of Hoxb8 cells expressing Cd45 and Cd11b in cell culture (Culture Day 0), before the transfer into mice (Culture Day 2), 6 days after the transfer isolated from several organs: blood, femur, vertebra, spinal cord, spleen, lymph nodes (lumbar, inguinal, mesenteric) **C.** Percentage of Cd45+Cd11b+ Hoxb8-derived (Live GFP+) cells (n=4 mice).

We then wanted to further characterize Hoxb8-derived myeloid cells found in the inflamed spinal cord by investigating the expression of several receptor markers by FACS staining. Among Cd45+Cd11b+ cells, some (~19%) expressed the neutrophil marker Ly6G+, but majority was negative for Ly6G. Among the monocyte (Ly6G-) population, we observed both Ly6C+ and Ly6C- monocytes with a majority of Ly6C- cells (~62%) (**Figure 15A,C**). Among the Ly6G- population, almost all cells (>97% for F4/80, ~87% for Cd11c) were positive for macrophage markers F4/80 and Cd11c, and some cells (~34%) were positive for activation marker MHCII (**Figure 15B,D**). Their endogenous counterparts (GFP-) cells also showed similar expression patterns with small differences probably because the GFP- population might include more heterogeneous cell populations such as microglia, NK cells, dendritic cells, eosinophils which we could not exclude with our staining panels. We also checked other organs for the expression of F4/80 and MHCII in Hoxb8-derived cells, MHCII+ cells were highly present in lymph nodes and spleen as well, indicating that their functional phenotype is not restricted to the spinal cord (**Supplementary Figure 5A,B**)

Interestingly, we observed differential Ly6G marker expression in different organs, Ly6G^{Low} to Ly6G^{High} ratio was highest in the spinal cord, suggesting that cells tend to be monocytes in the inflamed spinal cord (**Supplementary Figure 5C**). This could be due to the tissue-specific differentiation or recruitment signals. We also evaluated the blood for other potential cell types that can express Cd11b, and we confirmed that Hoxb8-derived cells are negative for eosinophil marker (SiglecF) and natural killer (NK) cell marker NK1.1 (**Supplementary Figure 5D,E**)
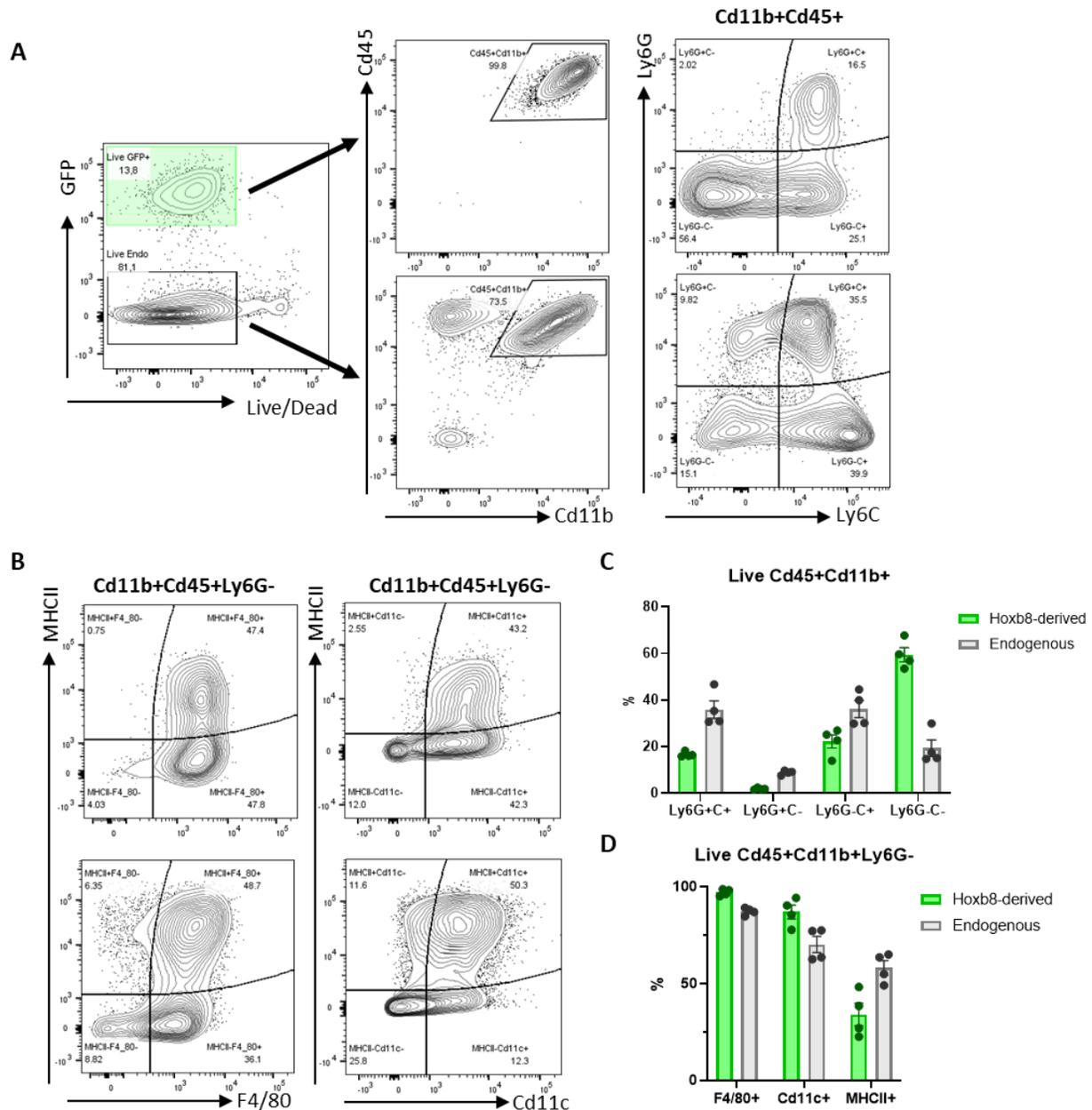
Figure 15 | Characterization of Hoxb8-derived myeloid cells in the spinal cord. A. Representative FACS plots of Live Hoxb8 (GFP+) and Endogenous (GFP-) cells for the expression of Cd45 and Cd11b, Ly6G and Ly6C (in Cd11b+Cd45+ gate) **B.** MHCII and F4/80 (in Cd11b+Cd45+Ly6G- gate), MHCII and Cd11c (in Cd11b+Cd45+Ly6G- gate). **C.** Percentage of Ly6G/C +/- in Live Cd45+Cd11b+ and **D.** F4/80+, Cd11c+, MHCII+ cells in Live Cd45+Cd11b+Ly6G- in Hoxb8 (GFP+) and Endogenous (GFP-) derived cells (n=4 mice).

We also histologically investigated the spinal cord of GFP+ Hoxb8 cells transferred animals. Dr. Paula Sanchez performed the staining, scanning, and analysis of the sections. We observed the presence of Cd11b+GFP+ Hoxb8-derived cells in EAE lesions. We observed no differences in the distribution of Hoxb8-derived cells in various lesion depths compared to their endogenous counterparts Cd11b+GFP- cells, confirming their natural recruitment to the inflamed spinal cord during EAE **(Figure 16A-C)**.
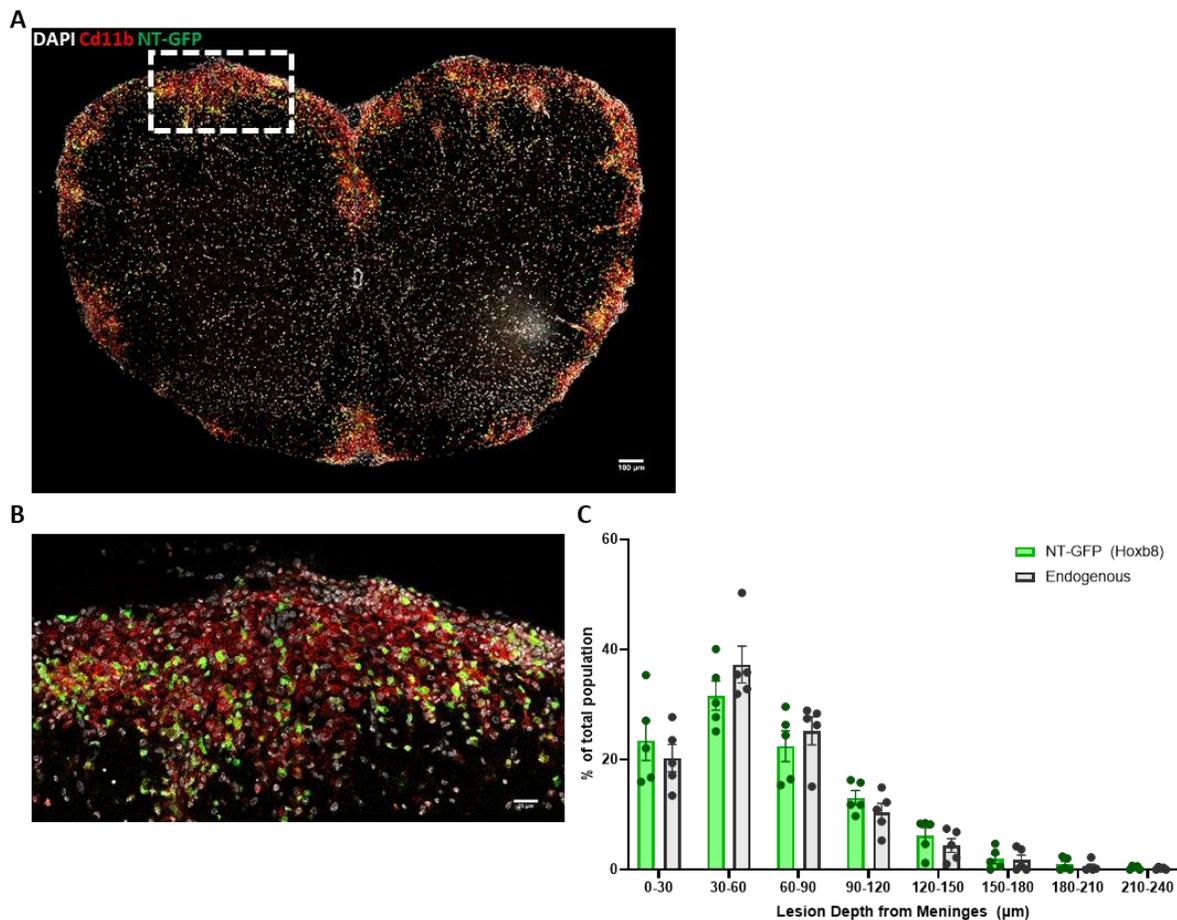
Figure 16 | Hoxb8-derived myeloid cells infiltrate the EAE spinal cord lesions A. A representative histology section of the spinal cord from EAE mice stained with DAPI for nucleus, Cd11b for the myeloid marker. NT-GFP represents Hoxb8-derived cells expressing NT sgRNA and GFP fluorophore. Scale:100µm. A white rectangular with dashes refer to B **B.** A closer look at the lesion site. Scale:25µm **C.** Percentage of Hoxb8-derived cells (Cd11b+GFP+) and Endogenous cells (Cd11b+GFP-) in total population in different lesion depth from meninges (µm). Each dot represents one lesion. Data are shown from one animal.

Overall, these results suggest that adoptively transferred Hoxb8 progenitor cells with myeloid potential can adapt to the physiological environment of the body and mimic their endogenous counterparts in terms of differentiation, recruitment, and activation in the spinal cord during EAE. They are also found in other organs, offering a valuable and simple tool to study large-scale genetic manipulations in monocytes/macrophages *in vivo*.

3.2.2 Migration of Hox8-derived monocytes to the inflamed spinal cord is CCR2-dependent

To assess whether Hoxb8-derived monocyte/macrophages infiltration to the inflamed spinal cord is an active or passive migration, we targeted Ccr2, a known chemokine receptor that is required for monocyte recruitment to inflammatory sites (C. L. Tsou et al., 2007). We deleted Ccr2 in Hoxb8 cells and transferred them to EAE induced animals. To control for experimental variation, we co-transferred GFP-expressing Ccr2KO Hoxb8 cells together with Tdtomato-expressing NT cells (**Figure 7A**). Ccr2 deficient monocytes (Ly6G-) were significantly diminished in the spinal cord but not in the spleen, relative to the blood (**Figure 7B**), indicating that Hoxb8-derived monocyte migration to the inflamed spinal cord is Ccr2-dependent. In line with previous studies (C. L. Tsou et al., 2007), Ccr2 deficient cells were enriched in the bone marrow. On the other hand, Ccr2 deficient neutrophils (Ly6G+) showed no impact on recruitment to the spinal cord, as expected. These results suggest that Hoxb8-derived monocytes are functionally recruited from the bone marrow and blood via Ccr2 to the inflamed spinal cord during EAE.
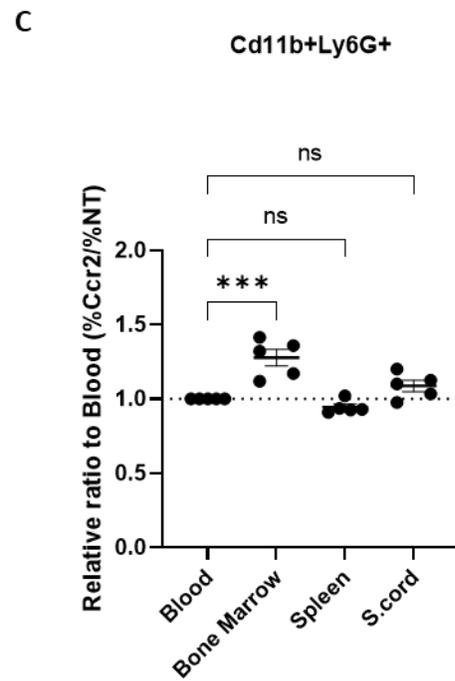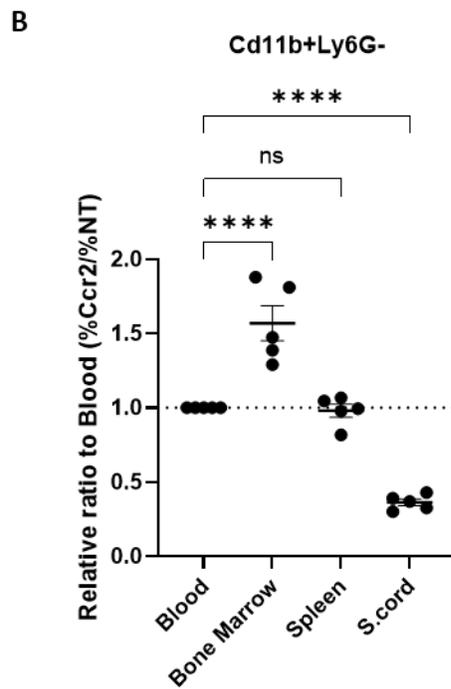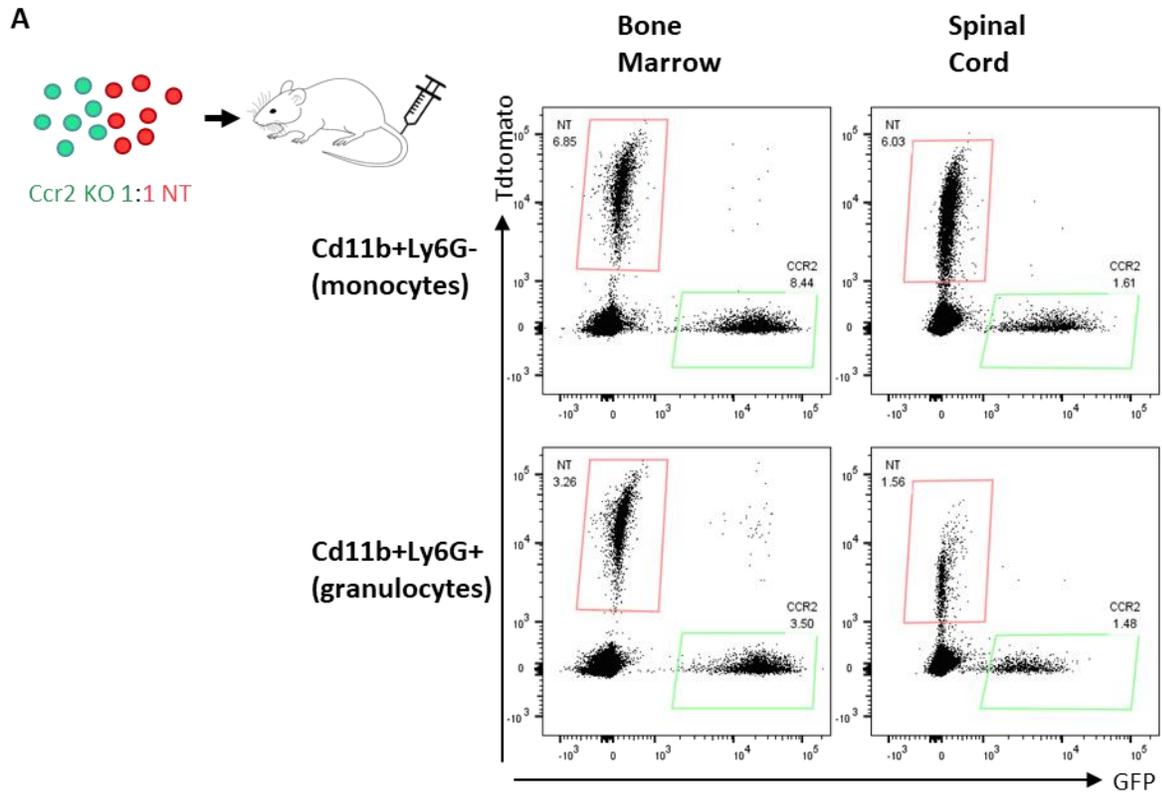
Figure 17 | Migration of Hoxb8-derived monocytes to the spinal cord in EAE is CCR2-dependent.
A. Representative FACS plots of Hoxb8 cells transduced with retroviral sgRNA vector, targeting
Ccr2 (with GFP backbone) or NT (with Tdtomato backbone) in the bone marrow and spinal cord.
B. One-way ANOVA with Dunnett's multiple comparisons test comparing blood (control) with
other tissues (bone marrow, spleen. spinal cord (s.cord)) in Cd11b+Ly6G- monocytes and **C.** in
Cd11b+Ly6G+ granulocytes. The ratio of %CCR2/%NT is normalized to 1 in the blood (n = 5 mice,
***P < 0.001, ****P < 0.0001, P=0.9926 for blood vs spleen in B, P=0.5613 for blood vs spleen
and P=0.2353 for blood and s.cord in C, mean ± sem)

3.2.3 Hox8-derived macrophages polarize to M_{Arg1} and M_{iNOS}

Next, we wanted to assess the functional phenotypes of macrophage polarization in Hoxb8-
derived cells in the spinal cord with our classical polarization markers Arg1 and iNOS. In the same
experiment, we also wanted to confirm that we can technically identify a polarization deficient
phenotype. To do so, we co-transferred GFP expressing Arg1 KO cells together with Tdtomato-
expressing NT cells as a control (**Figure 7A**). We observed overall a similar degree of polarization
in NT cells compared to their endogenous counterparts, although the iNOS+ population was
slightly higher than endogenous cells for both NT and Arg1 KO cells (**Figure 7B**). As expected we
saw significantly less Arg1 expression in Arg1 KO cells compared to the NT control, while iNOS
polarization was not significantly affected (**Figure 7B**). These results indicate that Hoxb8-derived
cells can gain polarization phenotypes similar to the endogenous population and we can
technically identify cells with an altered polarization phenotype.
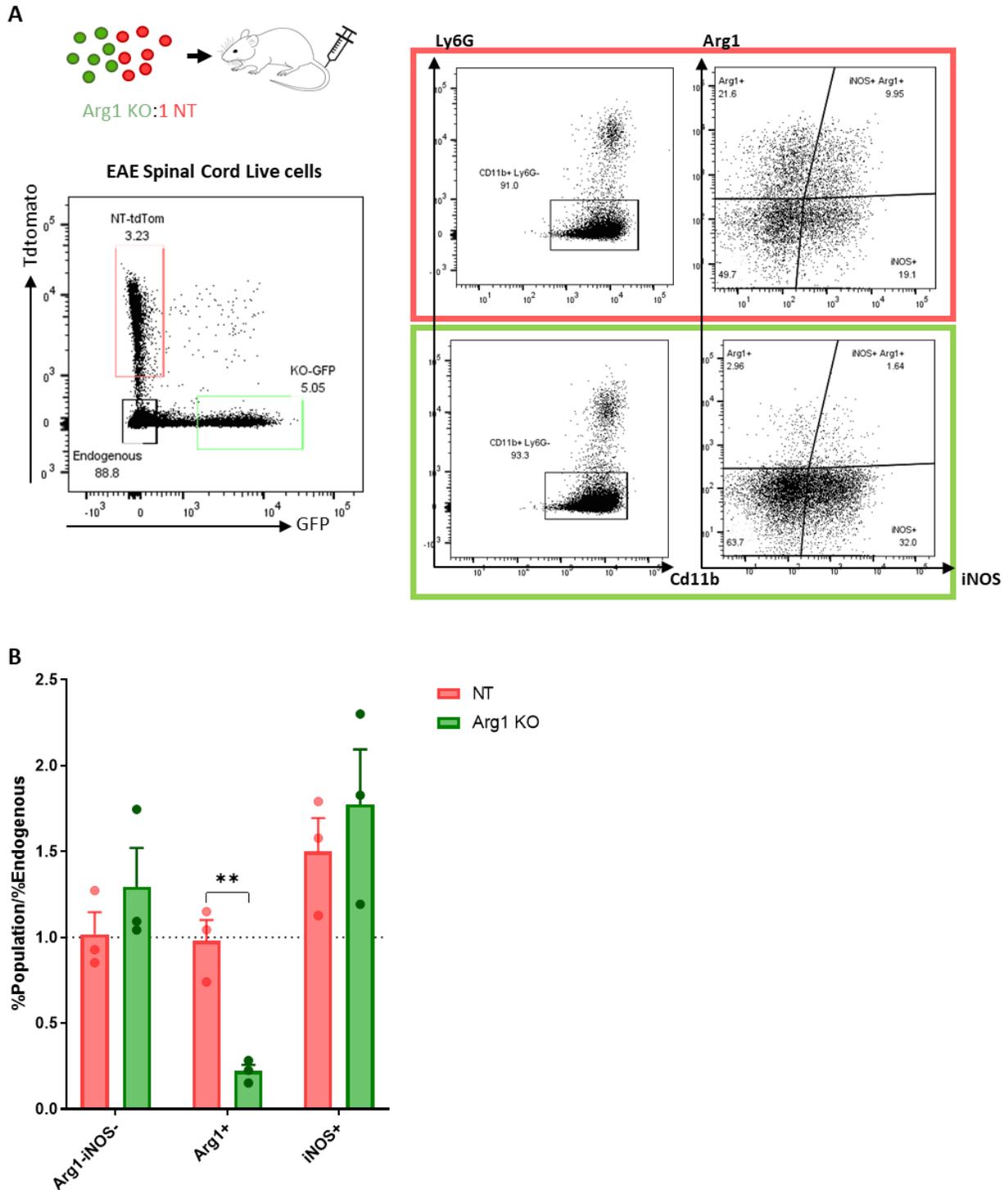
Figure 18 | Hoxb8-derived macrophages polarize to M$_{Arg1}$ and M$_{iNOS}$ in the spinal cord of EAE mice. A. Representative FACS plots of Hoxb8 cells transduced with retroviral sgRNA vector, targeting Arg1 (with GFP backbone) or NT (with Tdtomato backbone) in the spinal cord. **B.** Relative polarization of Cd11b+Ly6G- NT and Arg1 cells to endogenous cells (normalized to 1), unpaired two-tailed Student's t-test comparing NT and Arg1 KO in Arg1+ population (n=3 mice, **P < 0.01, P=0.0042, mean ± sem)

3.2.4 Transcriptome comparison of Hoxb8-derived Monocytes, M$_{Arg1}$ and M$_{iNOS}$ populations to the endogenous populations

To further characterize our Hoxb8 adoptive transfer system, we also investigated whether other markers in M$_{Arg1}$ and M$_{iNOS}$ populations correlate between Hoxb8-derived macrophages and endogenous macrophages. To do that, we isolated cells from the spinal cord of EAE induced Hoxb8 cells transferred animal, and we sorted Arg1+ and iNOS+ cells separately from both Hoxb8-derived and endogenous populations. We sorted Ly6C+ monocytes from the blood as a reference transcriptome. Transcriptome analysis showed that up- and down-regulated transcripts in Arg1+ and iNOS+ populations compared to the blood are correlating between Hoxb8-derived and endogenous macrophages (**Supplementary Figure 6A,B**), further confirming that Hoxb8-derived macrophages can acquire phenotypes similarly to their endogenous counterparts in the inflamed spinal cord.

We also observed that macrophage activation markers in both Arg1+ and iNOS+ populations, monocyte markers in the blood monocytes are similarly expressed between Hoxb8-derived and endogenous populations (**Supplementary Figure 6C-E**). Although Hoxb8-derived monocyte/macrophages express monocyte/macrophage markers at both protein and mRNA level, interestingly, Hoxb8 and Cd19 are still detected transcripts in Hoxb8-derived monocytes. This could be due to the leftover transcripts from progenitor states of Hoxb8 cells which are missing in the endogenous population.

Overall, these data indicate that Hoxb8-derived cells can be recruited into the spinal cord during EAE via the classic monocyte recruitment signaling and acquire functional macrophage phenotypes similar to their endogenous counterparts, confirming that they might be a useful tool for studying the role of monocytes and macrophages in EAE.

3.2.5 *In vivo* CRISPR screen to identify cytokines regulating M$_{Arg1}$ and M$_{iNOS}$ polarization during EAE

Cytokines have been shown to be central instructors of phagocyte phenotypes *in vitro and in vivo* (Sica & Mantovani, 2012). Therefore, we first wanted to identify cytokines driving macrophage polarization during EAE. We designed a CRISPR library containing sgRNAs targeting cytokine receptors and their corresponding key signaling pathway members ('Cytokine library'). We transduced Hoxb8 cells in culture with a retroviral vector expressing the library sgRNAs, transferred them to EAE induced animals and sorted four monocyte/macrophage (Cd11b+ Ly6G-) populations from the spinal cord: M0 (Arg1-iNOS-), Arg1+ (Arg1+iNOS-), iNOS+ (Arg1-iNOS+), double positive (DP) (Arg1+iNOS+) cells. We analyzed the results by MAGeCK. We first checked the migration phenotype among the cytokine receptors by comparing the sgRNA distribution between the bone marrow and spinal cord. We included Ccr2 gene in the library as a positive control for migration. Only Ccr2 KO cells were significantly depleted in the CNS with high fold change, suggesting that KO of cytokine receptors do not impact the migration of monocytes to the inflamed spinal cord (**Figure 19A**).

We then compared Arg1+ cells to M0 cells among the cytokine receptors (**Figure 19B**). We included Arg1 gene in the library as a positive control. Indeed, Arg1 KO was one of the top depleted hits in the Arg1+ population. Moreover, the TGF-β receptors (Tgfbr1 and Tgfbr2), the GM-CSF receptors (Csf2ra and Csf2rb) and the IL6 receptor (Il6r) were among the top depleted hits in the Arg1+ population. The TNF receptors (Tnfrsf1 and Tnfrsf2) also showed a minor depletion phenotype in the Arg1+ population. Interestingly, the KO of the IFN-γ receptors (Ifngr1 and Ifngr2) and IFN alpha/beta receptors (Ifnar1 and Ifnar2) were significantly enriched in the Arg1+ population, suggesting a negative role of IFNs on M$_{Arg1}$ polarization. Quite surprisingly, the well-known M$_{Arg1}$ inducer cytokines IL4, IL13 and IL10 receptors did not come up as candidates, suggesting that these cytokines do not play essential roles in polarizing macrophages to the M$_{Arg1}$ phenotype in the context of active EAE. To control whether the absence of well-known M$_{Arg1}$ polarizing cytokine IL-4 was due to low responsiveness by Hoxb8-derived macrophages, we performed a CRISPR screen experiment *in vitro* with Hoxb8-derived macrophages, polarizing cells with IL4 and sorting Arg1+ and Arg1- cells. We showed that IL4 receptors (Il4r, Il2rg) and their

signaling members (Jak3, Stat6) were significantly depleted in the Arg1+ population, confirming that Hoxb8-derived macrophages can respond to the IL4 cytokine (**Supplementary Figure 7**).

We next compared iNOS+ cells to M0 cells (**Figure 19B**). We included Nos2 gene as a positive control. Indeed, Nos2 KO was one of the top depleted hits in the iNOS+ population. The TNF receptors (Tnfrsf1 and Tnfrsf2), and the IFN-γ receptors (Ifngr1 and Ifngr2) were significantly depleted in the iNOS+ population. Interestingly, the KO of TGF-β receptors (Tgfbr1 and Tgfbr2) were enriched in the iNOS+ population, suggesting a negative role of TGF-β on M_{iNOS} polarization.

We also looked at the behavior of the key signaling members of each pathway for both Arg1+ vs M0 and iNOS+ vs M0 comparisons. A key signaling member of each pathway, namely, TGF-β-Smad4, IFN-γ-Stat1, GM-CSF-Stat5b, TNF-Nfkb1, IL6R-Stat3 showed the same phenotype as their receptors (**Figure 19C-G**), supporting the involvement of the pathways in respective M_{Arg1} and M_{iNOS} polarization.

The KO phenotypes of Ccr2, Arg1 and Nos2 confirm that *in vivo* CRISPR screens using our Hoxb8 cell-based method can identify physiological phenotypes in monocytes/macrophages. Overall, our data show that TGF-β and GM-CSF, but not IL4, IL13 or IL10, are essential for M_{Arg1} polarization, whereas TNF and IFN-γ are essential for M_{iNOS} polarization in active EAE model. Moreover, the TGF- β and IFN-γ pathways showed suppressive phenotypes on M_{iNOS} and M_{Arg1} polarization, respectively, suggesting a potential crosstalk between two pathways regulating macrophage polarization.
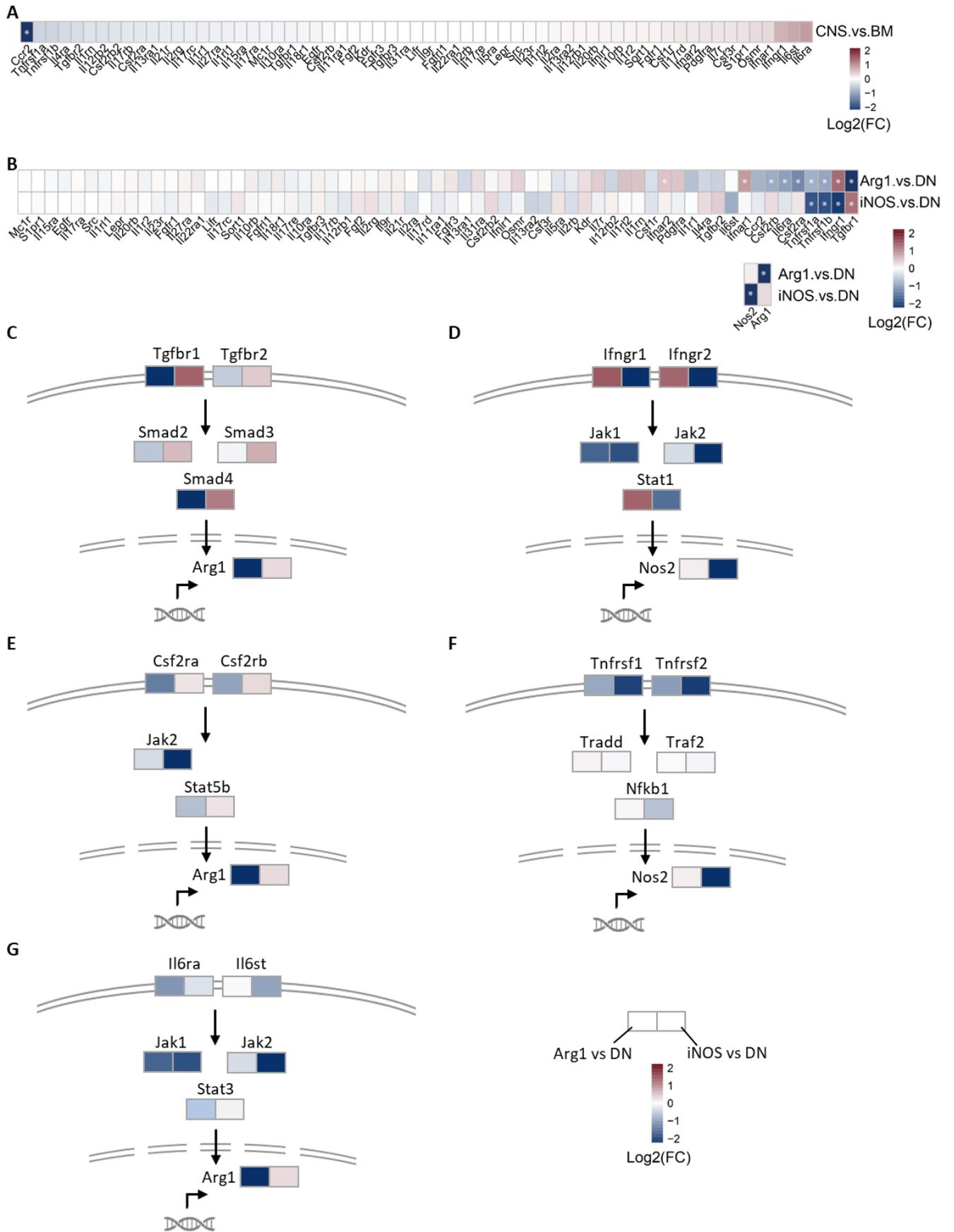
Figure 19 | *In vivo* CRISPR screen in Hoxb8-derived macrophages identified cytokines regulating M$_{Arg1}$ and M$_{iNOS}$ polarization during EAE. A. Heatmaps of the cytokine receptors for the CNS vs bone-marrow (BM) comparison, Ccr2 added as a positive control. **B.** Heatmaps of the cytokine receptors for Arg1+ vs double negative (DN, Arg1-iNOS-) and iNOS+ vs DN comparisons, Arg1 and Nos2 added as positive controls. Stars indicate significance (good sgRNAs ≥ 2, |log2(Fold-Change)| > 3 standard deviations from the log2(FC) distribution, adjusted p-value < 0.05). **C-G.** Schematic representation of TGF-β, IFN-γ, GMCSF, TNF-α, IL6 signaling pathways with heatmaps from the screen results.

3.2.6 Validation of hits with individually cloned sgRNAs

We next wanted to validate some of the top hits by single KO experiments. To control for experimental variation and to reduce the number of animals we co-transferred Tdtomato-expressing NT cells, GFP-expressing KO-1 cells and BFP-expressing KO-2 cells in an equal ratio to the same animal. We injected Tgfbr1 KO (GFP) together with Ifngr1 (BFP) cells (**Figure 20A).** Tgfbr1 KO cells showed significantly impaired M$_{Arg1}$ polarization and significantly enhanced M$_{iNOS}$ polarization compared to NT cells. On the contrary, Ifngr1 KO cells showed significantly enhanced M$_{Arg1}$ polarization and significantly impaired M$_{iNOS}$ polarization compared to NT cells (**Figure 20B**), confirming the CRISPR screen results. The opposite behavior of KOs indicates a potential balance between TGF-β and IFN-γ signaling pathways regulating macrophage polarization during active EAE.
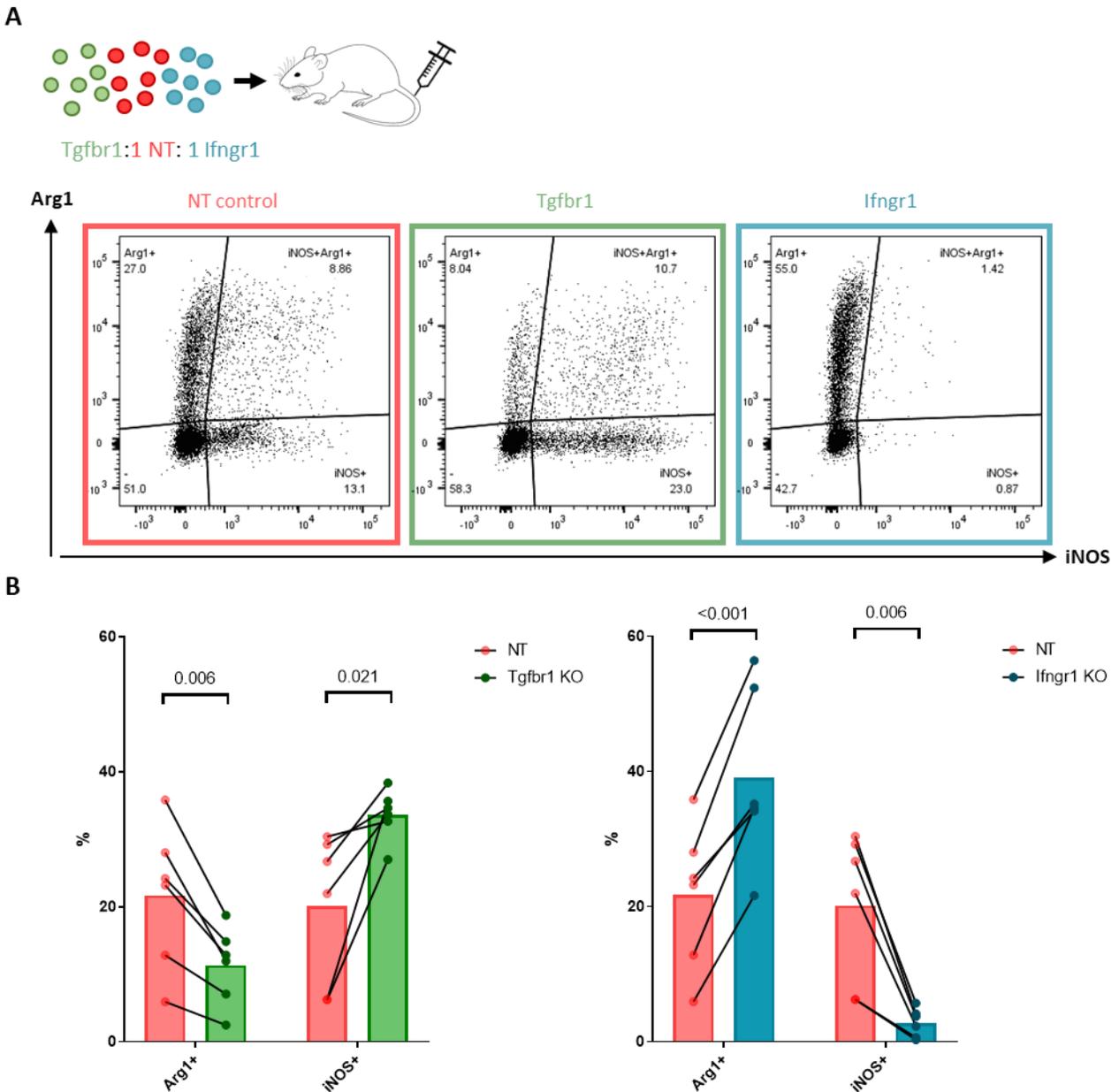
Figure 20 | Validation of Tgfbr1 and Ifngr1. A. Representative FACS plots of Hoxb8 cells transduced with retroviral sgRNA vector, targeting Tgfb1r (with GFP backbone) or Ifngr1 (with BFP backbone) and NT (with Tdtomato backbone) in the spinal cord for Arg1 and iNOS expression. **B.** Percentage of Arg1 and iNOS expression in Cd11b+Ly6G- Tgfbr1 KO and Ifngr1 KO cells compared to NT cells. Multiple paired two-tailed Student's t-test comparing KO cells to NT cells for Arg1+ and iNOS+ population (n=6 mice, p values are shown in the figure for each comparison), Experiments performed twice independently.

We injected Csf2ra KO (GFP) together with Il6ra (BFP) cells (**Figure 21A**). Csf2ra KO cells showed significantly impaired M_{Arg1} polarization compared to NT cells, whereas Il6ra KO cells had a mild but robust reduction in both M_{Arg1} and M_{iNOS} polarization compared to NT cells, confirming the CRISPR screen results. These results suggest that GM-CSF signaling is important to drive M_{Arg1} polarization, whereas IL6 signaling might have an impact on the general activation of macrophages in our active EAE model.
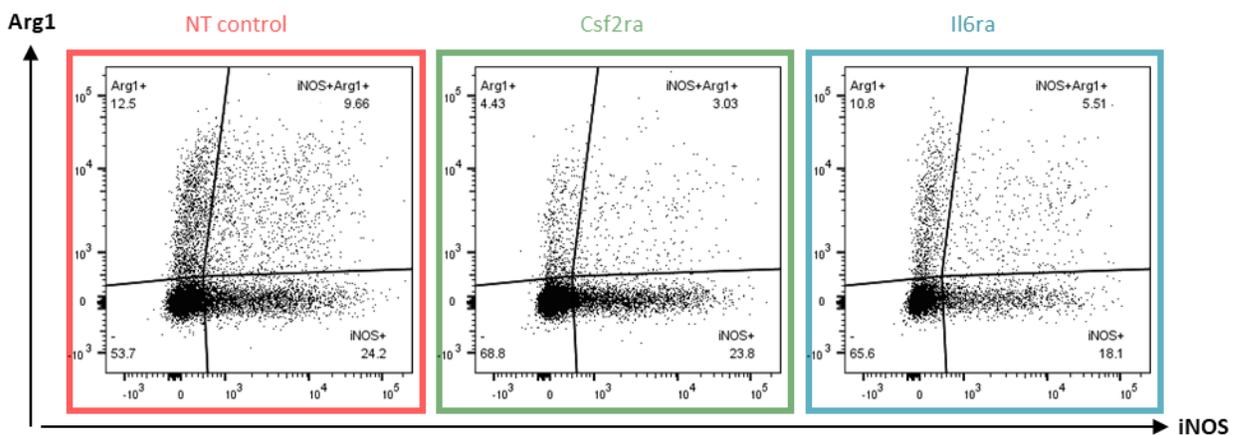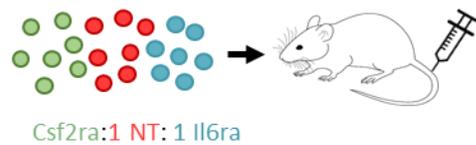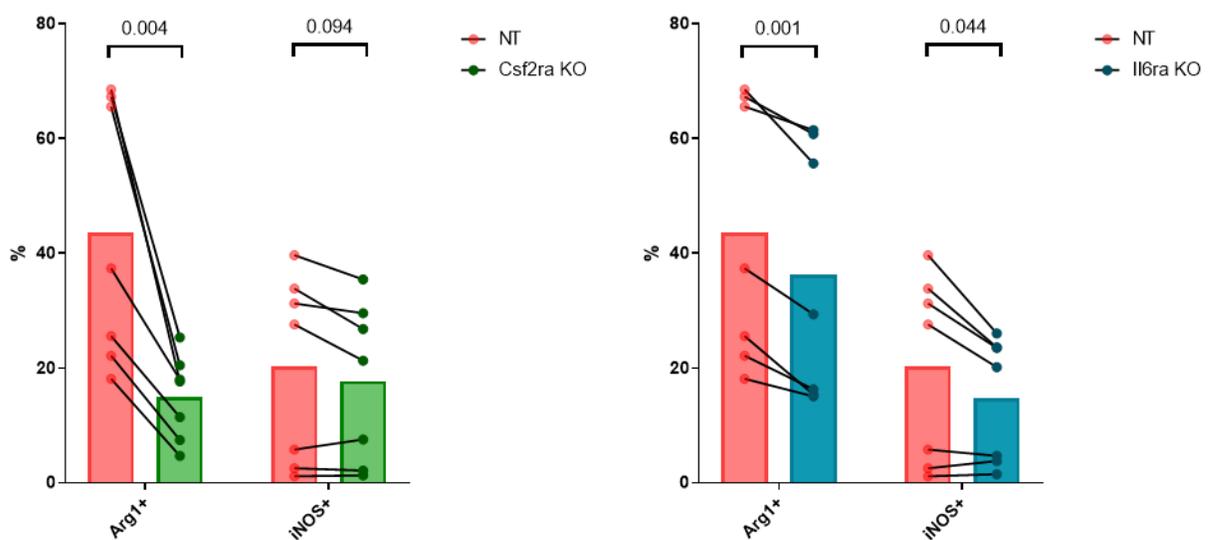
Figure 21 | Validation of Csf2ra and Il6ra. A. Representative FACS plots of Hoxb8 cells transduced with retroviral sgRNA vector, targeting Csf2ra (with GFP backbone) or Il6ra (with BFP backbone) and NT (with Tdtomato backbone) in the spinal cord for Arg1 and iNOS expression. **B.** Percentage of Arg1 and iNOS expression in Cd11b+Ly6G- Csf2ra KO and Il6ra KO cells compared to NT cells. Multiple paired two-tailed Student's t-test comparing KO cells to NT cells for Arg1+ and iNOS+ population (n=7 mice, p values are shown in the figure for each comparison), Experiments performed twice independently.

We injected Tnfrsf1a KO (GFP) together with Il4ra (BFP) cells (**Figure 22A**)**.** Tnfrsf1 KO cells had significantly impaired M_{iNOS} polarization compared to NT cells and had a mild but robust reduction in M_{Arg1} polarization. Il4ra KO cells showed no difference in M_{Arg1} polarization and showed a mild but significant increase in M_{iNOS} polarization compared to NT cells, confirming the CRISPR screen results. These results suggest that TNF-α signaling is mainly important to drive M_{iNOS} polarization but also slightly impairing M_{Arg1} polarization, whereas IL4 signaling, known as classical M_{Arg1} driver, does not play role in our active EAE model.

In all these experiments we confirmed target DNA perturbations for each gene by TIDE (**Supplementary Table 1**).

We further confirmed the lack of IL4 signaling in our EAE model on M_{Arg1} population by *in vivo* single KO experiment targeting Stat6 (**Supplementary Figure 8A**). Stat6 KO cells showed no change in M_{Arg1} polarization and showed a mild but significant increase in M_{iNOS} polarization compared to NT cells (**Supplementary Figure 8B**), replicating the Il4ra phenotype. We also sorted Arg1+ and Arg1- Stat6 KO cells and confirmed Arg1 expression in Stat6 KO cells by TIDE (**Supplementary Figure 8C**).

Overall, these data further confirms that TGF-β and GM-CSF, but not IL4, are the main drivers of M_{Arg1} polarization, whereas TNF-α and IFN-γ are the main drivers of M_{iNOS} polarization in our active EAE model.
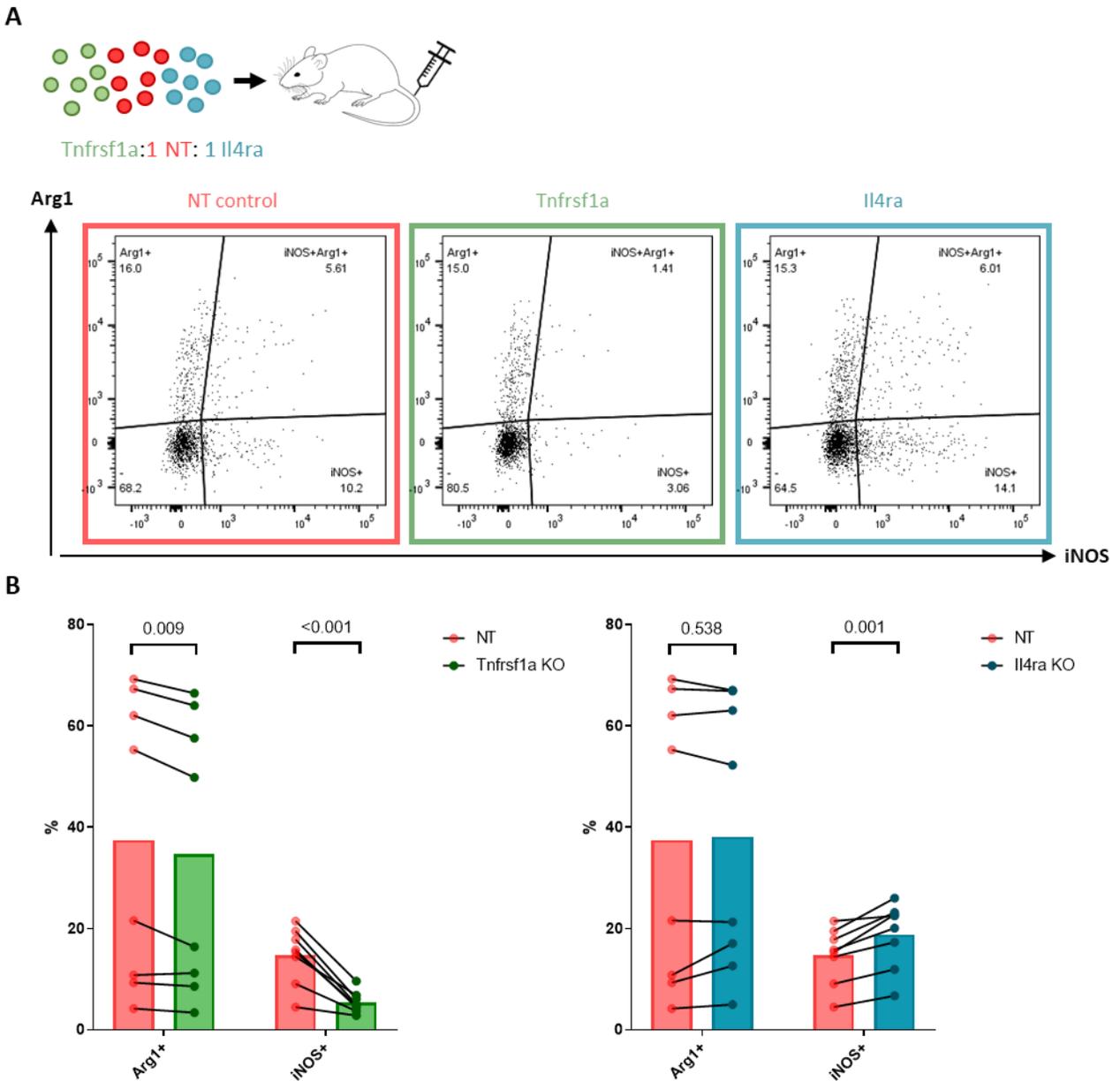
Figure 22 | Validation of Tnfrsf1a and Il4ra. A. Representative FACS plots of Hoxb8 cells transduced with retroviral sgRNA vector, targeting Tnfrsf1a (with GFP backbone) or Il4ra (with BFP backbone) and NT (with Tdtomato backbone) in the spinal cord for Arg1 and iNOS expression. **B.** Percentage of Arg1 and iNOS expression in Cd11b+Ly6G- Tnfrsf1a KO and Il4ra KO cells compared to NT cells. Multiple paired two-tailed Student's t-test comparing KO cells to NT cells for Arg1+ and iNOS+ population (n=8 mice, p values are shown in the figure for each comparison), Experiments performed twice independently.

3.2.7 *In vitro* cytokine combinations in BMDMs confirm the synergistic effect on M$_{Arg1}$ and M$_{iNOS}$

Our *in vivo* Cytokine library screen in macrophages during EAE revealed that TGF-β and GM-CSF are both required for M$_{Arg1}$ polarization, whereas IFN-γ and TNF-α are both required for M$_{iNOS}$ polarization. We wanted to test whether we can recapitulate the *in vivo* macrophage phenotypes *in vitro* by adding the respective recombinant cytokines. To do so, we used classical BMDM cultures and incubated them with different combinations of cytokines. We could indeed observe higher Arg1 expression at the protein level in TGF-β and GM-CSF co-treated cells, compared to individual cytokine treated cells (**Figure 23A**). Similarly, IFN-γ and TNF-α co-treated cells had higher iNOS expression compared to individual cytokines treated cells (**Figure 23B**). These results indicate that the combination of two cytokines has an increased impact on respective polarizations, recapitulating the *in vivo* phenotypes we observed with Hoxb8-derived macrophages *in vivo*. We also tested whether IL6 has an additive effect *in vitro*, however, we observed no impact of IL6 for both M$_{Arg1}$ and M$_{iNOS}$ polarization (**Figure 23C,D**). Surprisingly, treating cells with TGF-β, GM-CSF, IFN- γ, TNF-α at the same time enhanced M$_{Arg1}$ polarization and impaired M$_{iNOS}$ polarization (**Figure 23C,D**). We next wanted to investigate whether treating cells with four cytokines (TGF-β, GM-CSF, IFN- γ, TNF-α) induces the same phenotype as *in vivo* in Tgfbr1 and Ifngr1 KO cells. To do so, we used BMDM cells isolated from Cas9 animals. Tgfbr1 KO cells showed significantly impaired M$_{Arg1}$ polarization and significantly enhanced M$_{iNOS}$ polarization, whereas Ifngr1 KO cells showed significantly enhanced M$_{Arg1}$ polarization and significantly impaired M$_{iNOS}$ polarization compared to NT cells (**Figure 23E,F**), reproducing the *in vivo* phenotype obtained with Hoxb8-derived macrophages.

We then wanted to assess whether the synergistic effect of cytokine combinations is regulated at mRNA level. To do so, we incubated BMDMs with cytokines for 8h and performed 3' bulk mRNA sequencing. RNA levels also showed an increase in iNOS and Arg1 when the cytokines were present in combination (**Supplementary Figure 9A**). These results further confirm the synergistic effect of TGF-β and GM-CSF on M$_{Arg1}$, and IFN-γ and TNF-α on M$_{iNOS}$ also on transcriptome level. It should be noted that not only Arg1 and iNOS levels are getting affected but the rest of the

transcriptome also change by the combination of cytokines compared to individual cytokines (**Supplementary Figure 8B**).

Overall, these findings show that *in vitro* treatment of BMDM cells with respective recombinant cytokines supports the phenotypes of Hoxb8-derived macrophages in the inflamed spinal cord environment during active EAE, strengthening the validity of the Hoxb8 transfer method *in vivo*.
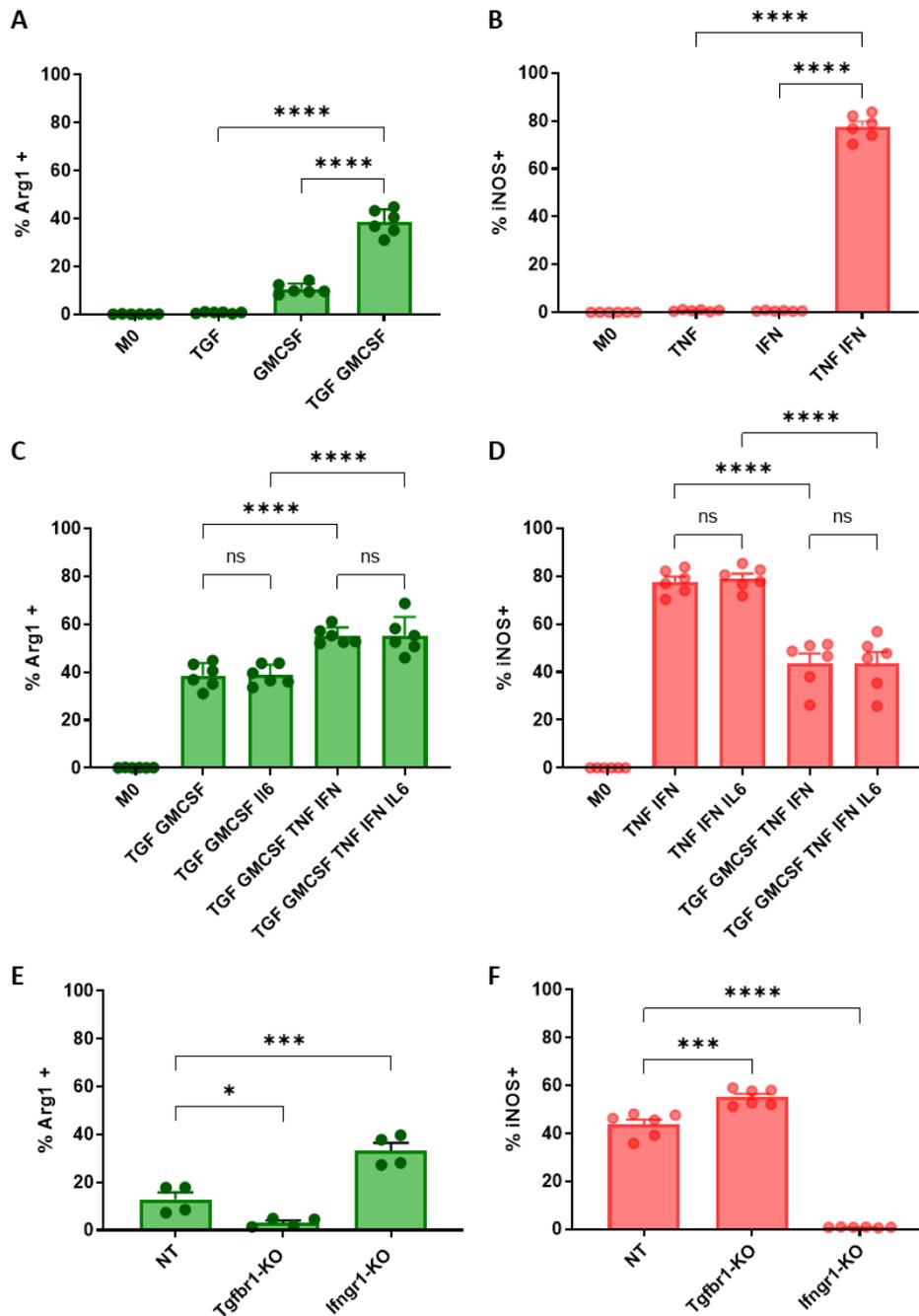
Figure 23 | *In vitro* treatmant of BMDMs with cytokine combinations. A. One-way ANOVA with Šídák's multiple comparisons test comparing TGF-β+GMCF treated cells with TGF-β and GMCSF only treated cells **B.** One-way ANOVA with Šídák's multiple comparisons test comparing TNF-α+IFN-γ treated cells with TNF-α and IFN-γ only treated cells. **C.** One-way ANOVA with Šídák's multiple comparisons test. **D.** One-way ANOVA with Šídák's multiple comparisons test. **E.** One-way ANOVA with Dunnett's multiple comparisons test comparing NT (control) cells with Tgfbr-KO and Ifngr KO cells treated with TGF-β+GMCF+TNF-α+IFN-γ (20ng/ml each) for 24h **F.** One-way ANOVA with Dunnett's multiple comparisons test comparing NT (control) cells with Tgfbr1-KO and Ifngr1 KO cells treated with TGF-β+GMCF+TNF-α+IFN-γ (20ng/ml each) for 24h. (each dot represents a biological replicate, (ns:not significant $P > 0.05$, *$P < 0.05$ ***$P < 0.001$, ****$P < 0.0001$, mean ± sem) (TGF:TGF-β, IFN:IFN-γ, TNF:TNF-α)

4. DISCUSSION

Here in my thesis, I established *in vivo* CRISPR KO screens to identify essential regulators of two key steps of neuroinflammation during EAE; transmigration of MBP specific T cells from the periphery to the CNS across the BBB, and the development of macrophage phenotypes that participate in the formation and resolution of lesions. We performed a genome-wide *in vivo* CRISPR screen in T_{MBP} cells in a passive EAE model in Lewis rats. We compared the sgRNA abundance between peripheral organs (blood and spleen) and CNS organs (meninges and parenchyma). Our CRISPR screen identified known regulators of transmigration such as Itga4, Fermt3, Itgb1, Tln1, Cxcr3, Hsp90b1 as well as unknown regulators such as Grk2, Gnai2, Arih1, Ube2l3, Ets1. We validated the selected candidates from the screen with *in vivo* single KO experiments. We showed that Grk2 deficiency inhibits T cells´ migration by its function on S1pr1 internalization. We also revealed that Ets1 inhibits T cell migration, and its absence results in increased T cell activation and cytotoxicity in the parenchyma.

Moreover, we performed an *in vivo* CRISPR screen targeting cytokine receptors and key members of the signaling pathways in Hoxb8-derived monocyte/macrophages in an active EAE mouse model. We compared the sgRNA abundance between M_{iNOS} (pro-inflammatory) and M_{Arg1} (anti-inflammatory) phenotypes in the inflamed spinal cord. Our CRISPR screen identified that TGF-β and GMCSF pathways primarily drive macrophages to the M_{Arg1} phenotype, whereas TNF-α and IFN-γ pathways primarily drive them to the M_{iNOS} phenotype. Notably, we revealed that well-known M_{Arg1} phenotype driver cytokines such as IL4, IL13 and IL10 do not play a role in our experimental setup. We validated the selected candidates from the screen with *in vivo* single KO experiments. We further showed that TGF-β and GMCSF act synergistically on M_{Arg1}, whereas IFN-γ and TNF-α act synergistically on M_{iNOS} phenotype in *in vitro* polarized BMDMs.

4.1 Migration of T_MBP cells across the BBB

4.1.1 *In vivo* vs *in vitro* BBB

The most challenging part about studying immune cell trafficking across the BBB *in vitro* is to mimic the physiological conditions of the barrier. So far, there have been several *in vitro* BBB models developed based on co-culturing brain endothelial cells together with astrocytes and/or pericytes on a transwell membrane, where the quality of the barrier is assessed by high transendothelial electrical resistance (TEER) (Wilhelm, Fazakas, & Krizbai, 2011). However, the endothelial cells used in *in vitro* BBB models show different characteristics. For example, monolayers of primary mouse brain microvascular endothelial cells maintain better BBB characteristics compared to the widely used monolayers of immortalized mouse brain endothelioma bEnd5 cells, as the latter do not express the necessary tight junction proteins (Steiner, Coisne, Engelhardt, & Lyck, 2010). Moreover, most of the *in vitro* BBB models lack shear flow, which is an indispensable parameter during T cell crawling *in vivo* against the direction of flow to search for sites for diapedesis, as observed by *in vivo* imaging of T cells during EAE (Bartholomäus et al., 2009). Although recent advances allowed researchers to develop newer *in vitro* BBB models, such as 3D culture systems which include flow conditions, vascularized brain organoids, brain endothelial cells derived from human induced pluripotent stem cells (iPSCs) (Erickson, Wilson, & Banks, 2020), further developments are still necessary to fully mimic the complex *in vivo* BBB characteristics. This becomes especially important during non-homeostatic conditions such as EAE, where inflammation changes the features of the BBB. Therefore, our genome-wide *in vivo* CRISPR screen to study MBP-specific T cell migration across the BBB provides valuable information as the BBB characteristics are fully preserved. To our knowledge, there is yet no study published in the literature studying T cell trafficking in an *in vivo* environment at a genome-wide scale. We performed our screen in Cd4+ MBP antigen-specific T cells, but similar screens could also be performed in different subtypes of T cells or in cells with different antigen specificity to compare patterns of migratory phenotypes. For example, β-synuclein, a protein found mainly in presynaptic terminals in the brain, can also behave as a CNS autoimmune antigen as β-synuclein specific T cells are enriched in the blood of MS patients. When T_MBP and T_β-syn cells are adoptively transferred to rats, T_β-syn cells exclusively infiltrate the gray matter of the cerebral

cortex, whereas T_{MBP} cells are only found in the white matter of the spinal cord and brain (Lodygin et al., 2019).

4.1.2 Trafficking of T_{MBP} cells

Our CRISPR screen identified Itga4, a well-known integrin molecule in the VLA-4 complex required for T cell adhesion to its endothelial ligand VCAM-1, as one of the top hits. This is in line with the strong therapeutic effect of targeting VLA-4 with the FDA-approved drug Natalizumab to avoid T cell infiltration into the CNS. T cell arrest is mediated by both LFA-1 interaction with ICAM-1 and VLA-4 interaction with VCAM-1, however, the KO of LFA-1 units (Itgal and Itgb2) did not show a depletion phenotype in our screen. Similar to our findings, in the same rat EAE model, anti-LFA-1 treatment did not block the migration of T_{MBP} cells into the CNS, whereas anti-VLA-4 antibody prevented cells crossing of the BBB (Bartholomäus et al., 2009), showing that in the absence of LFA-1 - ICAM-1 interaction, T_{MBP} cells can still migrate using VLA-4 - VCAM-1 interaction. These different migratory phenotypes could also be due to the preferential interaction used for adhesion by different T cell types in different EAE models. For example, it has been shown that migration of Th17 cells into the brain parenchyma is LFA1 – ICAM-1 dependent but VLA-4 – VCAM-1 independent, whereas Th1 migration into the spinal cord is dependent on VLA-4 – VCAM-1 interaction (Rothhammer et al., 2011) (Glatigny, Duhen, Oukka, & Bettelli, 2011). The adoptive T cell transfer EAE model that we used in the screen is a Th1 driven model and so our results are likely biased towards trafficking requirements of autoreactive Th1 cell. Therefore, it would be important to further investigate how different T cell types use different ways to reach the CNS, for a more complete understanding of T cell trafficking in the broader context of MS pathology.

Although Natalizumab is an effective treatment for RRMS, it, unfortunately, increases the risk of infectivity of oligodendrocytes by the John Cunningham (JC) virus causing a fatal disease called Progressive Multifocal Leukoencephalopathy (PML) (Weissert, 2011). The mechanism through which Natalizumab increases the risk of infection is thought to be through blocking the migration of virus specific Cd8+ T cells that function as a part of the CNS immunosurveillance. Therefore, developing alternative therapeutic targets for blocking the migration of CNS antigen-specific T cells without affecting the CNS immunosurveillance is critical (Young, MacLean, Dudani, Krishnan,

& Sad, 2011). Our study identified several potential targets for antigen-specific Cd4 T cell migration; however, future research should focus on how selective those targets are.

Interestingly, the KO of Itgb1, another component of VLA-4, had a significant but less strong effect on T cells migration to the CNS compared to the Itga4 KO. This might indicate that T_{MBP} cells can still migrate with a lower degree in the absence of Itgb1, whereas the presence of Itga4 is indispensable for CNS transmigration. It would be interesting to see how the absence of Itgb1 may affect the formation and function of the Itga4:Itgb1 dimer. Itga4 can also form a dimer with Itgb7 (LPAM-1), which did not show up as a hit in our screen. Similarly, Itgb1 can form a dimer with various other integrins, none of which showed a migration deficient phenotype in our screen. Upon activation by chemokines, integrin dimers undergo conformational changes with the binding of intracellular proteins Fermt3 (Kindlin-3) and Tln1 (Talin-1) (Hogg, Patzak, & Willenbrock, 2011) (S. Liu, Calderwood, & Ginsberg, 2000), which were also identified as hits in our screen. The KO of Tln1 had less strong effect compared to the Fermt3 KO, suggesting that T_{MBP} cells can still migrate with a lower degree in the absence of Tln1, whereas the presence of Fermt3 is indispensable for CNS transmigration. However, it should be noted that variations in the fold change might arise from the intrinsic variation of the sgRNA efficiency. Therefore, further confirmation of the KO efficiency is required to reach conclusions. Interestingly, Fermt3 has been shown to be required for passive EAE induction but not for active EAE induction, another example of the different regulation of T cell trafficking in different EAE models (Moretti et al., 2013). Like Fermt3 and Tln1, two isoforms of heat shock protein 90 (Hsp90), Hsp90aa1 and Hsp90ab1, have been shown to bind Itga4 in T cells during fever to mediate integrin mediated adhesion and transmigration (Lin et al., 2019). In our screen, the KO of Hsp90b1 (Hsp90 paralogue), but not Hsp90aa1 or Hsp90ab1 showed a significant depletion phenotype in CNS. The molecular chaperone function of Hsp90b1 on Toll-like receptors and integrins has also been described previously (Staron et al., 2010). Therefore, our results suggest that Hsp90b1 might play a role in T_{MBP} migration into the CNS by affecting Itga4/Itgb1 conformation.

Tethering and rolling are the initial steps of T cell migration, mediated by P-selectins (PSGL-1) expressed by T cells. However, mice deficient for P-selectins are not protected from EAE and from the invasion of T cells into the CNS parenchyma, although the rolling of T cells was abrogated

(Sathiyanadan et al., 2014). Our CRISPR screen also did not identify P-selectins as hits, confirming that the interaction of P/E selectins might be redundant for T cell transmigration, and integrin mediated adhesion and crawling might compensate for the tethering and rolling steps.

For the chemokine activation step, our screen identified Cxcr3 as one of the top hits and the only hit among the chemokine receptors. Upregulation of Cxcr3 in T_{MBP} cells and the presence of the corresponding cytokines, CXCL9/10/11, that are secreted by macrophages in the CNS, have been shown in a previous study with the same EAE model. Furthermore, in the same study, blocking Cxcr3 with antibody treatment prevented EAE (Schläger et al., 2016). These observations are in line with Cxcr3 KO being one of the strongest depleted hits in the CNS. Our data further suggest that in our model Cxcr3 is the only essential chemokine receptor involved in T_{MBP} cell trafficking into the CNS.

Overall, these data show that our genome-wide CRISPR KO screen in T_{MBP} cells could identify well-known positive regulators of T cell transmigration such as Itga4, Fermt3, Hsp90b1, Cxcr3, Itgb1, Tln1, confirming the confidence of our method. We could confirm the migration deficiency phenotype of Itga4, Hsp90b1, and Cxcr3 with single KO experiments in which we adoptively transferred control and KO T_{MBP} cells into the same animal and compared their accumulation in the CNS.

Since our analysis of known regulators confirmed the reliability of our screen, we next focused on less well-known candidates. Our library identified several TFs such as Cbfb, Foxo1, Prdm1 as depleted hits in the CNS. Cbfb plays role in Treg differentiation whereas Foxo1 is important for the formation of memory Cd8+ T cells (M. V. Kim, Ouyang, Liao, Zhang, & Li, 2013) (Rudra et al., 2009). Since both Cbfb and Foxo1 are important for T cell development and differentiation, their migration deficit phenotype might be due to abrogated function of Cd4 T cells. However, it should be noted that we delivered CRISPR perturbations to already differentiated, antigen-activated Cd4 T cells. Therefore, the question of whether Cbfb and Foxo1 might have a novel function in already differentiated Cd4 T cells should be addressed in the future. Prdm1 (Blimp1) has been also found to have broad functions in Cd8 and Tissue-resident memory (Trm) T cells (Welsh, 2009) (Mackay et al., 2016). Its role in T cell migration and egress has been reported in Cd8 and Trm cells but its effect in antigen-specific Cd4 T cells during neuroinflammation remains unknown.

Among the cluster of GPCR receptors, the deficiency of Grk2 and Gnai2 showed the highest depletion phenotype in the CNS. Gnai2 is one of the members of the Gαi protein family, which plays an important role in chemoattractant receptor signaling. Gnai2 deficient T cell transgenic models have disrupted T cell chemotaxis (I.-Y. Hwang, Harrison, Park, & Kehrl, 2017), which includes a lack of responsiveness to the three Cxcr3 ligands: CXCL9, CXCL10, and CXCL11 (B. D. Thompson et al., 2007). In addition to the Cxcr3 ligands, Gnai2 deficient cells also respond poorly to the S1pr1 ligand S1P, however, we did not observe a phenotype of disrupted migration of the S1pr1 KO from the blood into the CNS. Therefore, we concluded that the phenotype of Gnai2 in our CRISPR screen is linked to its effect on Cxcr3 signaling.

Grk2 drew our attention as a novel candidate for T cell transmigration into the CNS. Moreover, since kinases are druggable, targeting Grk2 could provide a potential therapeutic approach. Paroxetine, an FDA-approved serotonin reuptake inhibitor, is a potent inhibitor of Grk2 and Paroxetine-based Grk2 inhibitors have been being developed primarily for the treatment of cardiovascular diseases characterized by Grk2 overexpression (Seketoulie Keretsu, Swapnil P. Bhujbal, & Seung Joo Cho, 2019). Grk2 levels in lymphocytes have also been shown to be regulated in MS patients (Vroon et al., 2005). Grk2 phosphorylates GPCRs, typically on their C-terminal serine/threonine residues, leading to their desensitization and endocytosis. Besides its canonical kinase function, Grk2 can interact with many cellular partners as a multifunctional signaling hub in lymphocytes (J. Cheng, Lucas, & McAllister-Lucas, 2021). Lack of Grk2 correlates to less internalization of chemokine receptors, therefore causing an increase in chemokine response to several chemokines including CCL3, CCL4, CCL5 (Vroon et al., 2004). Because of the deficient CNS migration of the Grk2 KO T_{MBP} cells in our EAE model, we argue that Grk2-mediated Cxcr3 internalization cannot be the molecular mechanism mediating its phenotype, as an increased Cxcr3 response following lack of desensitization by Grk2 would be expected to boost the migration of T_{MBP} cells, rather than abrogate it. We also could not identify relevant regulated transcripts with bulk RNA sequencing of Grk2 KO cells in the spleen compared to NT cells, suggesting that the Grk2 KO phenotype is likely not mediated by transcriptional changes which was expected as kinases mostly drive post-translational changes. On the other hand, high levels of S1P in the blood is known to mediate S1pr1 desensitization through Grk2 function. It was reported that Grk2 mediated S1pr1 desensitization is required in T and B cells for the migration

of cells from blood into the lymph nodes against the S1P gradient, which was restored in S1P deficient mice (Arnon et al., 2011). Moreover, S1pr1 antagonist treated Grk2 deficient B cells showed partial recovery in their migration to lymph nodes and splenic follicles (I.-Y. Hwang et al., 2019). Therefore, we hypothesized that Grk2 mediated S1pr1 internalization might be the cause of migration-deficient phenotype in Grk2 KO T$_{MBP}$ cells that they are not able to leave the blood to transmigrate to the CNS, against the S1P gradient. Indeed, the KO of S1pr1 in Grk2 deficient cells rescued the migration phenotype of T$_{MBP}$ cells from the blood to the CNS. We could also track control NT and Grk2 KO T$_{MBP}$ cells by *in vivo* two-photon imaging. Grk2 KO T$_{MBP}$ cells showed no difference in adherence and crawling, but the number of extravasated T cells across the endothelial barrier was significantly diminished in Grk2 deficient cells.

Our CRISPR screen also identified negative regulators that limit T cell transmigration to the CNS. However, the number of such negative regulators that have a robust migration phenotype is less than positive regulators. This could be because all T$_{MBP}$ cells tend to migrate to CNS, as they are antigen-specific and activated, making the sensitivity to detect additional enhanced migration lower. Nevertheless, the KO of the Ets1 transcription factor showed an enhanced migration phenotype. Ets1 has been previously shown to be a suppressor of pathogenic T cell response in Atopic Dermatitis (C.-G. Lee et al., 2019) and a negative regulator of Th17 differentiation (Moisan, Grenningloh, Bettelli, Oukka, & Ho, 2007). It has been also identified as a risk locus in GWAS studies of T cells for Atopic Dermatitis (Paternoster et al., 2015). Its role in antigen-specific T cell migration to CNS during neuroinflammation holds potential interest and it has not been addressed yet. We showed that Ets1 deficient T$_{MBP}$ cells in the parenchyma exhibit a more aggressive T cell phenotype with higher activation and more cytotoxic markers. However, future research is required to unravel how the more aggressive phenotype is linked to the enriched migration phenotype in the passive EAE model.

Our CRISPR screen in T$_{MBP}$ cells did not only identify regulators of transmigration across the BBB but also identified regulators that control T cell entry into and egress from the spleen, the largest secondary lymphoid organ. For example, S1pr1 KO T$_{MBP}$ cells were unable to exit the spleen. T cells follow the gradient of S1P, and by regulating S1pr1 on their surface they can enter or leave tissues (Matloubian et al., 2004). The regulation of S1pr1 can happen in multiple ways. The

transcriptional regulation of S1pr1 is mediated by the TF Klf2, whose KO was also enriched in the spleen when compared to the blood in our library. Another regulatory mechanism is the agonist-induced internalization of the receptor. When S1P levels are high in the environment, S1pr1 gets internalized and is no longer available on the cell surface (Rivera, Proia, & Olivera, 2008). Agonist-induced internalization of S1pr1 is the mode of action of Fingolimod, an FDA-approved drug for MS. In our screen, the KOs of Arih1 and Ube2l3 are also highly enriched in the spleen when compared to the blood, however, their function in T cell egress has not previously been described. Arih1 and Ube2l3 interact together to mediate ubiquitination of target proteins. Further studies are required to search whether there is a link between Arih1/Ube2l3 and the regulation of S1pr1.

4.2 Macrophage polarization

4.2.1 A novel method to study monocyte/macrophages *in vivo*

Circulating monocytes are short-lived cells (1-7 days), they undergo spontaneous apoptosis and newly differentiated monocyte waves come from common myeloid progenitors in the bone marrow (Fahy, Doseff, & Wewers, 1999). Monocytes that infiltrate into tissues and mature to macrophages can survive up to months (Gonzalez-Mejia & Doseff, 2009). Because of the short lifespan of monocytes, genetic manipulations should be delivered at an earlier stage of differentiation to result in a continuous production of manipulated monocytes. To study the function of a gene specifically in monocytes/macrophages *in vivo*, transgenic animals carrying myeloid-specific deletions (e.g. LyzM-Cre Flox/Flox) need to be generated, thus screening for multiple genes is often costly and time consuming. Therefore, we started searching for alternative ways to perform *in vivo* CRISPR screens in the monocyte/macrophage population in the spinal cord of EAE. We have previously shown that direct injection of *in vitro* differentiated, and M$_{iNOS}$ polarized (LPS + IFN-γ) BMDMs to the spinal cord with a finely drawn glass capillary into the spinal cord of EAE mice can mimic the polarization phenotype switch from M$_{iNOS}$ to M$_{Arg1}$ as their endogenous counterparts to a certain degree (Locatelli et al., 2018). However, this method is not suitable for CRISPR screens for multiple reasons. First, functional recruitment of monocytes to the spinal cord during neuroinflammation, and their routes for infiltration might have an impact on the formation of polarization phenotypes. In addition, the injection would already cause tissue

damage to the spinal cord, potentially affecting the results of the polarization. Second, cytokines that are used *in vitro* to polarize macrophages might not be present *in vivo*. For instance, LPS, a bacteria-derived endotoxin, is absent in CNS during EAE. Finally, the number of cells that can be injected into the spinal cord is very limited for a screen. An alternative way to study macrophage polarization phenotypes *in vivo* could be to genetically manipulate hematopoietic stem cells (HSC) isolated from bone marrow and transfer them into lethally irradiated recipients to allow reconstitution of immune cell populations, which occurs in 6-8 weeks (Chappaz, Saunders, & Kile, 2021). Although several studies could show that manipulation of LSK (lineage negative, including HSC, Lin$^-$Sca-1$^+$c-Kit$^+$) cells with CRISPR allow to detection of KO phenotypes after reconstitution (LaFleur et al., 2019), there are still multiple limitations. First, the number of HSCs found in the bone marrow of mice is low (0.01% of total nucleated cells (Challen, Boles, Lin, & Goodell, 2009)) and culture conditions of HSCs do not offer unlimited proliferative capacity. Second, LSK cells contain HSCs together with distinct multipotent progenitors (MMPs) which have lower and variable lineage-differentiation potential (Sommerkamp et al., 2021), and there is yet no optimized protocol to fully keep the pluripotent capacity of HSCs. Even short-term cultures of HSCs shift their characteristic from long-term LT-HSC to short-term ST-HSC, resulting in short-term myeloid reconstitution ability (<1 month) (H. Cheng, Zheng, & Cheng, 2020) (Dykstra et al., 2007). Therefore, by the time EAE is induced (after 6-8 weeks of immune reconstitution + 2 weeks of EAE) edited monocyte numbers drop significantly. This problem is specific to myeloid linage as lymphoid lineage such as T and B cells are long-lived cells. Finally, lethal irradiation of mice might impact the development of active EAE by affecting mainly the BBB although those effects are shown to be transient (Lumniczky, Szatmári, & Sáfrány, 2017).

Hoxb8 cells are immortalized progenitor cells with myeloid differentiation potential *in vitro* and *in vivo* (Redecke et al., 2013). Hoxb8 cells have unlimited proliferation capacity *in vitro*, allowing the conditions for large-scale genetic manipulations. Considering that monocytes have a short lifespan, we hypothesized that injecting monocyte progenitor cells 6 to 7 days before we analyzed EAE spinal cords would enable us to catch the wave of monocyte differentiation *in vivo.* We first transferred WT (generated from B6 mouse) Hoxb8 cells, however, we failed to detect a high number of cells in mice (data not shown). Upon estrogen withdrawal, some of the Hoxb8 cells undergo an initial phase of cell death before starting differentiation and expansion to their

respective cell types in the presence of M-CSF or GM-CSF (Redecke et al., 2013). In line with *in vitro* observations, inhibition of the apoptotic program promotes the survival of monocytes *in vivo* (Parihar, Eubank, & Doseff, 2010). Therefore, we next transferred BCL-2 overexpressing Hoxb8 cells, in which the apoptotic program is suppressed by BCL-2 overexpression, and we managed to detect a high number of transferred Hoxb8-derived cells *in vivo*. Since Hoxb8 cells have both myeloid and lymphoid potential, we decided to pre-license Hoxb8 cells into the myeloid lineage by incubating them in M-CSF for 2 days prior to the transfer. We could show that transferred Hoxb8 cells complete their myeloid differentiation *in vivo*, were being functionally recruited to the inflamed spinal cord and acquired polarization phenotypes as their endogenous counterparts, therefore offering a valuable tool to study genetic manipulations in monocytes/macrophages at large scales *in vivo* without extra manipulations (no irradiation is required) and long waiting times (the cells were transferred during EAE). Notably, microglia and infiltrated macrophages can express similar activation markers during inflammatory conditions, causing difficulties in distinguishing these two morphologically and functionally similar cell types by FACS staining (Koeniger & Kuerten, 2017) (Göbel, Ruck, & Meuth, 2018). On the other hand, Hoxb8-derived macrophages eliminate this potential conflict between the identification of the two populations. Moreover, we observed that Hoxb8-derived myeloid cells can become Ly6G+ neutrophils, Ly6C- and + monocytes, and potentially myeloid-derived dendritic cells. Therefore, we believe that this method can easily be used to study myeloid lineage cells in different disease models. One major limitation of this method is the impact of BCL-2 overexpression in differentiated cells. Although the main function of BCL-2 is inhibiting apoptosis by primarily regulating mitochondria outer membrane permeabilization, it can also impact the physiological functions of mitochondrial dynamics, autophagy and calcium pathways (Hardwick & Soane, 2013) (Kale, Osterlund, & Andrews, 2018). However, it should be noted that we did not observe any of those pathways to be differentially regulated between Hoxb8-derived and endogenous monocyte/macrophages in our 3' bulk mRNA sequencing data.

4.2.2 Cytokine Library screen in Hoxb8-derived Macrophages

Cytokines in MS and EAE, secreted by a number of different cells, including innate and adaptive immune cells, endothelial cells and CNS resident cells, shape and govern the progress of the

disease. Cytokines may act differently on different cell types and some might function as both pro- and anti-inflammatory depending on the environmental conditions (Göbel et al., 2018). A better understanding of the complex nature of the cytokine networks will enable researchers to therapeutically target them more efficiently. By using our Hoxb8 transfer method, we first wanted to identify cytokines that regulate macrophage M_{iNOS} and M_{Arg1} polarization in the spinal cord of EAE mice. To do that, we designed a CRISPR library targeting cytokine receptors and their key signaling members (Cytokine Library). Our screen confirmed the literature findings that monocyte recruitment to the inflamed spinal cord during EAE is highly dependent on CCR2 . Upon entry of CCR2+ Ly6C+ monocytes to the CNS, they are exposed to the combination of cytokines, become activated, differentiate into macrophages and myeloid-derived dendritic cells and gain polarization phenotypes (Nally et al., 2019).

We identified that TGF-β and GM-CSF signaling were mainly necessary for M_{Arg1} polarization, whereas IFN-γ and TNF-α signaling were mainly necessary for M_{iNOS} polarization. We showed a synergistic effect of respective cytokine combinations on M_{iNOS} and M_{Arg1} polarization *in vitro* with BMDM cells both at the protein and mRNA levels. Notably, there are multiple cytokines involved in each phenotype and the contribution of each is necessary to polarize macrophages. Interestingly, GM-CSF is a well-studied pro-inflammatory cytokine known to drive CCR2+ monocytes towards pathogenic phenotype in EAE (Croxford et al., 2015), however, in our study, it is contributing to M_{Arg1} polarization which is associated with tissue repair and lesion resolution function. One should however note that the analysis of macrophage polarization based on two markers (Arg1 and iNOS) alone is certainly an oversimplification and does not reveal the full spectrum of macrophage polarization based on their plasticity (Prinz & Priller, 2014). Indeed, a recent single-cell RNA sequencing study in EAE monocytes showed the heterogeneity of monocyte populations and their differential contribution to the disease (Giladi et al., 2020). On the other hand, TGF-β is known as an anti-inflammatory cytokine with its role in wound healing and tissue repair and it is associated with remission in MS (P. W. Lee, Severin, & Lovett-Racke, 2017). Monocyte specific deletion of the TGF-β receptor (LysM-Cre Tgfbr2(fl/fl)) resulted in the development of a chronic form of EAE with extensive demyelination (Parsa et al., 2016). Similarly, IFN-γ and TNF-α are well-known as main pro-inflammatory cytokines in EAE, however, the beneficial effect of IFN-γ and IFN-γ receptor KO in EAE suggest that IFN-γ could be protective as

well (Sosa, Murphey, Robinson, & Forsthuber, 2015). Similarly, TNF and iNOS have been considered to have potentially beneficial roles in addition to their known detrimental roles (Lind et al., 2017) (Probert, 2015).

Interestingly, in our CRISPR screen, TGF-β signaling deficient cells were enriched in the M_{iNOS} population and IFN-γ signaling deficient cells were enriched in the M_{Arg1} population. These results might indicate potential crosstalk between TGF-β and IFN-γ signaling, where the balance between the two signaling pathways might control the macrophage polarization in EAE. Indeed, crosstalk of these two pathways has been reported previously in different cell types and disease conditions (Ishida, Kondo, Takayasu, Iwakura, & Mukaida, 2004) (Tian et al., 2018) (I.-K. Park, Letterio, & Gorham, 2007) (Göbel et al., 2018). On the other hand, TNF-α receptor KO cells showed a minor reduction also in M_{Arg1} population. These could be due to TNF signaling having an impact on the general activation of macrophages, rather than only on one polarization state. Moreover, although IL6 is known for its pro-inflammatory function in MS (Stampanoni Bassi et al., 2020) it can function as an anti-inflammatory signal as well (Scheller, Chalaris, Schmidt-Arras, & Rose-John, 2011). The IL6 receptor KO showed a mild depletion in both M_{iNOS} and M_{Arg1} populations. Again, this argues that pro-inflammatory cytokine IL6 might have an impact on general macrophage activation.

Notably, receptors for classical M_{Arg1} inducer cytokines IL-4, IL-13 and IL-10 did not show a phenotype in our EAE model. We indeed confirmed that IL-4 receptor and Stat6 KO cells can express Arg1 in EAE lesions by single KO experiments and TIDE assays. These findings were unexpected as the impact of IL-4 and IL-10 on alternatively activated M2 macrophages, and their positive impact in MS and EAE was widely discussed (Vogelaar et al., 2018) (Jiang, Jiang, & Zhang, 2014) (Mantovani et al., 2004). These results clearly illustrate that classical macrophage polarization paradigms developed *in vitro* mostly with LPS and IFN-γ for M1, with IL4 and IL13 for M2 (Murray, 2017) can be quite limited compared to the complex *in vivo* phenotypes.

So far, several transgenic models with cytokine expression deficiency have been tested for their impact on EAE incidence, however, it should be noted that studies with most cytokine deficient transgenic animals are impacting other cell types as well including T cells, thus any imbalance of cytokine regulation in T cells might impact EAE development (Göbel et al., 2018). Another

advantage of our Hoxb8 transfer model is having a monocyte/macrophage-specific manipulation only in a small percentage of cells leaving all the cell types involved in EAE as wild-type. We indeed observed transfer of Hoxb8 cells does not impact the EAE clinical course.

One of the major questions that remains unknown is the source of cytokines. In EAE, it has been shown that T cells can produce GM-CSF, IFN-γ and TNFα, whereas IL6 and TGF-β can be secreted by numerous cell types, including CNS resident cells. To what extent the contribution of each cytokine by each cell type impacts the cytokine milieu of EAE lesions should be addressed in the future. Depending on the source and the phenotype it induces, it might also be possible to target the source of a cytokine rather than the macrophage population.

Overall, our *in vivo* Cytokine CRISPR screen in monocytes could identify cytokines regulating the activation of macrophages and their polarization towards M_{Arg1} and M_{iNOS} phenotypes, shedding light into the complex cytokine network in EAE. Our next steps will be analyzing the Cytokine library in different EAE models to see which regulatory properties are conserved in different types of CNS inflammation. Moreover, we plan to perform single-cell RNA sequencing with the KO candidates to obtain a better understanding of the impact of each cytokine signaling on different subsets of monocytes.

4.3 EAE models vs MS

MS is a complex disease with the involvement of multiple cell types contributing to its clinical and pathological heterogeneity. Although different models of EAE have been established in several species, including rodents and primates, to mimic the several aspects of MS pathology, such as inflammation, demyelination, re-myelination, and neurodegeneration, there are major differences between EAE and MS which make it difficult to translate scientific findings to humans. On the other hand, it is not surprising that EAE and MS are not very similar as EAE models have their own complexity with clinical and pathological heterogeneity. For example, although murine EAE models are well-established and widely used, the disease incidence and severity depends on several factors, including strain, age, gender, stress level, and gut microbiota (Berer et al., 2011). Researchers have developed guidelines for EAE publications to improve the quality and transparency of studies which can be helpful for researchers to control the factors impacting the

EAE incidence (Baker & Amor, 2012). One of the major differences between EAE and MS is that MS is a spontaneous disease, whereas EAE is induced with strong immune adjuvants together with antigens or with the transfer of antigen-specific T cells. Although there are spontaneous EAE models that have been developed (Waldner, Whitters, Sobel, Collins, & Kuchroo, 2000), they are dependent on carrying transgenic receptors on immune cells, making their use in research limited. Most of the EAE models show a monophasic disease course, which requires the use of more than one EAE model to be able to cover several aspects of MS pathology. Another difference is that most EAE models induce lesions in the spinal cord, whereas in MS brain lesions are also prominent. Furthermore, EAE models are primarily based on a disease mediated by CD4+ T cells, whereas CD8+ T cells are more prevalent in MS, with B cells playing a larger role. Also, EAE studies are mostly based on inbred animals to prevent genetic heterogeneity for the sake of reproducibility. Finally, most EAE studies are performed in rodents, so the genetic and phenotypic differences of the immune system between rodents and humans might have an impact on the disease course (Dendrou, Fugger, & Friese, 2015).

Despite their limitations, EAE models have made a significant contribution to MS research, allowing researchers to better understand the disease's pathogenesis and shed light on how the immune system and CNS resident cells contribute to the disease. EAE models also paved the way for the development of therapeutics for MS. For example, Natalizumab, which blocks lymphocyte trafficking by targeting the α4β1 integrin, was discovered using EAE experiments (Yednock et al., 1992). Therefore, EAE models will continue to aid in the understanding of disease mechanisms and the development of better therapies, particularly with the help of emerging technologies such as single-cell RNA sequencing and CRISPR screens.

4.4 Moving from *in vitro* to *in vivo* CRISPR KO screens (and limitations)

CRISPR is a powerful gene-editing tool and CRISPR screens allow us to study the effect of genetic perturbations for particular phenotypes at a genome-wide scale (Przybyla & Gilbert, 2021). So far, most of the CRISPR screens have been performed in *in vitro* settings, mostly with cell types with a high capacity of proliferation. However, moving from *in vitro* to *in vivo* CRISPR screens has become essential, as *in vitro* conditions fail to mimic complex *in vivo* environments (Kuhn et al., 2021). One of the major limitations for *in vivo* screening is the number of cells required for

genome-wide CRISPR screens. CRISPR screens require a 1000-time coverage representation of each gRNA to obtain statistically meaningful data (Tim Wang, Lander, & Sabatini, 2016). When considering targeting each of the 20.000 genes in the genome with 10 sgRNA per gene, a library with 200k gRNA would require to be represented by 200 million cells. Currently, the most efficient way to deliver library sgRNA constructs is transduction with lentiviral or retroviral particles. To prevent multiple integrations by the virus, MOI of 0.4 or below (<30% transduction efficiency) should be used, bringing up the number of cells to start a CRISPR screen experiment to around 600 million. Nevertheless, recent advances in the design of sgRNAs increased their on-target efficiency and allowed researchers to reduce the number of sgRNAs per gene to 3 to 6 in CRISPR libraries. Two biological replicates for a library with 6 sgRNA per gene have been found to offer the best trade-off to obtain statistical power. However, despite the improvements, CRISPR screens have a 10-20% false hit discovery rate (Ong, Li, Koike-Yusa, & Yusa, 2017). Therefore, independent of the number of replicates performed and the number of sgRNA used, validation of the phenotype with single KO experiments is required. Accurate prediction of sgRNAs with high editing efficiency and low off-target score and more precise delivery methods will be helpful to scale down the size of the libraries in the future. In our *in vivo* CRISPR screens in T cells and macrophages we aimed to have at least >100x coverage for each gRNA since from some populations such as the meninges and the blood in T cell screen, and the Arg1+iNOS+ population in macrophage population, reaching 1000x coverage was not feasible. Lower coverage could increase our false discovery rate, therefore we always included positive controls and performed validation experiments with single KOs.

It should be noted that the KO of a gene means complete deletion of a protein, however, most of the therapeutic compounds increase or decrease the levels of target proteins or their activation. Reduction in protein levels or activity might cause a different phenotype than the complete deletion of the protein. Therefore, performing CRISPRi or CRISPRa screens can also be considered to fully elucidate the phenotype of a gene/protein. Furthermore, thanks to the recent advances in single-cell RNA sequencing technologies, combining CRISPR KO screens with single-cell RNA sequencing can provide deeper insight about the effect of each genetic perturbation on cellular phenotypes (Przybyla & Gilbert, 2021). Another limitation in CRISPR KO screen experiments is that the expression of the Cas9 nuclease is required for gene editing. Because of its large size,

delivering it with viral particles becomes difficult. Fortunately, Cas9 expressing transgenic mice have been developed to overcome this limitation (Platt et al., 2014). Although studies show that Cas9 expression has no detrimental effect on tissue health and metabolism and does not induces inflammation (Bond et al., 2021), stable expression of Cas9 and gRNA may cause disturbance in some cells. One solution is to deliver Cas9 protein with the sgRNA complex (RNP) with non-viral methods such as nucleofection, in which the presence of Cas9-gRNA complex is transient. We performed our single KO validation experiments in T cells by delivering Cas9-gRNA complex transiently by nucleofection. All genes that we picked for single KO experiments showed the same phenotype as in the screen, in which we delivered both Cas9 and sgRNA with two independent retroviral particles. Some studies, alternatively, developed a system in which removal of Cas9 and other proteins such as antibiotic resistance markers are possible by delivering CRE at a later time point after introducing Cas9 and gRNA backbones between two loxp sites (Dubrot et al., 2021). However, the necessity of several deliveries reduces the feasibility of this approach.

Overall, in both T cell and macrophage projects, I performed *in vivo* CRISPR screens to shed light on two key pathological aspects of neuroinflammation, T cell infiltration into the CNS and macrophage polarization that contributes to lesion formation and resolution. Identifying the essential regulators of the respective biological processes with *in vivo* CRISPR KO screens can allow us to target the disease driving pathways in future. CRISPR is a potent genome editing technique, and along with other emerging technologies, it will continue to be an important tool in dissecting molecular mechanisms of the disease pathogenesis and developing new therapeutics for MS.

5. SUPPLEMENTARY MATERIAL
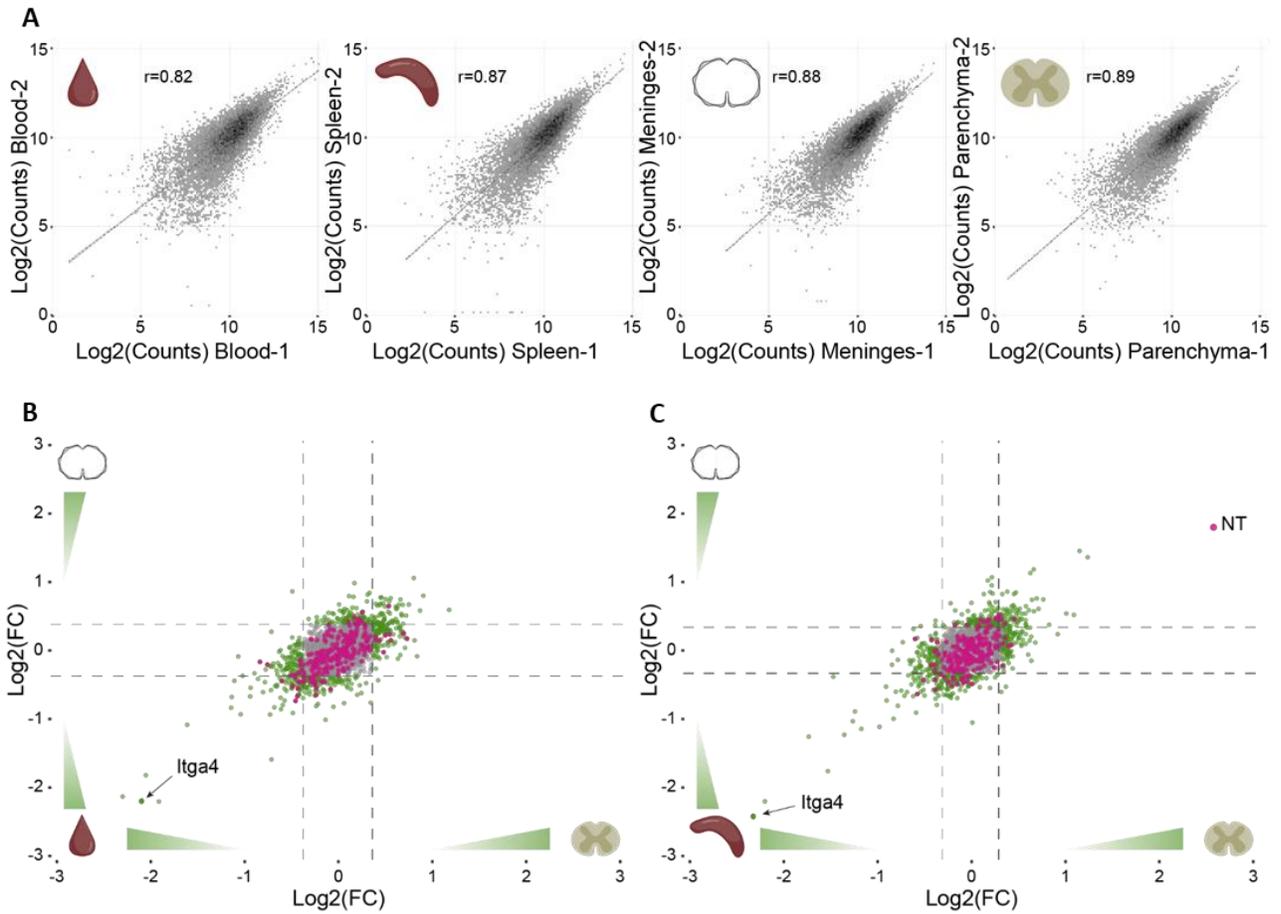
Supplementary Figure 1 | Validation CRISPR screen of T cell migration to the CNS. A. Correlation of individual replicates of the validation screen sgRNA log2 counts for (left to right) blood, spleen, meninges, and parenchyma. Correlation plot of migration from **B.** blood or **C.** spleen to meninges or parenchyma. Green indicates significant candidates at adjusted p-value < 0.05 and |log2(Fold-Change)| > 2 standard deviations of the log2(FC) distribution. Pink indicates Non-Targeted sgRNA controls.
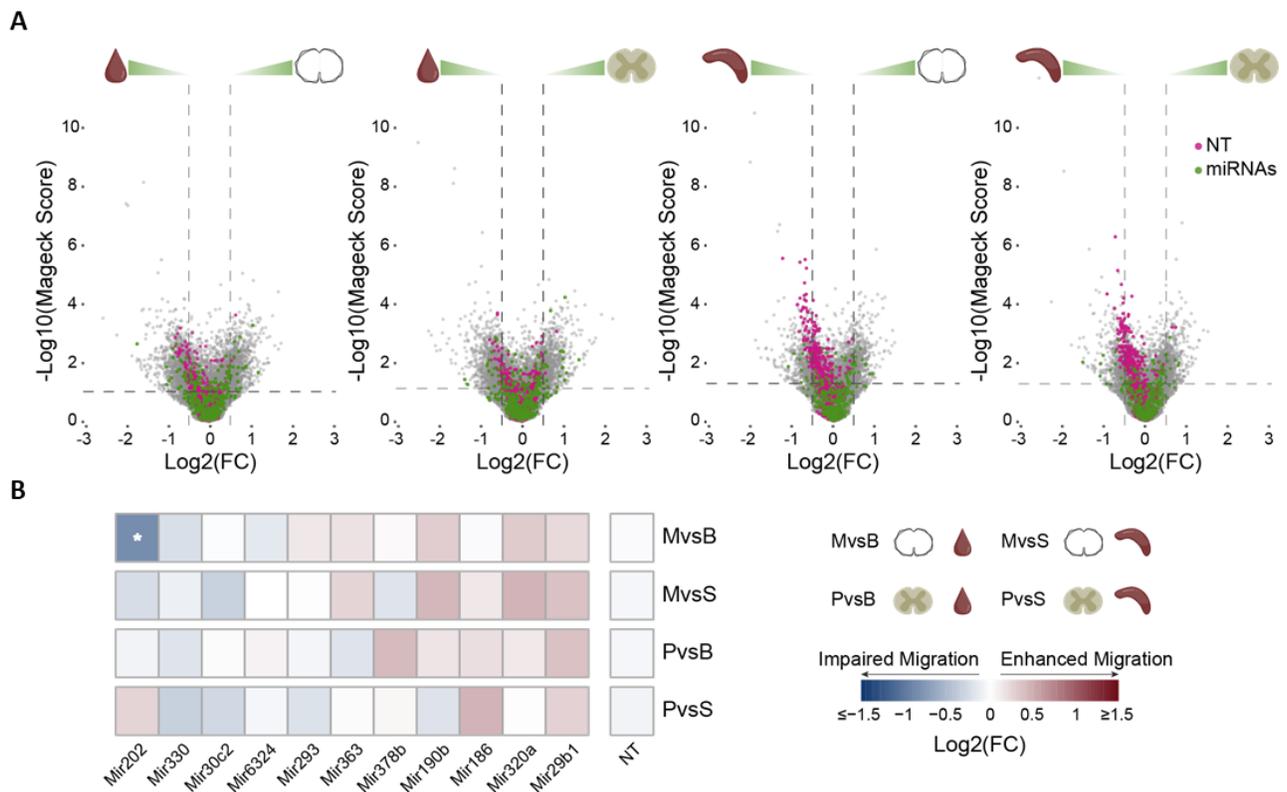
Supplementary Figure 2 | Regulation of T cell migration by miRNAs. A. Volcano plots of 4 comparisons (from left to right, Meninges vs Blood, Parenchyma vs Blood, Meninges vs Spleen and Parenchyma vs Spleen). Green indicates miRNAs, pink indicates Non-Targeted sgRNA controls. **B.** Heatmap of miRNAs across comparisons (from top to bottom Meninges vs Blood, Parenchyma vs Blood, Meninges vs Spleen and Parenchyma vs Spleen). Stars indicate significance (good sgRNAs > 3, |log2(Fold-Change)| > 3 standard deviations from the log2(FC) distribution, adjusted p-value < 0.05)

A
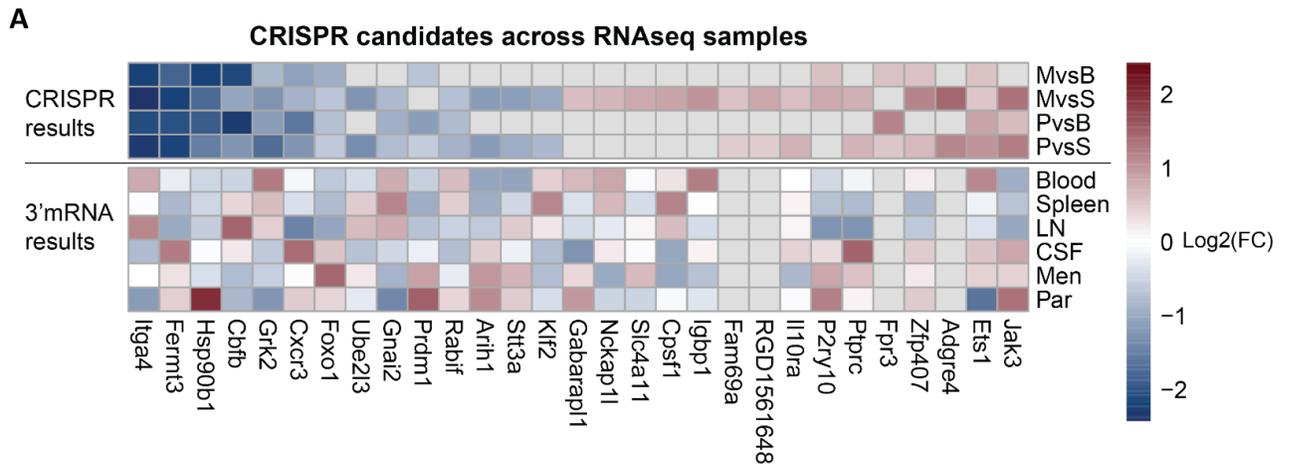
Supplementary Figure 3 | Transcriptional regulation of CRISPR candidates in T$_{MBP}$ cells. A. Bulk 3'mrna sequencing of sorted GFP expressing T$_{MBP}$ cells isolated from blood, spleen, lymph nodes (LN), CSF, meninges (Men), parenchyma (Par) on the onset of the disease (n=3 rats). Only top depleted and top enriched genes from the validation CRISPR screen are shown.
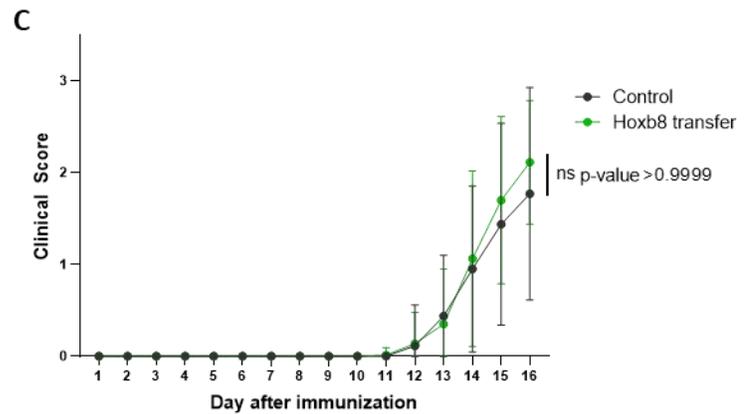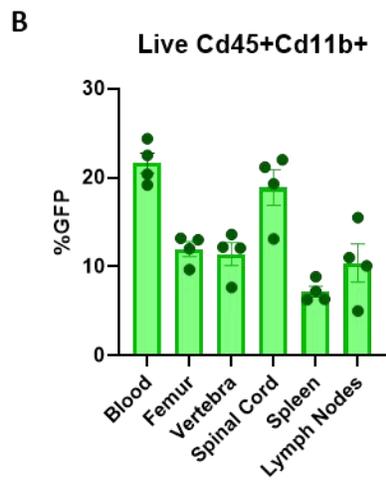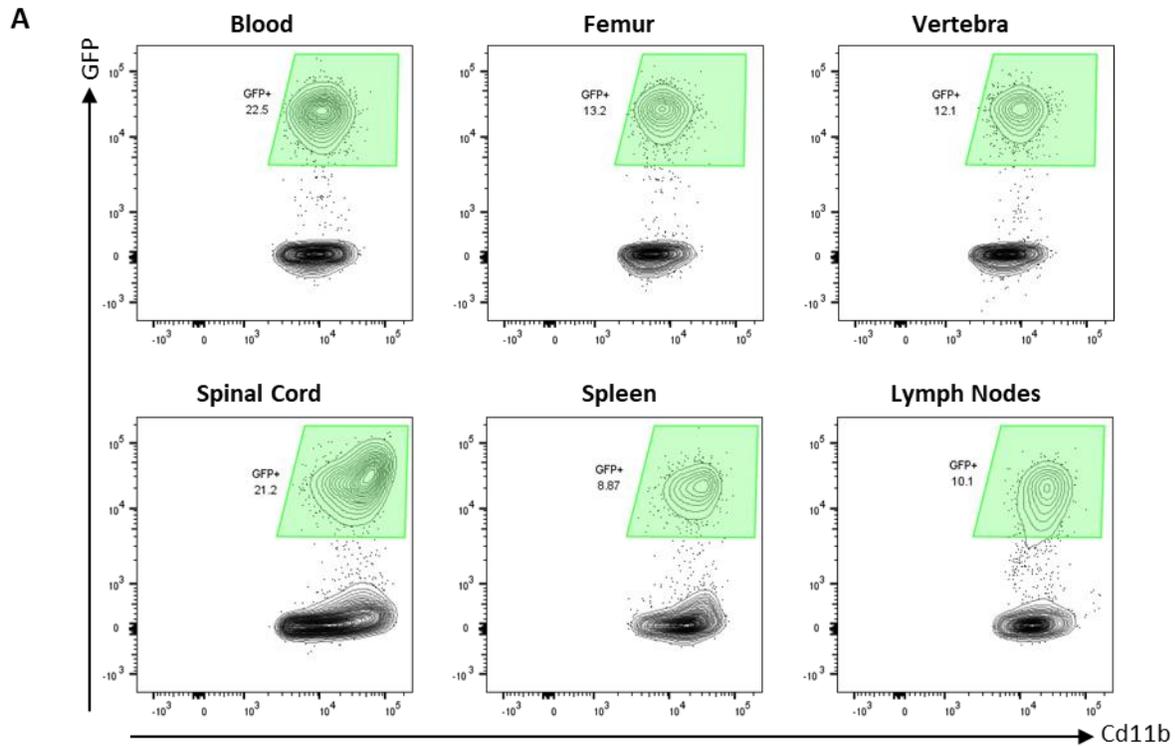
Supplementary Figure 4 | Hoxb8-derived myeloid cells in different organs A. Representative FACS plots of Live cells in different organs for GFP and Cd11b expression. **B.** Percentage of %GFP+ cells in myeloid lineage (Live Cd45+Cd11b) in different organs (n=4 mice). **C.** Kolmogorov-Smirnov test comparing clinical score of control and Hoxb8 injected EAE induced mice (n=40 mice for each group, data collected from independent experiments).
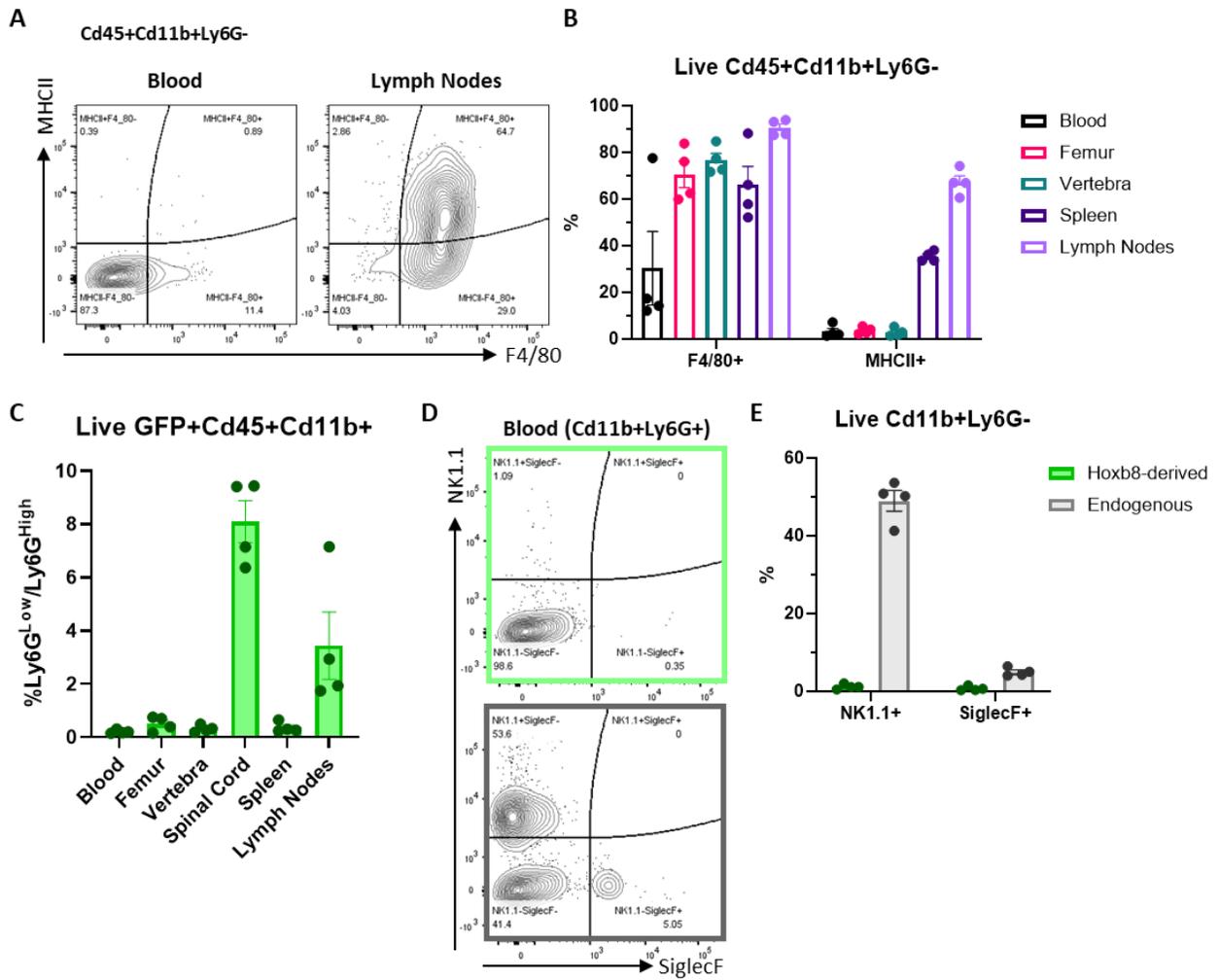
Supplementary Figure 5 | Characterization of Hoxb8-derived myeloid cells in EAE induced mice.
A. Representative FACS plots of Live Hoxb8 (GFP+) cells for the expression of F4/80 and MHCII (in Cd45+Cd11b+Ly6G- gate). **B.** Percentage of F4/80+ and MHCII+ cells in Live GFP+Cd45+Cd11b+Ly6G- Hoxb8-derived cells in different organs (n=4 mice)
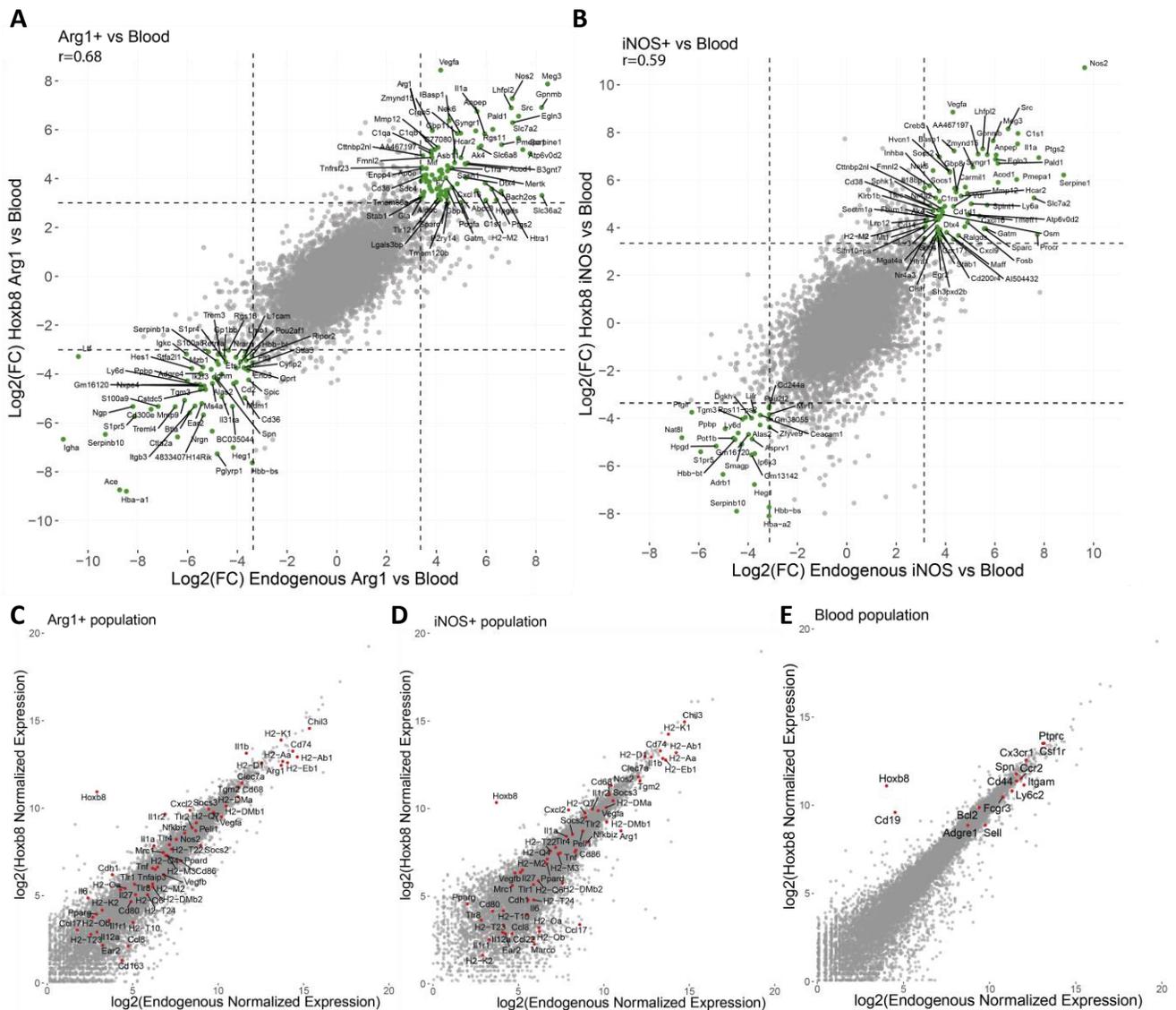
Supplementary Figure 6 | 3' Bulk mRNA sequencing of Hoxb8-derived and endogenous monocyte/macrophages. A. Correlation between Hoxb8 and Endogenous cells for up and down regulated transcripts in **A.** Arg1+population (r=0.68) **B.** iNOS+ population (r=0.59) compared to the blood Ly6C+monocytes. Green dots represent significantly regulated transcripts in both Hoxb8 and Endogenous populations. Normalized expression comparison between Hoxb8 and Endogenous populations in **C.** Arg1+ population **D.** iNOS+ population **E.** Blood Ly6C+ population. Red dots represent macrophage activation markers for C and D and monocyte markers for E. All RNA data obtained from 3 different mice.
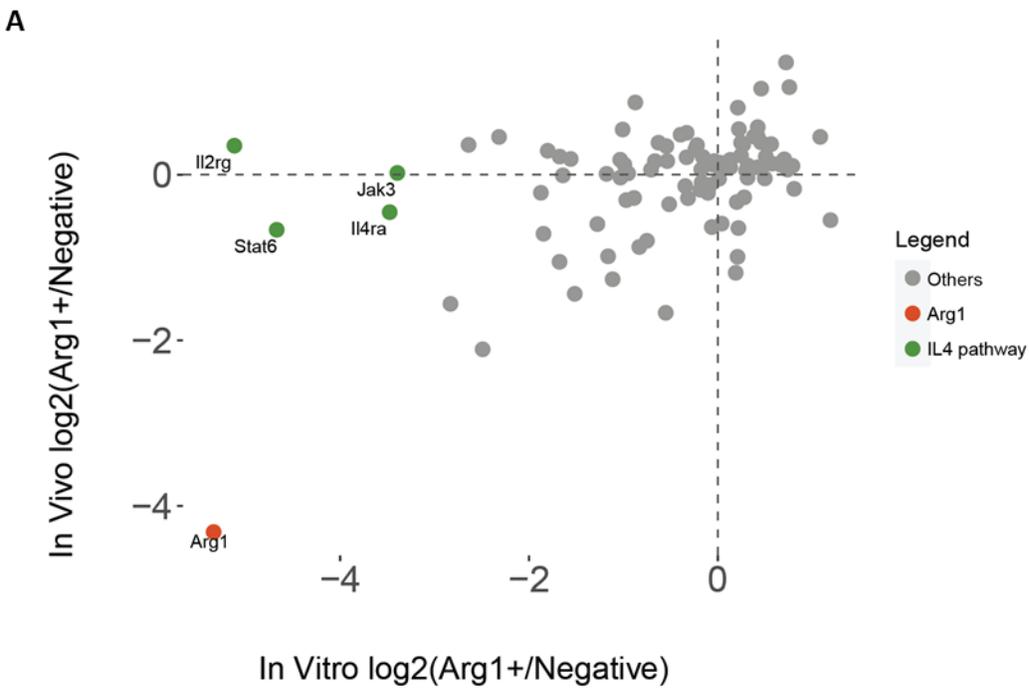
Supplementary Figure 7 | *In vivo* **vs** *in vitro* **results of CRISPR screen in Hoxb8-derived macrophages. A.** Log2 fold change comparison of IL4 signaling members between *in vivo* CRISPR screen during EAE and *in vitro* CRISPR screen by IL4 cytokine. Each screen was performed twice. All genes are targeted by 3 different sgRNA.
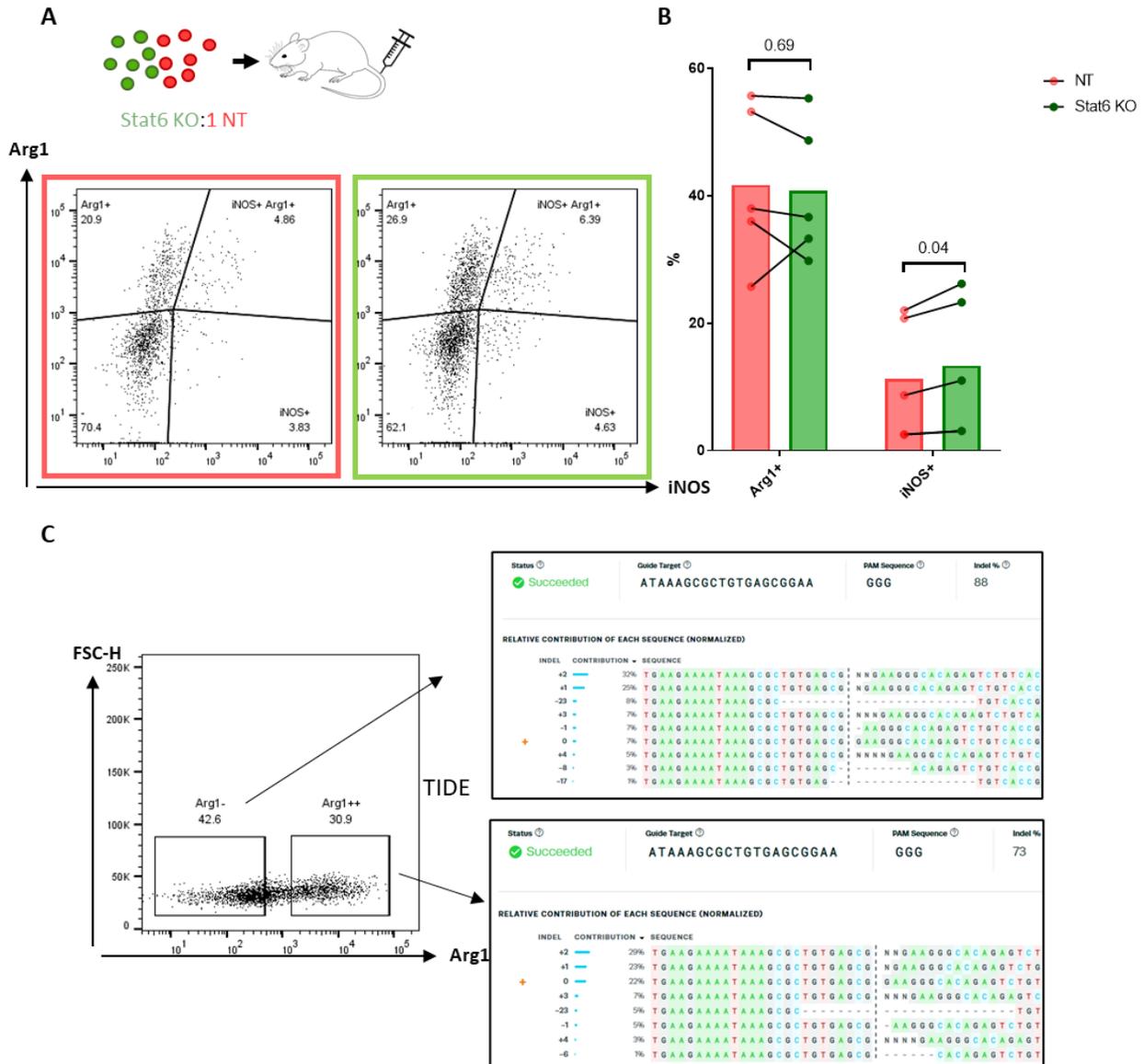
Supplementary Figure 8 | Stat6 KO cells replicate the phenotype of Il4ra KO cells. A. Representative FACS plots of Hoxb8 cells transduced with retroviral sgRNA vector, targeting Stat6 (with GFP backbone) and NT (with Tdtomato backbone) in the spinal cord for Arg1 and iNOS expression. **B.** Percentage of Arg1 and iNOS expression in Cd11b+Ly6G- Stat6 KO cells compared to NT cells. Multiple paired two-tailed Student's t-test comparing KO cells to NT cells for Arg1+ and iNOS+ population (n=5 mice, p values are shown in the figure for each comparison). **C.** Sorting of Arg1- and Arg1+ Stat6 KO for gDNA isolation and TIDE.

A
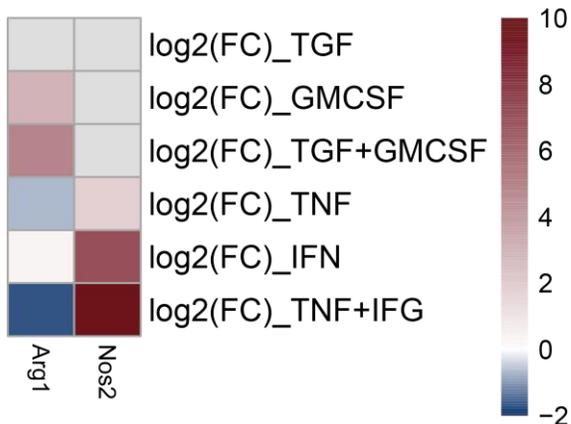
B
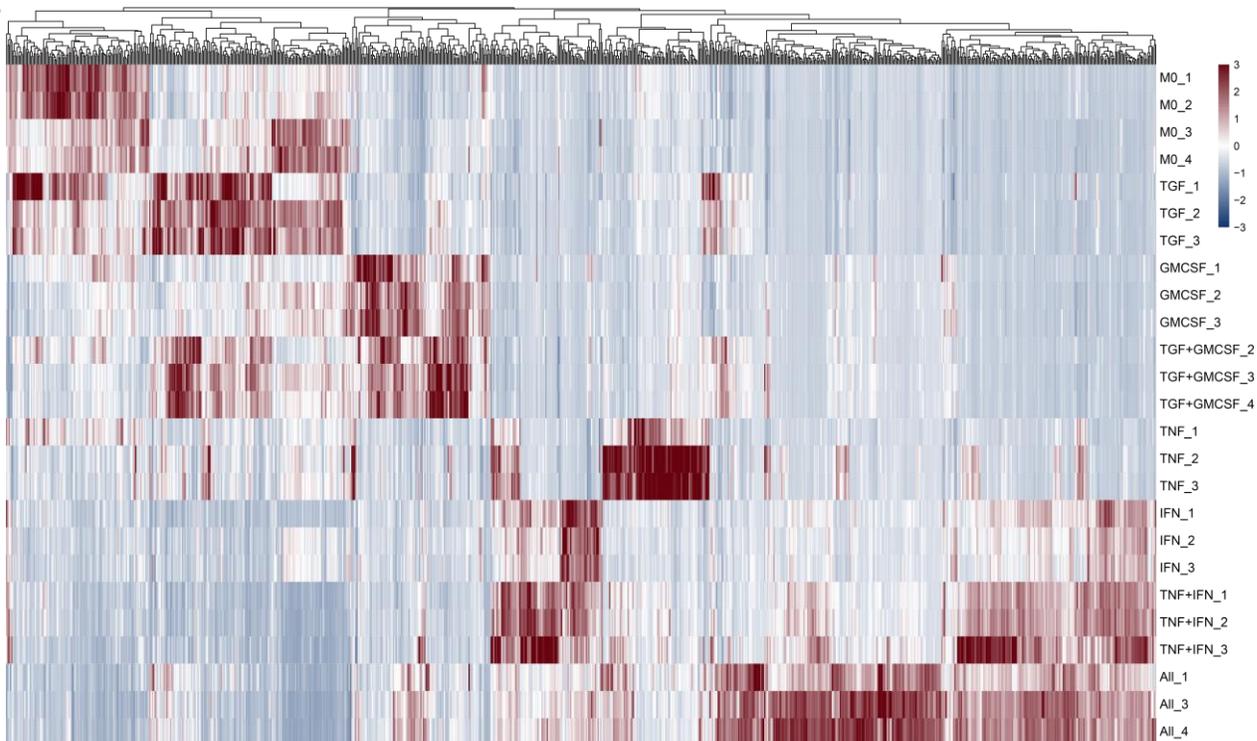
Supplementary Figure 9 | 3' Bulk mRNA sequencing of *In vitro* treated BMDMs with cytokine combinations. A. Transcriptome levels of Arg1 and Nos2 upon treatmant of cytokine combinations. **B.** Whole transcriptome change in each treatment. M0 represents untreated BMDMs, ALL represents BMDMs treated with four cytokines (TGF-β, GM-CSF, IFN-γ, TNF-α).

Sample	gRNA	Indel %	R²	KO Score
Grk2	GATTTGTCAGAACCTCCGAG	99	0.99	99
Hsp90b1	GTCTCACGGGAAACATTGAG	88	0.98	88
Ube2l3	GCTTGAAGGGATACTCTGCT	96	0.98	88
Ets1	TGCTGCTCGGAGTTAACAGT	85	0.95	67
S1pr1	GCGGCTTCGAGTCCTCACCA	92	0.95	86
Cxcr3	TCTGCGTGTACTGCAGCTAG	81	0.94	76
Itga4	GATGCTGTTGCTGTACTTCG	98	0.98	98
Gnai2	TGGGTGGTCAGCGATCTGAG	97	0.97	88
Tgfbr1	AGAGCGTTCATGGTTCCGAG	99	0.99	99
Ifngr1	TTCAGGGTGAAATACGAGGA	70	0.98	66
Csf2ra	TTGGTCGTGACCGGTCGGAG	90	0.93	65
Il6ra	CTGTGCGTTGCAAACAGTGT	82	0.94	82
Tnfrsf1a	AGACCTAGCAAGATAACCAG	91	0.94	88
Il4ra	ATCCAGGAACCACTCACACG	83	0.94	76

Supplementary Table 1 | TIDE assay of sgRNAs for INDEL calculation.

6. CONTRIBUTIONS

In the T cell project, initial optimization experiments were performed together with PD. Dr. Naoto Kawakami (NK). NK performed all the animal work. Clara de la Rosa del Val (CRV) helped with the screen experiments and performed all the bioinformatics analyses. NK, Katrin Lämmle (KL) performed the single KO validation experiments, *in vivo* two-photon imaging experiment and double KO experiment.

In the macrophage project, all the experiments were performed together with CRV. Niel Mehraein (NM) performed the *in vitro* experiments. Dr. Paula Sanchez performed the histology experiment. Hoxb8 cells were provided by Seren Baygün from Prof. Marc Schmidt-Supprian lab. Selin Baygün kindly generated figure 2, 3 and 4 for my thesis.

7. REFERENCES

Abadier, M., Haghayegh Jahromi, N., Cardoso Alves, L., Boscacci, R., Vestweber, D., Barnum, S., . . . Lyck, R. (2015). Cell surface levels of endothelial ICAM-1 influence the transcellular or paracellular T-cell diapedesis across the blood-brain barrier. *Eur J Immunol, 45*(4), 1043-1058. doi:10.1002/eji.201445125

Abbott, N. J., Patabendige, A. A. K., Dolman, D. E. M., Yusof, S. R., & Begley, D. J. (2010). Structure and function of the blood–brain barrier. *Neurobiology of Disease, 37*(1), 13-25. doi:https://doi.org/10.1016/j.nbd.2009.07.030

Abudayyeh, O. O., Gootenberg, J. S., Konermann, S., Joung, J., Slaymaker, I. M., Cox, D. B., . . . Zhang, F. (2016). C2c2 is a single-component programmable RNA-guided RNA-targeting CRISPR effector. *Science, 353*(6299), aaf5573. doi:10.1126/science.aaf5573

Accarias, S., Sanchez, T., Labrousse, A., Ben-Neji, M., Boyance, A., Poincloux, R., . . . Le Cabec, V. (2020). Genetic engineering of Hoxb8-immortalized hematopoietic progenitors – a potent tool to study macrophage tissue migration. *Journal of Cell Science, 133*(5). doi:10.1242/jcs.236703

Adli, M. (2018). The CRISPR tool kit for genome editing and beyond. *Nature Communications, 9*(1), 1911. doi:10.1038/s41467-018-04252-2

Afgan, E., Baker, D., Batut, B., van den Beek, M., Bouvier, D., Čech, M., . . . Blankenberg, D. (2018). The Galaxy platform for accessible, reproducible and collaborative biomedical analyses: 2018 update. *Nucleic Acids Research, 46*(W1), W537-W544. doi:10.1093/nar/gky379

Agrawal, S., Anderson, P., Durbeej, M., van Rooijen, N., Ivars, F., Opdenakker, G., & Sorokin, L. M. (2006). Dystroglycan is selectively cleaved at the parenchymal basement membrane at sites of leukocyte extravasation in experimental autoimmune encephalomyelitis. *J Exp Med, 203*(4), 1007-1019. doi:10.1084/jem.20051342

Ajami, B., Bennett, J. L., Krieger, C., McNagny, K. M., & Rossi, F. M. (2011). Infiltrating monocytes trigger EAE progression, but do not contribute to the resident microglia pool. *Nat Neurosci, 14*(9), 1142-1149. doi:10.1038/nn.2887

Alonso, A., & Hernán, M. A. (2008). Temporal trends in the incidence of multiple sclerosis: a systematic review. *Neurology, 71*(2), 129-135. doi:10.1212/01.wnl.0000316802.35974.34

Altae-Tran, H., Kannan, S., Demircioglu, F. E., Oshiro, R., Nety, S. P., McKay, L. J., . . . Zhang, F. (2021). The widespread IS200/605 transposon family encodes diverse programmable RNA-guided endonucleases. *Science, 0*(0), eabj6856. doi:doi:10.1126/science.abj6856

Amor, S., Groome, N., Linington, C., Morris, M. M., Dornmair, K., Gardinier, M. V., . . . Baker, D. (1994). Identification of epitopes of myelin oligodendrocyte glycoprotein for the induction of experimental allergic encephalomyelitis in SJL and Biozzi AB/H mice. *J Immunol, 153*(10), 4349-4356.

Anders, C., Niewoehner, O., Duerst, A., & Jinek, M. (2014). Structural basis of PAM-dependent target DNA recognition by the Cas9 endonuclease. *Nature, 513*(7519), 569-573. doi:10.1038/nature13579

Anzalone, A. V., Randolph, P. B., Davis, J. R., Sousa, A. A., Koblan, L. W., Levy, J. M., . . . Liu, D. R. (2019). Search-and-replace genome editing without double-strand breaks or donor DNA. *Nature, 576*(7785), 149-157. doi:10.1038/s41586-019-1711-4

Arnon, T. I., Xu, Y., Lo, C., Pham, T., An, J., Coughlin, S., . . . Cyster, J. G. (2011). GRK2-dependent S1PR1 desensitization is required for lymphocytes to overcome their attraction to blood. *Science, 333*(6051), 1898-1903. doi:10.1126/science.1208248

Ascherio, A. (2013). Environmental factors in multiple sclerosis. *Expert Rev Neurother, 13*(12 Suppl), 3-9. doi:10.1586/14737175.2013.865866

Bahbouhi, B., Berthelot, L., Pettré, S., Michel, L., Wiertlewski, S., Weksler, B., . . . Soulillou, J. P. (2009). Peripheral blood CD4+ T lymphocytes from multiple sclerosis patients are characterized by higher PSGL-1 expression and transmigration capacity across a human blood-brain barrier-derived endothelial cell line. *J Leukoc Biol, 86*(5), 1049-1063. doi:10.1189/jlb.1008666

Bai, A., Hu, H., Yeung, M., & Chen, J. (2007). Kruppel-like factor 2 controls T cell trafficking by activating L-selectin (CD62L) and sphingosine-1-phosphate receptor 1 transcription. *J Immunol, 178*(12), 7632-7639. doi:10.4049/jimmunol.178.12.7632

Baker, D., & Amor, S. (2012). Publication guidelines for refereeing and reporting on animal use in experimental autoimmune encephalomyelitis. *J Neuroimmunol, 242*(1-2), 78-83. doi:10.1016/j.jneuroim.2011.11.003

Bar-Or, A. (2008). The immunology of multiple sclerosis. *Semin Neurol, 28*(1), 29-45. doi:10.1055/s-2007-1019124

Bar-Or, A., Fawaz, L., Fan, B., Darlington, P. J., Rieger, A., Ghorayeb, C., . . . Smith, C. H. (2010). Abnormal B-cell cytokine responses a trigger of T-cell-mediated disease in MS? *Ann Neurol, 67*(4), 452-461. doi:10.1002/ana.21939

Bartholomäus, I., Kawakami, N., Odoardi, F., Schläger, C., Miljkovic, D., Ellwart, J. W., . . . Flügel, A. (2009). Effector T cell interactions with meningeal vascular structures in nascent autoimmune CNS lesions. *Nature, 462*(7269), 94-98. doi:10.1038/nature08478

Basso, A. S., Frenkel, D., Quintana, F. J., Costa-Pinto, F. A., Petrovic-Stojkovic, S., Puckett, L., . . . Weiner, H. L. (2008). Reversal of axonal loss and disability in a mouse model of progressive multiple sclerosis. *J Clin Invest, 118*(4), 1532-1543. doi:10.1172/jci33464

Beecham, A. H., Patsopoulos, N. A., Xifara, D. K., Davis, M. F., Kemppinen, A., Cotsapas, C., . . . McCauley, J. L. (2013). Analysis of immune-related loci identifies 48 new susceptibility variants for multiple sclerosis. *Nat Genet, 45*(11), 1353-1360. doi:10.1038/ng.2770

Ben-Nun, A., Wekerle, H., & Cohen, I. R. (1981). The rapid isolation of clonable antigen-specific T lymphocyte lines capable of mediating autoimmune encephalomyelitis. *Eur J Immunol, 11*(3), 195-199. doi:10.1002/eji.1830110307

Berer, K., Mues, M., Koutrolos, M., Rasbi, Z. A., Boziki, M., Johner, C., . . . Krishnamoorthy, G. (2011). Commensal microbiota and myelin autoantigen cooperate to trigger autoimmune demyelination. *Nature, 479*(7374), 538-541. doi:10.1038/nature10554

Berger, T., Weerth, S., Kojima, K., Linington, C., Wekerle, H., & Lassmann, H. (1997). Experimental autoimmune encephalomyelitis: the antigen specificity of T lymphocytes determines the topography of lesions in the central and peripheral nervous system. *Lab Invest, 76*(3), 355-364.

Bernard, C. C., & Carnegie, P. R. (1975). Experimental autoimmune encephalomyelitis in mice: immunologic response to mouse spinal cord and myelin basic proteins. *J Immunol, 114*(5), 1537-1540.

Bester, A. C., Lee, J. D., Chavez, A., Lee, Y. R., Nachmani, D., Vora, S., . . . Pandolfi, P. P. (2018). An Integrated Genome-wide CRISPRa Approach to Functionalize lncRNAs in Drug Resistance. *Cell, 173*(3), 649-664.e620. doi:10.1016/j.cell.2018.03.052

Bettadapura, J., Menon, K. K., Moritz, S., Liu, J., & Bernard, C. C. A. (1998). Expression, Purification, and Encephalitogenicity of Recombinant Human Myelin Oligodendrocyte Glycoprotein. *Journal of Neurochemistry, 70*(4), 1593-1599. doi:https://doi.org/10.1046/j.1471-4159.1998.70041593.x

Bielekova, B., Sung, M. H., Kadom, N., Simon, R., McFarland, H., & Martin, R. (2004). Expansion and functional relevance of high-avidity myelin-specific CD4+ T cells in multiple sclerosis. *J Immunol, 172*(6), 3893-3904. doi:10.4049/jimmunol.172.6.3893

Bjornevik, K., Cortese, M., Healy Brian, C., Kuhle, J., Mina Michael, J., Leng, Y., . . . Ascherio, A. (2022). Longitudinal analysis reveals high prevalence of Epstein-Barr virus associated with multiple sclerosis. *Science, 0*(0). doi:10.1126/science.abj8222

Boettcher, M., & McManus, M. T. (2015). Choosing the Right Tool for the Job: RNAi, TALEN, or CRISPR. *Molecular cell, 58*(4), 575-585. doi:10.1016/j.molcel.2015.04.028

Bond, S. T., Zhuang, A., Yang, C., Gould, E. A. M., Sikora, T., Liu, Y., . . . Drew, B. G. (2021). Detailed metabolic phenotyping of four tissue specific Cas9 transgenic mouse lines. *bioRxiv*, 2021.2003.2031.436695. doi:10.1101/2021.03.31.436695

Bö, L., Dawson, T. M., Wesselingh, S., Mörk, S., Choi, S., Kong, P. A., . . . Trapp, B. D. (1994). Induction of nitric oxide synthase in demyelinating regions of multiple sclerosis brains. *Ann Neurol, 36*(5), 778-786. doi:10.1002/ana.410360515

Bradley, C. A. (2019). In vivo T cell CRISPR screens reveal immunotherapeutic targets. *Nature Reviews Cancer, 19*(11), 606-606. doi:10.1038/s41568-019-0207-8

Brinkman, E. K., Chen, T., Amendola, M., & van Steensel, B. (2014). Easy quantitative assessment of genome editing by sequence trace decomposition. *Nucleic Acids Research, 42*(22), e168-e168. doi:10.1093/nar/gku936

Brioschi, S., Wang, W. L., Peng, V., Wang, M., Shchukina, I., Greenberg, Z. J., . . . Colonna, M. (2021). Heterogeneity of meningeal B cells reveals a lymphopoietic niche at the CNS borders. *Science, 373*(6553). doi:10.1126/science.abf9277

Brück, W., Sommermeier, N., Bergmann, M., Zettl, U., Goebel, H. H., Kretzschmar, H. A., & Lassmann, H. (1996). Macrophages in multiple sclerosis. *Immunobiology, 195*(4-5), 588-600. doi:10.1016/s0171-2985(96)80024-6

Cao, Y., Goods, B. A., Raddassi, K., Nepom, G. T., Kwok, W. W., Love, J. C., & Hafler, D. A. (2015). Functional inflammatory profiles distinguish myelin-reactive T cells from patients with multiple sclerosis. *Sci Transl Med, 7*(287), 287ra274. doi:10.1126/scitranslmed.aaa8038

Carman, C. V., & Springer, T. A. (2004). A transmigratory cup in leukocyte diapedesis both through individual vascular endothelial cells and between them. *J Cell Biol, 167*(2), 377-388. doi:10.1083/jcb.200404129

Carrieri, P. B., Provitera, V., Bruno, R., Perrella, M., Tartaglia, G., Busto, A., & Perrella, O. (1997). Possible role of transforming growth factor-beta in relapsing-remitting multiple sclerosis. *Neurol Res, 19*(6), 599-600. doi:10.1080/01616412.1997.11740866

Challen, G. A., Boles, N., Lin, K. K.-Y., & Goodell, M. A. (2009). Mouse hematopoietic stem cell identification and analysis. *Cytometry. Part A : the journal of the International Society for Analytical Cytology, 75*(1), 14-24. doi:10.1002/cyto.a.20674

Chappaz, S., Saunders, T. L., & Kile, B. T. (2021). Generation of Murine Bone Marrow and Fetal Liver Chimeras. *Current Protocols, 1*(4), e79. doi:https://doi.org/10.1002/cpz1.79

Chard, D. T., Griffin, C. M., Parker, G. J., Kapoor, R., Thompson, A. J., & Miller, D. H. (2002). Brain atrophy in clinically early relapsing-remitting multiple sclerosis. *Brain, 125*(Pt 2), 327-337. doi:10.1093/brain/awf025

Chen, X., Winkler-Pickett, R. T., Carbonetti, N. H., Ortaldo, J. R., Oppenheim, J. J., & Howard, O. M. (2006). Pertussis toxin as an adjuvant suppresses the number and function of CD4+CD25+ T regulatory cells. *Eur J Immunol, 36*(3), 671-680. doi:10.1002/eji.200535353

Cheng, H., Zheng, Z., & Cheng, T. (2020). New paradigms on hematopoietic stem cell differentiation. *Protein & Cell, 11*(1), 34-44. doi:10.1007/s13238-019-0633-0

Cheng, J., Lucas, P. C., & McAllister-Lucas, L. M. (2021). Canonical and Non-Canonical Roles of GRK2 in Lymphocytes. *Cells, 10*(2), 307. doi:10.3390/cells10020307

Coisne, C., & Engelhardt, B. (2011). Tight junctions in brain barriers during central nervous system inflammation. *Antioxid Redox Signal, 15*(5), 1285-1303. doi:10.1089/ars.2011.3929

Cong, L., Ran, F. A., Cox, D., Lin, S., Barretto, R., Habib, N., . . . Zhang, F. (2013). Multiplex genome engineering using CRISPR/Cas systems. *Science, 339*(6121), 819-823. doi:10.1126/science.1231143

Cotsapas, C., & Mitrovic, M. (2018). Genome-wide association studies of multiple sclerosis. *Clinical & translational immunology, 7*(6), e1018-e1018. doi:10.1002/cti2.1018

Croxford, A. L., Lanzinger, M., Hartmann, F. J., Schreiner, B., Mair, F., Pelczar, P., . . . Becher, B. (2015). The Cytokine GM-CSF Drives the Inflammatory Signature of CCR2+ Monocytes and Licenses Autoimmunity. *Immunity, 43*(3), 502-514. doi:10.1016/j.immuni.2015.08.010

Cruz-Orengo, L., Holman, D. W., Dorsey, D., Zhou, L., Zhang, P., Wright, M., . . . Klein, R. S. (2011). CXCR7 influences leukocyte entry into the CNS parenchyma by controlling abluminal CXCL12 abundance during autoimmunity. *J Exp Med, 208*(2), 327-339. doi:10.1084/jem.20102010

Cugurra, A., Mamuladze, T., Rustenhoven, J., Dykstra, T., Beroshvili, G., Greenberg, Z. J., . . . Kipnis, J. (2021). Skull and vertebral bone marrow are myeloid cell reservoirs for the meninges and CNS parenchyma. *Science, 373*(6553). doi:10.1126/science.abf7844

Cyster, J. G., & Schwab, S. R. (2012). Sphingosine-1-phosphate and lymphocyte egress from lymphoid organs. *Annu Rev Immunol, 30*, 69-94. doi:10.1146/annurev-immunol-020711-075011

Daneman, R. (2012). The blood–brain barrier in health and disease. *Annals of Neurology, 72*(5), 648-672. doi:https://doi.org/10.1002/ana.23648

De Stefano, N., Giorgio, A., Tintoré, M., Pia Amato, M., Kappos, L., Palace, J., . . . Rovira, À. (2018). Radiologically isolated syndrome or subclinical multiple sclerosis: MAGNIMS consensus recommendations. *Mult Scler, 24*(2), 214-221. doi:10.1177/1352458517717808

Dendrou, C. A., Fugger, L., & Friese, M. A. (2015). Immunopathology of multiple sclerosis. *Nature Reviews Immunology, 15*(9), 545-558. doi:10.1038/nri3871

Dubrot, J., Lane-Reticker, S. K., Kessler, E. A., Ayer, A., Mishra, G., Wolfe, C. H., . . . Manguso, R. T. (2021). In vivo screens using a selective CRISPR antigen removal lentiviral vector system reveal immune dependencies in renal cell carcinoma. *Immunity, 54*(3), 571-585.e576. doi:https://doi.org/10.1016/j.immuni.2021.01.001

Dykstra, B., Kent, D., Bowie, M., McCaffrey, L., Hamilton, M., Lyons, K., . . . Eaves, C. (2007). Long-term propagation of distinct hematopoietic differentiation programs in vivo. *Cell Stem Cell, 1*(2), 218-229. doi:10.1016/j.stem.2007.05.015

Elbashir, S. M., Harborth, J., Lendeckel, W., Yalcin, A., Weber, K., & Tuschl, T. (2001). Duplexes of 21-nucleotide RNAs mediate RNA interference in cultured mammalian cells. *Nature, 411*(6836), 494-498. doi:10.1038/35078107

Engelhardt, B., & Ransohoff, R. M. (2005). The ins and outs of T-lymphocyte trafficking to the CNS: anatomical sites and molecular mechanisms. *Trends Immunol, 26*(9), 485-495. doi:10.1016/j.it.2005.07.004

Engelhardt, B., & Ransohoff, R. M. (2012). Capture, crawl, cross: the T cell code to breach the blood-brain barriers. *Trends Immunol, 33*(12), 579-589. doi:10.1016/j.it.2012.07.004

Erickson, M. A., Wilson, M. L., & Banks, W. A. (2020). In vitro modeling of blood–brain barrier and interface functions in neuroimmune communication. *Fluids and Barriers of the CNS, 17*(1), 26. doi:10.1186/s12987-020-00187-3

Fahy, R. J., Doseff, A. I., & Wewers, M. D. (1999). Spontaneous human monocyte apoptosis utilizes a caspase-3-dependent pathway that is blocked by endotoxin and is independent of caspase-1. *J Immunol, 163*(4), 1755-1762.

Fife, B. T., Huffnagle, G. B., Kuziel, W. A., & Karpus, W. J. (2000). CC chemokine receptor 2 is critical for induction of experimental autoimmune encephalomyelitis. *J Exp Med, 192*(6), 899-905. doi:10.1084/jem.192.6.899

Filippi, M., Bar-Or, A., Piehl, F., Preziosa, P., Solari, A., Vukusic, S., & Rocca, M. A. (2018). Multiple sclerosis. *Nat Rev Dis Primers, 4*(1), 43. doi:10.1038/s41572-018-0041-4

Filippi, M., Bar-Or, A., Piehl, F., Preziosa, P., Solari, A., Vukusic, S., & Rocca, M. A. (2018). Multiple sclerosis. *Nature Reviews Disease Primers, 4*(1), 43. doi:10.1038/s41572-018-0041-4

Filippini, G., Del Giovane, C., Vacchi, L., D'Amico, R., Di Pietrantonj, C., Beecher, D., & Salanti, G. (2013). Immunomodulators and immunosuppressants for multiple sclerosis: a network meta-analysis. *Cochrane Database Syst Rev*(6), Cd008933. doi:10.1002/14651858.CD008933.pub2

Fire, A., Xu, S., Montgomery, M. K., Kostas, S. A., Driver, S. E., & Mello, C. C. (1998). Potent and specific genetic interference by double-stranded RNA in Caenorhabditis elegans. *Nature, 391*(6669), 806-811. doi:10.1038/35888

Flügel, A., Berkowicz, T., Ritter, T., Labeur, M., Jenne, D. E., Li, Z., . . . Wekerle, H. (2001). Migratory activity and functional changes of green fluorescent effector cells before and during experimental autoimmune encephalomyelitis. *Immunity, 14*(5), 547-560. doi:10.1016/s1074-7613(01)00143-1

Forrester, J. V., McMenamin, P. G., & Dando, S. J. (2018). CNS infection and immune privilege. *Nature Reviews Neuroscience, 19*(11), 655-671. doi:10.1038/s41583-018-0070-8

Frischer, J. M., Bramow, S., Dal-Bianco, A., Lucchinetti, C. F., Rauschka, H., Schmidbauer, M., . . . Lassmann, H. (2009). The relation between inflammation and neurodegeneration in multiple sclerosis brains. *Brain : a journal of neurology, 132*(Pt 5), 1175-1189. doi:10.1093/brain/awp070

Frischer, J. M., Bramow, S., Dal-Bianco, A., Lucchinetti, C. F., Rauschka, H., Schmidbauer, M., . . . Lassmann, H. (2009). The relation between inflammation and neurodegeneration in multiple sclerosis brains. *Brain, 132*(Pt 5), 1175-1189. doi:10.1093/brain/awp070

Frohman, E. M., Racke, M. K., & Raine, C. S. (2006). Multiple sclerosis--the plaque and its pathogenesis. *N Engl J Med, 354*(9), 942-955. doi:10.1056/NEJMra052130

Gaj, T., Gersbach, C. A., & Barbas, C. F. (2013). ZFN, TALEN, and CRISPR/Cas-based methods for genome engineering. *Trends in Biotechnology, 31*(7), 397-405. doi:https://doi.org/10.1016/j.tibtech.2013.04.004

Gaudelli, N. M., Komor, A. C., Rees, H. A., Packer, M. S., Badran, A. H., Bryson, D. I., & Liu, D. R. (2017). Programmable base editing of A•T to G•C in genomic DNA without DNA cleavage. *Nature, 551*(7681), 464-471. doi:10.1038/nature24644

Giladi, A., Wagner, L. K., Li, H., Dörr, D., Medaglia, C., Paul, F., . . . Mildner, A. (2020). Cxcl10+ monocytes define a pathogenic subset in the central nervous system during autoimmune neuroinflammation. *Nature Immunology, 21*(5), 525-534. doi:10.1038/s41590-020-0661-1

Giles, D. A., Washnock-Schmid, J. M., Duncker, P. C., Dahlawi, S., Ponath, G., Pitt, D., & Segal, B. M. (2018). Myeloid cell plasticity in the evolution of central nervous system autoimmunity. *Ann Neurol, 83*(1), 131-141. doi:10.1002/ana.25128

Glatigny, S., Duhen, R., Oukka, M., & Bettelli, E. (2011). Cutting edge: loss of α4 integrin expression differentially affects the homing of Th1 and Th17 cells. *Journal of immunology (Baltimore, Md. : 1950), 187*(12), 6176-6179. doi:10.4049/jimmunol.1102515

Goldmann, T., Wieghofer, P., Jordão, M. J. C., Prutek, F., Hagemeyer, N., Frenzel, K., . . . Prinz, M. (2016). Origin, fate and dynamics of macrophages at central nervous system interfaces. *Nature Immunology, 17*(7), 797-805. doi:10.1038/ni.3423

Goldschmidt, T., Antel, J., König, F. B., Brück, W., & Kuhlmann, T. (2009). Remyelination capacity of the MS brain decreases with disease chronicity. *Neurology, 72*(22), 1914-1921. doi:10.1212/WNL.0b013e3181a8260a

Gonzalez-Mejia, M. E., & Doseff, A. I. (2009). Regulation of monocytes and macrophages cell fate. *Front Biosci (Landmark Ed), 14*, 2413-2431. doi:10.2741/3387

Göbel, K., Ruck, T., & Meuth, S. G. (2018). Cytokine signaling in multiple sclerosis: Lost in translation. *Mult Scler, 24*(4), 432-439. doi:10.1177/1352458518763094

Greenfield, A. L., & Hauser, S. L. (2018). B-cell Therapy for Multiple Sclerosis: Entering an era. *Ann Neurol, 83*(1), 13-26. doi:10.1002/ana.25119

Greenwood, J., Wang, Y., & Calder, V. L. (1995). Lymphocyte adhesion and transendothelial migration in the central nervous system: the role of LFA-1, ICAM-1, VLA-4 and VCAM-1. off. *Immunology, 86*(3), 408-415.

Hardwick, J. M., & Soane, L. (2013). Multiple functions of BCL-2 family proteins. *Cold Spring Harbor perspectives in biology, 5*(2), a008722. doi:10.1101/cshperspect.a008722

Henderson, A. P., Barnett, M. H., Parratt, J. D., & Prineas, J. W. (2009). Multiple sclerosis: distribution of inflammatory cells in newly forming lesions. *Ann Neurol, 66*(6), 739-753. doi:10.1002/ana.21800

Hill, K. E., Zollinger, L. V., Watt, H. E., Carlson, N. G., & Rose, J. W. (2004). Inducible nitric oxide synthase in chronic active multiple sclerosis plaques: distribution, cellular expression and association with myelin damage. *J Neuroimmunol, 151*(1-2), 171-179. doi:10.1016/j.jneuroim.2004.02.005

Hogg, N., Patzak, I., & Willenbrock, F. (2011). The insider's guide to leukocyte integrin signalling and function. *Nature Reviews Immunology, 11*(6), 416-426. doi:10.1038/nri2986

Hohlfeld, R., Kerschensteiner, M., Stadelmann, C., Lassmann, H., & Wekerle, H. (2000). The neuroprotective effect of inflammation: implications for the therapy of multiple sclerosis. *J Neuroimmunol, 107*(2), 161-166. doi:10.1016/s0165-5728(00)00233-2

Holman, D. W., Klein, R. S., & Ransohoff, R. M. (2011). The blood-brain barrier, chemokines and multiple sclerosis. *Biochim Biophys Acta, 1812*(2), 220-230. doi:10.1016/j.bbadis.2010.07.019

Hooijmans, C. R., Hlavica, M., Schuler, F. A. F., Good, N., Good, A., Baumgartner, L., . . . Ineichen, B. V. (2019). Remyelination promoting therapies in multiple sclerosis animal models: a systematic review and meta-analysis. *Scientific Reports, 9*(1), 822. doi:10.1038/s41598-018-35734-4

Horlbeck, M. A., Gilbert, L. A., Villalta, J. E., Adamson, B., Pak, R. A., Chen, Y., . . . Weissman, J. S. (2016). Compact and highly active next-generation libraries for CRISPR-mediated gene repression and activation. *Elife, 5*. doi:10.7554/eLife.19760

Housden, B. E., Muhar, M., Gemberling, M., Gersbach, C. A., Stainier, D. Y. R., Seydoux, G., . . . Perrimon, N. (2017). Loss-of-function genetic tools for animal models: cross-species and cross-platform differences. *Nature reviews. Genetics, 18*(1), 24-40. doi:10.1038/nrg.2016.118

Hsiau, T., Conant, D., Rossi, N., Maures, T., Waite, K., Yang, J., . . . Stoner, R. (2019). Inference of CRISPR Edits from Sanger Trace Data. *bioRxiv*, 251082. doi:10.1101/251082

Huang, D. R., Wang, J., Kivisakk, P., Rollins, B. J., & Ransohoff, R. M. (2001). Absence of monocyte chemoattractant protein 1 in mice leads to decreased local macrophage recruitment and antigen-specific T helper cell type 1 immune response in experimental autoimmune encephalomyelitis. *J Exp Med, 193*(6), 713-726. doi:10.1084/jem.193.6.713

Hutchinson, M. (2007). Natalizumab: A new treatment for relapsing remitting multiple sclerosis. *Therapeutics and clinical risk management, 3*(2), 259-268. doi:10.2147/tcrm.2007.3.2.259

Hwang, I.-Y., Harrison, K., Park, C., & Kehrl, J. H. (2017). Loss of Gαi proteins impairs thymocyte development, disrupts T-cell trafficking, and leads to an expanded population of splenic CD4+PD-1+CXCR5+/− T-cells. *Scientific Reports, 7*(1), 4156. doi:10.1038/s41598-017-04537-4

Hwang, I.-Y., Park, C., Harrison, K., & Kehrl, J. H. (2019). Biased S1PR1 Signaling in B Cells Subverts Responses to Homeostatic Chemokines, Severely Disorganizing Lymphoid Organ Architecture. *The Journal of Immunology, 203*(9), 2401. doi:10.4049/jimmunol.1900678

Hwang, I. Y., Park, C., & Kehrl, J. H. (2007). Impaired trafficking of Gnai2+/- and Gnai2-/- T lymphocytes: implications for T cell movement within lymph nodes. *J Immunol, 179*(1), 439-448. doi:10.4049/jimmunol.179.1.439

International Multiple Sclerosis Genetics Consortium. (2019). Multiple sclerosis genomic map implicates peripheral immune cells and microglia in susceptibility. *Science, 365*(6460). doi:10.1126/science.aav7188

Ishida, Y., Kondo, T., Takayasu, T., Iwakura, Y., & Mukaida, N. (2004). The Essential Involvement of Cross-Talk between IFN-γ and TGF-β in the Skin Wound-Healing Process. *The Journal of Immunology, 172*(3), 1848-1855. doi:10.4049/jimmunol.172.3.1848

Jafari, M., Schumacher, A.-M., Snaidero, N., Ullrich Gavilanes, E. M., Neziraj, T., Kocsis-Jutka, V., . . . Kerschensteiner, M. (2021). Phagocyte-mediated synapse removal in cortical neuroinflammation is promoted by local calcium accumulation. *Nature Neuroscience, 24*(3), 355-367. doi:10.1038/s41593-020-00780-7

Jäger, A., Dardalhon, V., Sobel, R. A., Bettelli, E., & Kuchroo, V. K. (2009). Th1, Th17, and Th9 Effector Cells Induce Experimental Autoimmune Encephalomyelitis with Different Pathological Phenotypes. *The Journal of Immunology, 183*(11), 7169. doi:10.4049/jimmunol.0901906

Jiang, Z., Jiang, J. X., & Zhang, G. X. (2014). Macrophages: a double-edged sword in experimental autoimmune encephalomyelitis. *Immunol Lett, 160*(1), 17-22. doi:10.1016/j.imlet.2014.03.006

Jürgens, T., Jafari, M., Kreutzfeldt, M., Bahn, E., Brück, W., Kerschensteiner, M., & Merkler, D. (2016). Reconstruction of single cortical projection neurons reveals primary spine loss in multiple sclerosis. *Brain, 139*(Pt 1), 39-46. doi:10.1093/brain/awv353

Kabat, E. A., Wolf, A., Bezer, A. E., & Murray, J. P. (1951). Studies on acute disseminated encephalomyelitis produced experimentally in rhesus monkeys. *J Exp Med, 93*(6), 615-633. doi:10.1084/jem.93.6.615

Kale, J., Osterlund, E. J., & Andrews, D. W. (2018). BCL-2 family proteins: changing partners in the dance towards death. *Cell Death & Differentiation, 25*(1), 65-80. doi:10.1038/cdd.2017.186

Kampmann, M. (2018). CRISPRi and CRISPRa Screens in Mammalian Cells for Precision Biology and Medicine. *ACS Chem Biol, 13*(2), 406-416. doi:10.1021/acschembio.7b00657

Kamradt, T., Soloway, P. D., Perkins, D. L., & Gefter, M. L. (1991). Pertussis toxin prevents the induction of peripheral T cell anergy and enhances the T cell response to an encephalitogenic peptide of myelin basic protein. *J Immunol, 147*(10), 3296-3302.

Kapoor, R., Ho, P. R., Campbell, N., Chang, I., Deykin, A., Forrestal, F., . . . Steiner, D. (2018). Effect of natalizumab on disease progression in secondary progressive multiple sclerosis (ASCEND): a phase 3, randomised, double-blind, placebo-controlled trial with an open-label extension. *Lancet Neurol, 17*(5), 405-415. doi:10.1016/s1474-4422(18)30069-3

Kapoor, T., & Mehan, S. (2021). Neuroprotective Methodologies in the Treatment of Multiple Sclerosis Current Status of Clinical and Pre-clinical Findings. *Curr Drug Discov Technol, 18*(1), 31-46. doi:10.2174/1570163817666200207100903

Kaskow, B. J., & Baecher-Allan, C. (2018). Effector T Cells in Multiple Sclerosis. *Cold Spring Harb Perspect Med, 8*(4). doi:10.1101/cshperspect.a029025

Kawakami, N., Nägerl, U. V., Odoardi, F., Bonhoeffer, T., Wekerle, H., & Flügel, A. (2005). Live imaging of effector cell trafficking and autoantigen recognition within the unfolding autoimmune encephalomyelitis lesion. *J Exp Med, 201*(11), 1805-1814. doi:10.1084/jem.20050011

Kebir, H., Ifergan, I., Alvarez, J. I., Bernard, M., Poirier, J., Arbour, N., . . . Prat, A. (2009). Preferential recruitment of interferon-gamma-expressing TH17 cells in multiple sclerosis. *Ann Neurol, 66*(3), 390-402. doi:10.1002/ana.21748

Kennedy, M. K., Torrance, D. S., Picha, K. S., & Mohler, K. M. (1992). Analysis of cytokine mRNA expression in the central nervous system of mice with experimental autoimmune encephalomyelitis reveals that IL-10 mRNA expression correlates with recovery. *J Immunol, 149*(7), 2496-2505.

Keretsu, S., Bhujbal, S. P., & Joo Cho, S. (2019). Computational study of paroxetine-like inhibitors reveals new molecular insight to inhibit GRK2 with selectivity over ROCK1. *Scientific Reports, 9*(1), 13053. doi:10.1038/s41598-019-48949-w

Keretsu, S., Bhujbal, S. P., & Joo Cho, S. (2019). Computational study of paroxetine-like inhibitors reveals new molecular insight to inhibit GRK2 with selectivity over ROCK1. *Sci Rep, 9*(1), 13053. doi:10.1038/s41598-019-48949-w

Kerfoot, S. M., & Kubes, P. (2002). Overlapping roles of P-selectin and alpha 4 integrin to recruit leukocytes to the central nervous system in experimental autoimmune encephalomyelitis. *J Immunol, 169*(2), 1000-1006. doi:10.4049/jimmunol.169.2.1000

Kim, H. J., Ifergan, I., Antel, J. P., Seguin, R., Duddy, M., Lapierre, Y., . . . Bar-Or, A. (2004). Type 2 monocyte and microglia differentiation mediated by glatiramer acetate therapy in patients with multiple sclerosis. *J Immunol, 172*(11), 7144-7153. doi:10.4049/jimmunol.172.11.7144

Kim, M. V., Ouyang, W., Liao, W., Zhang, M. Q., & Li, M. O. (2013). The transcription factor Foxo1 controls central-memory CD8+ T cell responses to infection. *Immunity, 39*(2), 286-297. doi:10.1016/j.immuni.2013.07.013

King, I. L., Dickendesher, T. L., & Segal, B. M. (2009). Circulating Ly-6C+ myeloid precursors migrate to the CNS and play a pathogenic role during autoimmune demyelinating disease. *Blood, 113*(14), 3190-3197. doi:10.1182/blood-2008-07-168575

Kleinstiver, B. P., Sousa, A. A., Walton, R. T., Tak, Y. E., Hsu, J. Y., Clement, K., . . . Joung, J. K. (2019). Engineered CRISPR-Cas12a variants with increased activities and improved targeting ranges for gene, epigenetic and base editing. *Nat Biotechnol, 37*(3), 276-282. doi:10.1038/s41587-018-0011-0

Koeniger, T., & Kuerten, S. (2017). Splitting the "Unsplittable": Dissecting Resident and Infiltrating Macrophages in Experimental Autoimmune Encephalomyelitis. *Int J Mol Sci, 18*(10). doi:10.3390/ijms18102072

Komor, A. C., Kim, Y. B., Packer, M. S., Zuris, J. A., & Liu, D. R. (2016). Programmable editing of a target base in genomic DNA without double-stranded DNA cleavage. *Nature, 533*(7603), 420-424. doi:10.1038/nature17946

Krienke, C., Kolb, L., Diken, E., Streuber, M., Kirchhoff, S., Bukur, T., . . . Sahin, U. (2021). A noninflammatory mRNA vaccine for treatment of experimental autoimmune encephalomyelitis. *Science, 371*(6525), 145-153. doi:10.1126/science.aay3638

Kuhn, M., Santinha, A. J., & Platt, R. J. (2021). Moving from in vitro to in vivo CRISPR screens. *Gene and Genome Editing, 2*, 100008. doi:https://doi.org/10.1016/j.ggedit.2021.100008

La Mantia, L., Eoli, M., Milanese, C., Salmaggi, A., Dufour, A., & Torri, V. (1994). Double-blind trial of dexamethasone versus methylprednisolone in multiple sclerosis acute relapses. *Eur Neurol, 34*(4), 199-203. doi:10.1159/000117038

LaFleur, M. W., Nguyen, T. H., Coxe, M. A., Yates, K. B., Trombley, J. D., Weiss, S. A., . . . Sharpe, A. H. (2019). A CRISPR-Cas9 delivery system for in vivo screening of genes in the immune system. *Nature Communications, 10*(1), 1668. doi:10.1038/s41467-019-09656-2

Lassmann, H., & Bradl, M. (2017). Multiple sclerosis: experimental models and reality. *Acta Neuropathol, 133*(2), 223-244. doi:10.1007/s00401-016-1631-4

Lee, C.-G., Kwon, H.-K., Kang, H., Kim, Y., Nam, J. H., Won, Y. H., . . . Im, S.-H. (2019). Ets1 suppresses atopic dermatitis by suppressing pathogenic T cell responses. *JCI Insight, 4*(5). doi:10.1172/jci.insight.124202

Lee, P. W., Severin, M. E., & Lovett-Racke, A. E. (2017). TGF-β regulation of encephalitogenic and regulatory T cells in multiple sclerosis. *European Journal of Immunology, 47*(3), 446-453. doi:https://doi.org/10.1002/eji.201646716

Leray, E., Yaouanq, J., Le Page, E., Coustans, M., Laplaud, D., Oger, J., & Edan, G. (2010). Evidence for a two-stage disability progression in multiple sclerosis. *Brain : a journal of neurology, 133*(Pt 7), 1900-1913. doi:10.1093/brain/awq076

Li, L., Hu, S., & Chen, X. (2018). Non-viral delivery systems for CRISPR/Cas9-based genome editing: Challenges and opportunities. *Biomaterials, 171*, 207-218. doi:10.1016/j.biomaterials.2018.04.031

Li, W., Xu, H., Xiao, T., Cong, L., Love, M. I., Zhang, F., . . . Liu, X. S. (2014). MAGeCK enables robust identification of essential genes from genome-scale CRISPR/Cas9 knockout screens. *Genome biology, 15*(12), 554. doi:10.1186/s13059-014-0554-4

Lin, C., Zhang, Y., Zhang, K., Zheng, Y., Lu, L., Chang, H., . . . Chen, J. (2019). Fever Promotes T Lymphocyte Trafficking via a Thermal Sensory Pathway Involving Heat Shock Protein 90 and α4 Integrins. *Immunity, 50*(1), 137-151.e136. doi:https://doi.org/10.1016/j.immuni.2018.11.013

Lind, M., Hayes, A., Caprnda, M., Petrovic, D., Rodrigo, L., Kruzliak, P., & Zulli, A. (2017). Inducible nitric oxide synthase: Good or bad? *Biomed Pharmacother, 93*, 370-375. doi:10.1016/j.biopha.2017.06.036

Liu, B. S., Janssen, H. L., & Boonstra, A. (2012). Type I and III interferons enhance IL-10R expression on human monocytes and macrophages, resulting in IL-10-mediated suppression of TLR-induced IL-12. *Eur J Immunol, 42*(9), 2431-2440. doi:10.1002/eji.201142360

Liu, S., Calderwood, D. A., & Ginsberg, M. H. (2000). Integrin cytoplasmic domain-binding proteins. *J Cell Sci, 113 (Pt 20)*, 3563-3571.

Locatelli, G., Theodorou, D., Kendirli, A., Jordão, M. J. C., Staszewski, O., Phulphagar, K., . . . Kerschensteiner, M. (2018). Mononuclear phagocytes locally specify and adapt their phenotype in a multiple sclerosis model. *Nat Neurosci, 21*(9), 1196-1208. doi:10.1038/s41593-018-0212-3

Lodygin, D., Hermann, M., Schweingruber, N., Flügel-Koch, C., Watanabe, T., Schlosser, C., . . . Flügel, A. (2019). β-Synuclein-reactive T cells induce autoimmune CNS grey matter degeneration. *Nature, 566*(7745), 503-508. doi:10.1038/s41586-019-0964-2

Lopes Pinheiro, M. A., Kamermans, A., Garcia-Vallejo, J. J., van Het Hof, B., Wierts, L., O'Toole, T., . . . Unger, W. W. (2016). Internalization and presentation of myelin antigens by the brain endothelium guides antigen-specific T cell migration. *Elife, 5*. doi:10.7554/eLife.13149

Lu, C., Pelech, S., Zhang, H., Bond, J., Spach, K., Noubade, R., . . . Teuscher, C. (2008). Pertussis toxin induces angiogenesis in brain microvascular endothelial cells. *J Neurosci Res, 86*(12), 2624-2640. doi:10.1002/jnr.21716

Lublin, F. D., Reingold, S. C., Cohen, J. A., Cutter, G. R., Sørensen, P. S., Thompson, A. J., . . . Polman, C. H. (2014). Defining the clinical course of multiple sclerosis: the 2013 revisions. *Neurology, 83*(3), 278-286. doi:10.1212/WNL.0000000000000560

Lumniczky, K., Szatmári, T., & Sáfrány, G. (2017). Ionizing Radiation-Induced Immune and Inflammatory Reactions in the Brain. *Frontiers in Immunology, 8*(517). doi:10.3389/fimmu.2017.00517

Mackay, L. K., Minnich, M., Kragten, N. A., Liao, Y., Nota, B., Seillet, C., . . . van Gisbergen, K. P. (2016). Hobit and Blimp1 instruct a universal transcriptional program of tissue residency in lymphocytes. *Science, 352*(6284), 459-463. doi:10.1126/science.aad2035

Mantovani, A., Sica, A., Sozzani, S., Allavena, P., Vecchi, A., & Locati, M. (2004). The chemokine system in diverse forms of macrophage activation and polarization. *Trends Immunol, 25*(12), 677-686. doi:10.1016/j.it.2004.09.015

Martinelli, R., Gegg, M., Longbottom, R., Adamson, P., Turowski, P., & Greenwood, J. (2009). ICAM-1-mediated endothelial nitric oxide synthase activation via calcium and AMP-activated protein kinase is required for transendothelial lymphocyte migration. *Mol Biol Cell, 20*(3), 995-1005. doi:10.1091/mbc.e08-06-0636

Martinez, F. O., & Gordon, S. (2014). The M1 and M2 paradigm of macrophage activation: time for reassessment. *F1000prime reports, 6*, 13-13. doi:10.12703/P6-13

Matloubian, M., Lo, C. G., Cinamon, G., Lesneski, M. J., Xu, Y., Brinkmann, V., . . . Cyster, J. G. (2004). Lymphocyte egress from thymus and peripheral lymphoid organs is dependent on S1P receptor 1. *Nature, 427*(6972), 355-360. doi:10.1038/nature02284

McAlpine, D., Lumsden, C. E., & Acheson, D. (1972). *Multiple Sclerosis: A Reappraisal*: Churchill Livingstone.

McQualter, J. L., Darwiche, R., Ewing, C., Onuki, M., Kay, T. W., Hamilton, J. A., . . . Bernard, C. C. (2001). Granulocyte macrophage colony-stimulating factor: a new putative therapeutic target in multiple sclerosis. *J Exp Med, 194*(7), 873-882. doi:10.1084/jem.194.7.873

Mendel, I., Kerlero de Rosbo, N., & Ben-Nun, A. (1995). A myelin oligodendrocyte glycoprotein peptide induces typical chronic experimental autoimmune encephalomyelitis in H-2b mice: fine specificity and T cell receptor V beta expression of encephalitogenic T cells. *Eur J Immunol, 25*(7), 1951-1959. doi:10.1002/eji.1830250723

Mickael, M. E., Kubick, N., Klimovich, P., Flournoy, P. H., Bieńkowska, I., & Sacharczuk, M. (2021). Paracellular and Transcellular Leukocytes Diapedesis Are Divergent but Interconnected Evolutionary Events. *Genes (Basel), 12*(2). doi:10.3390/genes12020254

Mikita, J., Dubourdieu-Cassagno, N., Deloire, M. S., Vekris, A., Biran, M., Raffard, G., . . . Petry, K. G. (2011). Altered M1/M2 activation patterns of monocytes in severe relapsing experimental rat model of multiple sclerosis. Amelioration of clinical status by M2 activated monocyte administration. *Mult Scler, 17*(1), 2-15. doi:10.1177/1352458510379243

Millán, J., Hewlett, L., Glyn, M., Toomre, D., Clark, P., & Ridley, A. J. (2006). Lymphocyte transcellular migration occurs through recruitment of endothelial ICAM-1 to caveola- and F-actin-rich domains. *Nature Cell Biology, 8*(2), 113-123. doi:10.1038/ncb1356

Miller, T. E., Liau, B. B., Wallace, L. C., Morton, A. R., Xie, Q., Dixit, D., . . . Rich, J. N. (2017). Transcription elongation factors represent in vivo cancer dependencies in glioblastoma. *Nature, 547*(7663), 355-359. doi:10.1038/nature23000

Miron, V. E., Boyd, A., Zhao, J.-W., Yuen, T. J., Ruckh, J. M., Shadrach, J. L., . . . Ffrench-Constant, C. (2013). M2 microglia and macrophages drive oligodendrocyte differentiation during CNS remyelination. *Nature Neuroscience, 16*(9), 1211-1218. doi:10.1038/nn.3469

Moisan, J., Grenningloh, R., Bettelli, E., Oukka, M., & Ho, I. C. (2007). Ets-1 is a negative regulator of Th17 differentiation. *J Exp Med, 204*(12), 2825-2835. doi:10.1084/jem.20070994

Montalban, X., Hauser, S. L., Kappos, L., Arnold, D. L., Bar-Or, A., Comi, G., . . . Wolinsky, J. S. (2017). Ocrelizumab versus Placebo in Primary Progressive Multiple Sclerosis. *N Engl J Med, 376*(3), 209-220. doi:10.1056/NEJMoa1606468

Moretti, F. A., Moser, M., Lyck, R., Abadier, M., Ruppert, R., Engelhardt, B., & Fässler, R. (2013). Kindlin-3 regulates integrin activation and adhesion reinforcement of effector T cells.

Proceedings of the National Academy of Sciences of the United States of America, 110(42), 17005-17010. doi:10.1073/pnas.1316032110

Murray, P. J. (2017). Macrophage Polarization. *Annual Review of Physiology, 79*(1), 541-566. doi:10.1146/annurev-physiol-022516-034339

Murray, P. J., Allen, J. E., Biswas, S. K., Fisher, E. A., Gilroy, D. W., Goerdt, S., . . . Wynn, T. A. (2014). Macrophage activation and polarization: nomenclature and experimental guidelines. *Immunity, 41*(1), 14-20. doi:10.1016/j.immuni.2014.06.008

Nally, F. K., De Santi, C., & McCoy, C. E. (2019). Nanomodulation of Macrophages in Multiple Sclerosis. *Cells, 8*(6). doi:10.3390/cells8060543

Napier, M. D., Poole, C., Satten, G. A., Ashley-Koch, A., Marrie, R. A., & Williamson, D. M. (2016). Heavy metals, organic solvents, and multiple sclerosis: An exploratory look at gene-environment interactions. *Archives of environmental & occupational health, 71*(1), 26-34. doi:10.1080/19338244.2014.937381

Newton, R. H., Shrestha, S., Sullivan, J. M., Yates, K. B., Compeer, E. B., Ron-Harel, N., . . . Turka, L. A. (2018). Maintenance of CD4 T cell fitness through regulation of Foxo1. *Nature Immunology, 19*(8), 838-848. doi:10.1038/s41590-018-0157-4

Nikić, I., Merkler, D., Sorbara, C., Brinkoetter, M., Kreutzfeldt, M., Bareyre, F. M., . . . Kerschensteiner, M. (2011). A reversible form of axon damage in experimental autoimmune encephalomyelitis and multiple sclerosis. *Nat Med, 17*(4), 495-499. doi:10.1038/nm.2324

Nimmerjahn, A., Kirchhoff, F., & Helmchen, F. (2005). Resting microglial cells are highly dynamic surveillants of brain parenchyma in vivo. *Science, 308*(5726), 1314-1318. doi:10.1126/science.1110647

Odoardi, F., Sie, C., Streyl, K., Ulaganathan, V. K., Schläger, C., Lodygin, D., . . . Flügel, A. (2012). T cells become licensed in the lung to enter the central nervous system. *Nature, 488*(7413), 675-679. doi:10.1038/nature11337

Okuda, D. T., Siva, A., Kantarci, O., Inglese, M., Katz, I., Tutuncu, M., . . . Lebrun, C. (2014). Radiologically isolated syndrome: 5-year risk for an initial clinical event. *PLoS One, 9*(3), e90509. doi:10.1371/journal.pone.0090509

Olsson, T., Barcellos, L. F., & Alfredsson, L. (2017). Interactions between genetic, lifestyle and environmental risk factors for multiple sclerosis. *Nat Rev Neurol, 13*(1), 25-36. doi:10.1038/nrneurol.2016.187

Ong, S. H., Li, Y., Koike-Yusa, H., & Yusa, K. (2017). Optimised metrics for CRISPR-KO screens with second-generation gRNA libraries. *Scientific Reports, 7*(1), 7384. doi:10.1038/s41598-017-07827-z

Ortiz, G. G., Pacheco-Moisés, F. P., Macías-Islas, M., Flores-Alvarado, L. J., Mireles-Ramírez, M. A., González-Renovato, E. D., . . . Alatorre-Jiménez, M. A. (2014). Role of the blood-brain barrier in multiple sclerosis. *Arch Med Res, 45*(8), 687-697. doi:10.1016/j.arcmed.2014.11.013

Owens, T., Bechmann, I., & Engelhardt, B. (2008). Perivascular spaces and the two steps to neuroinflammation. *J Neuropathol Exp Neurol, 67*(12), 1113-1121. doi:10.1097/NEN.0b013e31818f9ca8

Palacios, N., Alonso, A., Brønnum-Hansen, H., & Ascherio, A. (2011). Smoking and increased risk of multiple sclerosis: parallel trends in the sex ratio reinforce the evidence. *Ann Epidemiol, 21*(7), 536-542. doi:10.1016/j.annepidem.2011.03.001

Parihar, A., Eubank, T. D., & Doseff, A. I. (2010). Monocytes and macrophages regulate immunity through dynamic networks of survival and cell death. *Journal of innate immunity, 2*(3), 204-215. doi:10.1159/000296507

Park, E. J., Yuki, Y., Kiyono, H., & Shimaoka, M. (2015). Structural basis of blocking integrin activation and deactivation for anti-inflammation. *Journal of Biomedical Science, 22*(1), 51. doi:10.1186/s12929-015-0159-6

Park, I.-K., Letterio, J. J., & Gorham, J. D. (2007). TGF-beta 1 inhibition of IFN-gamma-induced signaling and Th1 gene expression in CD4+ T cells is Smad3 independent but MAP kinase dependent. *Molecular immunology, 44*(13), 3283-3290. doi:10.1016/j.molimm.2007.02.024

Parnas, O., Jovanovic, M., Eisenhaure, T. M., Herbst, R. H., Dixit, A., Ye, C. J., . . . Regev, A. (2015). A Genome-wide CRISPR Screen in Primary Immune Cells to Dissect Regulatory Networks. *Cell, 162*(3), 675-686. doi:10.1016/j.cell.2015.06.059

Parsa, R., Lund, H., Tosevski, I., Zhang, X. M., Malipiero, U., Beckervordersandforth, J., . . . Harris, R. A. (2016). TGFβ regulates persistent neuroinflammation by controlling Th1 polarization and ROS production via monocyte-derived dendritic cells. *Glia, 64*(11), 1925-1937. doi:10.1002/glia.23033

Paternoster, L., Standl, M., Waage, J., Baurecht, H., Hotze, M., Strachan, D. P., . . . Weidinger, S. (2015). Multi-ancestry genome-wide association study of 21,000 cases and 95,000 controls identifies new risk loci for atopic dermatitis. *Nature Genetics, 47*(12), 1449-1456. doi:10.1038/ng.3424

Penela, P., Ribas, C., Sánchez-Madrid, F., & Mayor, F., Jr. (2019). G protein-coupled receptor kinase 2 (GRK2) as a multifunctional signaling hub. *Cell Mol Life Sci, 76*(22), 4423-4446. doi:10.1007/s00018-019-03274-3

Peters, A., Pitcher, L. A., Sullivan, J. M., Mitsdoerffer, M., Acton, S. E., Franz, B., . . . Kuchroo, V. K. (2011). Th17 cells induce ectopic lymphoid follicles in central nervous system tissue inflammation. *Immunity, 35*(6), 986-996. doi:10.1016/j.immuni.2011.10.015

Piccio, L., Rossi, B., Scarpini, E., Laudanna, C., Giagulli, C., Issekutz, A. C., . . . Constantin, G. (2002). Molecular mechanisms involved in lymphocyte recruitment in inflamed brain microvessels: critical roles for P-selectin glycoprotein ligand-1 and heterotrimeric G(i)-linked receptors. *J Immunol, 168*(4), 1940-1949. doi:10.4049/jimmunol.168.4.1940

Platt, R. J., Chen, S., Zhou, Y., Yim, M. J., Swiech, L., Kempton, H. R., . . . Zhang, F. (2014). CRISPR-Cas9 knockin mice for genome editing and cancer modeling. *Cell, 159*(2), 440-455. doi:10.1016/j.cell.2014.09.014

Prinz, M., & Priller, J. (2014). Microglia and brain macrophages in the molecular age: from origin to neuropsychiatric disease. *Nat Rev Neurosci, 15*(5), 300-312. doi:10.1038/nrn3722

Probert, L. (2015). TNF and its receptors in the CNS: The essential, the desirable and the deleterious effects. *Neuroscience, 302*, 2-22. doi:10.1016/j.neuroscience.2015.06.038

Przybyla, L., & Gilbert, L. A. (2021). A new era in functional genomics screens. *Nature Reviews Genetics*. doi:10.1038/s41576-021-00409-w

R Development Core Team. (2021). R: A Language and Environment for Statistical Computing: R Foundation for Statistical Computing. Retrieved from http://www.R-project.org/

Ramagopalan, S. V., Dobson, R., Meier, U. C., & Giovannoni, G. (2010). Multiple sclerosis: risk factors, prodromes, and potential causal pathways. *Lancet Neurol, 9*(7), 727-739. doi:10.1016/s1474-4422(10)70094-6

Ran, F. A., Hsu, P. D., Wright, J., Agarwala, V., Scott, D. A., & Zhang, F. (2013). Genome engineering using the CRISPR-Cas9 system. *Nature protocols, 8*(11), 2281-2308. doi:10.1038/nprot.2013.143

Rasouli, J., Ciric, B., Imitola, J., Gonnella, P., Hwang, D., Mahajan, K., . . . Rostami, A. (2015). Expression of GM-CSF in T Cells Is Increased in Multiple Sclerosis and Suppressed by IFN-β Therapy. *J Immunol, 194*(11), 5085-5093. doi:10.4049/jimmunol.1403243

Redecke, V., Wu, R., Zhou, J., Finkelstein, D., Chaturvedi, V., High, A. A., & Häcker, H. (2013). Hematopoietic progenitor cell lines with myeloid and lymphoid potential. *Nat Methods, 10*(8), 795-803. doi:10.1038/nmeth.2510

Redford, E. J., Smith, K. J., Gregson, N. A., Davies, M., Hughes, P., Gearing, A. J., . . . Hughes, R. A. (1997). A combined inhibitor of matrix metalloproteinase activity and tumour necrosis factor-alpha processing attenuates experimental autoimmune neuritis. *Brain, 120 (Pt 10)*, 1895-1905. doi:10.1093/brain/120.10.1895

Rivera, J., Proia, R. L., & Olivera, A. (2008). The alliance of sphingosine-1-phosphate and its receptors in immunity. *Nature reviews. Immunology, 8*(10), 753-763. doi:10.1038/nri2400

Rivers, T. M., Sprunt, D. H., & Berry, G. P. (1933). OBSERVATIONS ON ATTEMPTS TO PRODUCE ACUTE DISSEMINATED ENCEPHALOMYELITIS IN MONKEYS. *J Exp Med, 58*(1), 39-53. doi:10.1084/jem.58.1.39

Rothhammer, V., Heink, S., Petermann, F., Srivastava, R., Claussen, M. C., Hemmer, B., & Korn, T. (2011). Th17 lymphocytes traffic to the central nervous system independently of α4 integrin expression during EAE. *J Exp Med, 208*(12), 2465-2476. doi:10.1084/jem.20110434

Rudra, D., Egawa, T., Chong, M. M. W., Treuting, P., Littman, D. R., & Rudensky, A. Y. (2009). Runx-CBFbeta complexes control expression of the transcription factor Foxp3 in regulatory T cells. *Nature Immunology, 10*(11), 1170-1177. doi:10.1038/ni.1795

Sathiyanadan, K., Coisne, C., Enzmann, G., Deutsch, U., & Engelhardt, B. (2014). PSGL-1 and E/P-selectins are essential for T-cell rolling in inflamed CNS microvessels but dispensable for initiation of EAE. *Eur J Immunol, 44*(8), 2287-2294. doi:10.1002/eji.201344214

Scheller, J., Chalaris, A., Schmidt-Arras, D., & Rose-John, S. (2011). The pro- and anti-inflammatory properties of the cytokine interleukin-6. *Biochimica et Biophysica Acta (BBA) - Molecular Cell Research, 1813*(5), 878-888. doi:https://doi.org/10.1016/j.bbamcr.2011.01.034

Schläger, C., Körner, H., Krueger, M., Vidoli, S., Haberl, M., Mielke, D., . . . Flügel, A. (2016). Effector T-cell trafficking between the leptomeninges and the cerebrospinal fluid. *Nature, 530*(7590), 349-353. doi:10.1038/nature16939

Seki, A., & Rutz, S. (2018). Optimized RNP transfection for highly efficient CRISPR/Cas9-mediated gene knockout in primary T cells. *Journal of Experimental Medicine, 215*(3), 985-997. doi:10.1084/jem.20171626

Shalem, O., Sanjana, N. E., & Zhang, F. (2015). High-throughput functional genomics using CRISPR-Cas9. *Nature reviews. Genetics, 16*(5), 299-311. doi:10.1038/nrg3899

Sica, A., & Mantovani, A. (2012). Macrophage plasticity and polarization: in vivo veritas. *The Journal of Clinical Investigation, 122*(3), 787-795. doi:10.1172/JCI59643

Siewert, K., Malotka, J., Kawakami, N., Wekerle, H., Hohlfeld, R., & Dornmair, K. (2012). Unbiased identification of target antigens of CD8+ T cells with combinatorial libraries coding for short peptides. *Nat Med, 18*(5), 824-828. doi:10.1038/nm.2720

Sixt, M., Engelhardt, B., Pausch, F., Hallmann, R., Wendler, O., & Sorokin, L. M. (2001). Endothelial cell laminin isoforms, laminins 8 and 10, play decisive roles in T cell recruitment across the blood-brain barrier in experimental autoimmune encephalomyelitis. *J Cell Biol, 153*(5), 933-946. doi:10.1083/jcb.153.5.933

Sobel, R. A., Mitchell, M. E., & Fondren, G. (1990). Intercellular adhesion molecule-1 (ICAM-1) in cellular immune reactions in the human central nervous system. *The American journal of pathology, 136*(6), 1309-1316. Retrieved from https://pubmed.ncbi.nlm.nih.gov/1972610

https://www.ncbi.nlm.nih.gov/pmc/articles/PMC1877574/

Sommerkamp, P., Romero-Mulero, M. C., Narr, A., Ladel, L., Hustin, L., Schönberger, K., . . . Cabezas-Wallscheid, N. (2021). Mouse multipotent progenitor 5 cells are located at the interphase between hematopoietic stem and progenitor cells. *Blood, 137*(23), 3218-3224. doi:10.1182/blood.2020007876

Song, J., Wu, C., Korpos, E., Zhang, X., Agrawal, S. M., Wang, Y., . . . Sorokin, L. (2015). Focal MMP-2 and MMP-9 activity at the blood-brain barrier promotes chemokine-induced leukocyte migration. *Cell Rep, 10*(7), 1040-1054. doi:10.1016/j.celrep.2015.01.037

Sosa, R. A., Murphey, C., Robinson, R. R., & Forsthuber, T. G. (2015). IFN-γ ameliorates autoimmune encephalomyelitis by limiting myelin lipid peroxidation. *Proc Natl Acad Sci U S A, 112*(36), E5038-5047. doi:10.1073/pnas.1505955112

Stampanoni Bassi, M., Iezzi, E., Drulovic, J., Pekmezovic, T., Gilio, L., Furlan, R., . . . Buttari, F. (2020). IL-6 in the Cerebrospinal Fluid Signals Disease Activity in Multiple Sclerosis. *Frontiers in Cellular Neuroscience, 14*(120). doi:10.3389/fncel.2020.00120

Staron, M., Yang, Y., Liu, B., Li, J., Shen, Y., Zúñiga-Pflücker, J. C., . . . Li, Z. (2010). gp96, an endoplasmic reticulum master chaperone for integrins and Toll-like receptors, selectively regulates early T and B lymphopoiesis. *Blood, 115*(12), 2380-2390. doi:10.1182/blood-2009-07-233031

Steffen, B. J., Butcher, E. C., & Engelhardt, B. (1994). Evidence for involvement of ICAM-1 and VCAM-1 in lymphocyte interaction with endothelium in experimental autoimmune encephalomyelitis in the central nervous system in the SJL/J mouse. *Am J Pathol, 145*(1), 189-201.

Steiner, O., Coisne, C., Cecchelli, R., Boscacci, R., Deutsch, U., Engelhardt, B., & Lyck, R. (2010). Differential Roles for Endothelial ICAM-1, ICAM-2, and VCAM-1 in Shear-Resistant T Cell Arrest, Polarization, and Directed Crawling on Blood–Brain Barrier Endothelium. *The Journal of Immunology, 185*(8), 4846. doi:10.4049/jimmunol.0903732

Steiner, O., Coisne, C., Engelhardt, B., & Lyck, R. (2010). Comparison of Immortalized bEnd5 and Primary Mouse Brain Microvascular Endothelial Cells as in vitro Blood–Brain Barrier Models for the Study of T Cell Extravasation. *Journal of Cerebral Blood Flow & Metabolism, 31*(1), 315-327. doi:10.1038/jcbfm.2010.96

Steinman, L. (2001). Multiple sclerosis: a two-stage disease. *Nature Immunology, 2*(9), 762-764. doi:10.1038/ni0901-762

Strijbis, E. M. M., Kooi, E. J., van der Valk, P., & Geurts, J. J. G. (2017). Cortical Remyelination Is Heterogeneous in Multiple Sclerosis. *J Neuropathol Exp Neurol, 76*(5), 390-401. doi:10.1093/jnen/nlx023

The Multiple Sclerosis International Federation. (September 2020). Atlas of MS. (3rd Edition).

Thompson, A. J., Banwell, B. L., Barkhof, F., Carroll, W. M., Coetzee, T., Comi, G., . . . Cohen, J. A. (2018). Diagnosis of multiple sclerosis: 2017 revisions of the McDonald criteria. *Lancet Neurol, 17*(2), 162-173. doi:10.1016/s1474-4422(17)30470-2

Thompson, B. D., Jin, Y., Wu, K. H., Colvin, R. A., Luster, A. D., Birnbaumer, L., & Wu, M. X. (2007). Inhibition of G alpha i2 activation by G alpha i3 in CXCR3-mediated signaling. *The Journal of biological chemistry, 282*(13), 9547-9555. doi:10.1074/jbc.M610931200

Tian, X., Guan, W., Zhang, L., Sun, W., Zhou, D., Lin, Q., . . . Xu, G. (2018). Physical interaction of STAT1 isoforms with TGF-β receptors leads to functional crosstalk between two signaling pathways in epithelial ovarian cancer. *Journal of Experimental & Clinical Cancer Research, 37*(1), 103. doi:10.1186/s13046-018-0773-8

Tsou, C.-L., Peters, W., Si, Y., Slaymaker, S., Aslanian, A. M., Weisberg, S. P., . . . Charo, I. F. (2007). Critical roles for CCR2 and MCP-3 in monocyte mobilization from bone marrow and recruitment to inflammatory sites. *The Journal of Clinical Investigation, 117*(4), 902-909. doi:10.1172/JCI29919

Tsou, C. L., Peters, W., Si, Y., Slaymaker, S., Aslanian, A. M., Weisberg, S. P., . . . Charo, I. F. (2007). Critical roles for CCR2 and MCP-3 in monocyte mobilization from bone marrow and recruitment to inflammatory sites. *J Clin Invest, 117*(4), 902-909. doi:10.1172/jci29919

Vercellino, M., Masera, S., Lorenzatti, M., Condello, C., Merola, A., Mattioda, A., . . . Cavalla, P. (2009). Demyelination, inflammation, and neurodegeneration in multiple sclerosis deep gray matter. *J Neuropathol Exp Neurol, 68*(5), 489-502. doi:10.1097/NEN.0b013e3181a19a5a

Vogel, D. Y., Vereyken, E. J., Glim, J. E., Heijnen, P. D., Moeton, M., van der Valk, P., . . . Dijkstra, C. D. (2013). Macrophages in inflammatory multiple sclerosis lesions have an intermediate activation status. *J Neuroinflammation, 10*, 35. doi:10.1186/1742-2094-10-35

Vogelaar, C. F., Mandal, S., Lerch, S., Birkner, K., Birkenstock, J., Bühler, U., . . . Zipp, F. (2018). Fast direct neuronal signaling via the IL-4 receptor as therapeutic target in neuroinflammation. *Sci Transl Med, 10*(430). doi:10.1126/scitranslmed.aao2304

Vroon, A., Heijnen, C. J., Lombardi, M. S., Cobelens, P. M., Mayor, F., Jr., Caron, M. G., & Kavelaars, A. (2004). Reduced GRK2 level in T cells potentiates chemotaxis and signaling in response to CCL4. *J Leukoc Biol, 75*(5), 901-909. doi:10.1189/jlb.0403136

Vroon, A., Kavelaars, A., Limmroth, V., Lombardi, M. S., Goebel, M. U., Van Dam, A. M., . . . Heijnen, C. J. (2005). G protein-coupled receptor kinase 2 in multiple sclerosis and experimental autoimmune encephalomyelitis. *J Immunol, 174*(7), 4400-4406. doi:10.4049/jimmunol.174.7.4400

Waldner, H., Whitters, M. J., Sobel, R. A., Collins, M., & Kuchroo, V. K. (2000). Fulminant spontaneous autoimmunity of the central nervous system in mice transgenic for the myelin proteolipid protein-specific T cell receptor. *Proc Natl Acad Sci U S A, 97*(7), 3412-3417. doi:10.1073/pnas.97.7.3412

Wang, G. G., Calvo, K. R., Pasillas, M. P., Sykes, D. B., Häcker, H., & Kamps, M. P. (2006). Quantitative production of macrophages or neutrophils ex vivo using conditional Hoxb8. *Nat Methods, 3*(4), 287-293. doi:10.1038/nmeth865

Wang, T., Lander, E. S., & Sabatini, D. M. (2016). Viral Packaging and Cell Culture for CRISPR-Based Screens. *Cold Spring Harbor protocols, 2016*(3), pdb.prot090811-pdb.prot090811. doi:10.1101/pdb.prot090811

Wang, T., Yu, H., Hughes, N. W., Liu, B., Kendirli, A., Klein, K., . . . Sabatini, D. M. (2017). Gene Essentiality Profiling Reveals Gene Networks and Synthetic Lethal Interactions with Oncogenic Ras. *Cell, 168*(5), 890-903.e815. doi:10.1016/j.cell.2017.01.013

Weber, J., Braun, C. J., Saur, D., & Rad, R. (2020). In vivo functional screening for systems-level integrative cancer genomics. *Nature Reviews Cancer, 20*(10), 573-593. doi:10.1038/s41568-020-0275-9

Weissert, R. (2011). Progressive multifocal leukoencephalopathy. *J Neuroimmunol, 231*(1-2), 73-77. doi:10.1016/j.jneuroim.2010.09.021

Wekerle, H., Kojima, K., Lannes-Vieira, J., Lassmann, H., & Linington, C. (1994). Animal models. *Ann Neurol, 36 Suppl*, S47-53. doi:10.1002/ana.410360714

Welsh, R. M. (2009). Blimp hovers over T cell immunity. *Immunity, 31*(2), 178-180. doi:10.1016/j.immuni.2009.08.005

Wenzel, D. M., Lissounov, A., Brzovic, P. S., & Klevit, R. E. (2011). UBCH7 reactivity profile reveals parkin and HHARI to be RING/HECT hybrids. *Nature, 474*(7349), 105-108. doi:10.1038/nature09966

Whitham, R. H., Bourdette, D. N., Hashim, G. A., Herndon, R. M., Ilg, R. C., Vandenbark, A. A., & Offner, H. (1991). Lymphocytes from SJL/J mice immunized with spinal cord respond selectively to a peptide of proteolipid protein and transfer relapsing demyelinating experimental autoimmune encephalomyelitis. *The Journal of Immunology, 146*(1), 101. Retrieved from http://www.jimmunol.org/content/146/1/101.abstract

Wilhelm, I., Fazakas, C., & Krizbai, I. A. (2011). In vitro models of the blood-brain barrier. *Acta Neurobiol Exp (Wars), 71*(1), 113-128.

Winger, R. C., Koblinski, J. E., Kanda, T., Ransohoff, R. M., & Muller, W. A. (2014). Rapid remodeling of tight junctions during paracellular diapedesis in a human model of the blood-brain barrier. *J Immunol, 193*(5), 2427-2437. doi:10.4049/jimmunol.1400700

Wu, C., Ivars, F., Anderson, P., Hallmann, R., Vestweber, D., Nilsson, P., . . . Sorokin, L. M. (2009). Endothelial basement membrane laminin alpha5 selectively inhibits T lymphocyte extravasation into the brain. *Nat Med, 15*(5), 519-527. doi:10.1038/nm.1957

Yang, H., Wang, H., Shivalila, C. S., Cheng, A. W., Shi, L., & Jaenisch, R. (2013). One-step generation of mice carrying reporter and conditional alleles by CRISPR/Cas-mediated genome engineering. *Cell, 154*(6), 1370-1379. doi:10.1016/j.cell.2013.08.022

Yednock, T. A., Cannon, C., Fritz, L. C., Sanchez-Madrid, F., Steinman, L., & Karin, N. (1992). Prevention of experimental autoimmune encephalomyelitis by antibodies against alpha 4 beta 1 integrin. *Nature, 356*(6364), 63-66. doi:10.1038/356063a0

Young, K. G., MacLean, S., Dudani, R., Krishnan, L., & Sad, S. (2011). CD8^{+} T Cells Primed in the Periphery Provide Time-Bound Immune-Surveillance to the Central Nervous System. *The Journal of Immunology, 187*(3), 1192-1200. doi:10.4049/jimmunol.1100695

Zetsche, B., Gootenberg, J. S., Abudayyeh, O. O., Slaymaker, I. M., Makarova, K. S., Essletzbichler, P., . . . Zhang, F. (2015). Cpf1 is a single RNA-guided endonuclease of a class 2 CRISPR-Cas system. *Cell, 163*(3), 759-771. doi:10.1016/j.cell.2015.09.038

Zhang, H. X., Zhang, Y., & Yin, H. (2019). Genome Editing with mRNA Encoding ZFN, TALEN, and Cas9. *Mol Ther, 27*(4), 735-746. doi:10.1016/j.ymthe.2019.01.014

Zhao, L., Cannons, J. L., Anderson, S., Kirby, M., Xu, L., Castilla, L. H., . . . Liu, P. P. (2007). CBFB-MYH11 hinders early T-cell development and induces massive cell death in the thymus. *Blood, 109*(8), 3432-3440. doi:10.1182/blood-2006-10-051508

8. ACKNOWLEDGMENT

I'd like to start by thanking my adviser, Prof. Martin Kerschensteiner, for being an excellent mentor one could wish for. His problem-solving abilities, smart guidance and most importantly his understanding throughout my PhD years were very precious. I am specifically grateful to him for always being supportive to my project ideas, which allowed me to pursue all my scientific questions freely from the beginning. Maybe one thing I would have appreciated more: if the lab meetings had started at 9.05 am instead of 9.00 am. I'd also like to thank Dr. Giuseppe Locatelli and Dr. Delphine Theodorou for their help in the early stages of my PhD, Dr. Eduardo Beltran for his assistance with initial CRISPR data analysis, and Jutta Marks and Anja Schmalz for their help with the never-ending paperwork. I'd like to thank our technician and our bench-neighbor Berni Fiedler for always dealing with all of my orders and genotyping PCRs in a cheerful manner.

I particularly thank my thesis advisory committee members, Prof. Thomas Korn and Prof. Marc Schmidt-Supprian, for their time, guidance, and constant encouragement. Special thanks to Marc-Schmidt-Supprian for always making the extra time to listen to my projects and contribute with his ideas and tools. Discussing science projects with him is always a pleasure. Special thanks to PD Dr. Naoto Kawakami for his close collaboration from the start and for attending my thesis advisory committee meetings voluntarily. It's a pleasure to work with him, and I'm grateful for his constant positive attitude and assistance with my experimental trial ideas, which helped me overcome many technical difficulties. I would also want to thank Katrin Lämmle for her critical contribution to our T cell study, which considerably accelerated the project.

I'd like to thank Dr. Lisa Richter and Pardis Khosravani for their assistance with the flow cytometry machines, as I spent a significant portion of my PhD time with sorting. I'd also like to thank Stefan Krebs from LAFUGA for his patience with my seemingly endless supply of NGS samples. I'd also like to thank the Sanger sequencing service team at the faculty of biology, particularly Gisela Brinkmann, for running my samples on the same day, despite the fact that I was always late in bringing them.

I want to thank all the students who worked with me during my PhD, namely Clara, Daniela, Zala, Seray, Ryan, and Niel for their contributions to the projects, for giving me new perspectives on

List of Publications

1. Locatelli, G., Theodorou, D., **Kendirli, A.,** Jordao, M. J. C., Staszewski, O., Phulphagar, K., Cantuti-Castelvetri L., Dagkalis A., Bessis A., Simons M., Meissner F., Prinz M., Kerschensteiner, M. (2018). Mononuclear phagocytes locally specify and adapt their phenotype in a multiple sclerosis model. **Nature Neuroscience.** 21(9), 1196-1208. doi:10.1038/s41593-018-0212-3

2. Wang T., Yu H., Hughes N.W., Liu B., **Kendirli A.**, Klein K., Chen W.W., Lander E.S., Sabatini D.M. (2017). Gene essentiality profiling reveals gene networks and synthetic lethal interactions with oncogenic Ras. **Cell.** 168(5), 890-903.e815. doi: 10.1016/j.cell.2017.01.013